**Carderock Division**
**Naval Surface Warfare Center**
West Bethesda, MD 20817-5700

**NSWCCD-61-TR–2001/05** February 2000

Survivability, Structures and Materials Directorate
Technical Report

# Dynamic Fracture Toughness Characterization of HY-100 Under-matched Welds

by

Stephen M. Graham
*Vector Research*

and

Michael D. McLaughlin

20010823 010



**NSWCCD-61-TR–2001/05** **Dynamic Fracture Toughness Characterization of HY-100 Under-matched Welds**

Naval Surface Warfare Center
**Carderock Division**
West Bethesda, MD 20817-5700

**NSWCCD-61-TR—2000/05** **February 2000**

Survivability, Structures, and Materials Directorate
Technical Report

# Dynamic Fracture Toughness Characterization of HY-100 Under-matched Welds

by

Stephen M. Graham
*Vector Research*

and

Michael D. McLaughlin

# REPORT DOCUMENTATION PAGE

*Form Approved*
*OMB No. 0704-0188*

| 1. AGENCY USE ONLY (Leave blank) | 2. REPORT DATE | 3. REPORT TYPE AND DATES COVERED |
|---|---|---|
| | | Final Report, March 1998 – February 2000 |

| 4. TITLE AND SUBTITLE | 5. FUNDING NUMBERS |
|---|---|
| Dynamic Fracture Toughness Characterization of HY-100 Under-matched Welds | |
| 6. AUTHOR(S)<br>Stephen M. Graham and Michael D. McLaughlin | |
| 7. PERFORMING ORGANIZATION NAME(S) AND ADDRESS(ES)<br>Naval Surface Warfare Center<br>Carderock Division (Code 614)<br>9500 MacArthur Boulevard<br>West Bethesda, MD 20817-5700 | 8. PERFORMING ORGANIZATION REPORT NUMBER<br>NSWCCD-61-TR-2000/05 |
| 9. SPONSORING/MONITORING AGENCY NAME(S) AND ADDRESS(ES)<br>Dr. George Yoder, Materials Science and Technology Division (ONR 332)<br>Office of Naval Research<br>Ballston Centre, Tower One<br>800 North Quincy Street<br>Arlington, VA 22217-5660 | 10. SPONSORING/MONITORING AGENCY REPORT NUMBER |

11. SUPPLEMENTARY NOTES

| 12a. DISTRIBUTION/AVAILABILITY STATEMENT | 12b. DISTRIBUTION CODE |
|---|---|
| Approved for public release; distribution is unlimited. | |

13. ABSTRACT (Maximum 200 words)

Welds in marine structures are typically fabricated such that the yield strength of the weld metal is higher than the base plate (over-matched). Allowing the weld metal yield strength to be less than the base metal (under-matching) can increase productivity and weld metal toughness; however, there is some concern that under-matching increases the crack driving force and decreases the weld metal tearing resistance. This study examined fracture behavior of two HY-100 under-matched welds under dynamic loading. A new test fixture that provided greater control of specimen deflection during impact testing of SE(B) specimens was developed, as was a procedure for applying the Normalization Method to the analysis of dynamic fracture toughness tests. Successful application of Normalization involved using multiple specimens with varying ductile crack growth to establish the correct form for the plasticity function. The accuracy of the measured $J_{Id}$ was verified by comparing with multi-specimen $J_{Id}$ values. The results from these tests showed that the proximity of the crack tip to the fusion line had more effect on fracture behavior than mismatch level. Narrower fusion line margins led to lower tearing resistance and a greater propensity for fracture instability.

| 14. SUBJECT TERMS | 15. NUMBER OF PAGES |
|---|---|
| Under-matched Welds, Dynamic Fracture Toughness, HY-100, Normalization, $J_{Id}$ | |
| | 16. PRICE CODE |

| 17. SECURITY CLASSIFICATION OF REPORT | 18. SECURITY CLASSIFICATION OF THIS PAGE | 19. SECURITY CLASSIFICATION OF ABSTRACT | 20. LIMITATION OF ABSTRACT |
|---|---|---|---|
| Unclassified | Unclassified | Unclassified | Unclassified |

NSN 7540-01-280-5500

Standard Form 298 (Rev. 2-89)
Prescribed by ANSI Std Z39-18

# TABLE OF CONTENTS

## FIGURES

## TABLES

## ADMINISTRATIVE INFORMATION

This work was performed through contract with Analysis & Technology (contract N00167-96-D-0045) and by the Metals Department (Code 61) of the Survivability, Structures and Materials Directorate at the Naval Surface Warfare Center, Carderock Division (NSWCCD) under the supervision of Mr. Thomas Montemarano, Branch Head, Fatigue and Fracture (Code 614). The work was sponsored by Dr. George Yoder of the Office of Naval Research, Materials Science and Technology Division (ONR 332), as part of the Seaborne Structural Materials Task, and managed by Dr. William Messick (Code 0115). The Technical Agent at NAVSEA was Allen Manuel (05P4).

## SUMMARY

Fusion welded marine structures are typically fabricated with welding consumables and procedures that produce welds with a higher yield strengths than the base plates being joined (over-matched). Allowing the weld metal yield strength to be less than the base metal (under-matching) can increase productivity and weld metal toughness. However, there is some concern that the rate of increase in crack driving force to fracture (J) with increasing plastic strain can be much greater for a crack in an under-matched weld. There is also come concern that when the crack tip is close to the fusion line of an under-matched weld, it can cause a significant decrease in the tearing resistance. The objective of this study was to examine under-matched weld fracture behavior under dynamic loading. Currently there are no standardized test methods for dynamic fracture toughness testing of ductile materials. Consequently, test procedures and analysis methods had to be developed. Two under-matched systems were examined in this study, both of which were made from 50.8 mm (2 in.) thick HY steel plate with a yield of about 690 MPa (100 ksi) and MIL 100S-1 weld wire. A new test fixture that provides greater control of specimen deflection during impact testing of SE(B) specimens was developed, as was a procedure for applying the Normalization Method to the analysis of dynamic fracture toughness tests. Successful application of the Normalization Method was achieved by using multiple specimens with varying ductile crack growth to establish the correct form for the plasticity function. The accuracy of the procedure for determining $J_{Id}$ was verified by comparing values from Normalization with a multi-specimen approach. The results from these tests showed that the proximity of the crack tip to the fusion line had more effect on fracture behavior than mismatch level. Narrower fusion line margins led to lower tearing resistance and a greater propensity for fracture instability.


## INTRODUCTION

Fusion welded marine structures are typically fabricated with welding consumables and procedures that produce welds with higher yield strengths than the base plates being joined (over-matched). This is done to prevent development of high strains in the weld metal, which typically has lower fracture toughness and more defects than the base metal. This works well for lower strength structural steels, but can be problematic for high strength marine steels because of the high pre-heats required to prevent hydrogen cracking and the lower deposition rates. Allowing the weld metal yield strength to be less than the base metal (under-matching) can increase productivity and weld metal toughness. However, it is not known what effect the concentration of strain in the weld metal may have on the integrity of the structure.

Various investigators have studied the fracture behavior of under-matched welds [1 - 5]. Kirk conducted a literature review of overall deformation and fracture behavior of mismatched steel butt welds [1]. He found that the rate of increase in crack driving force to fracture (J) with increasing plastic strain can be much greater for a crack in an under-matched weld than in an over-matched weld. This is consistent with observations of strain variation across under-matched welds. These strain variations complicate the calculation of J in an under-matched weld. However, Kirk also found that for deeply cracked SE(B) specimens, treating the specimen as homogeneous with weld metal properties provides reasonably accurate estimates of J provided that plastic deformation is confined to the weld metal. Mismatching can have more effect on J for shallow cracks in SE(B)'s because of the proximity of the free edge to the crack tip plastic zone. In a later study, Kirk and Dodds [2] found that treating weld specimens as all weld improperly accounts for the effects of weld mismatch on the limit load and plastic work distribution; however, these two errors are opposite and thus tend to cancel each other out. Therefore, they concluded that accurate J's could be estimated by treating the specimen as homogeneous using weld metal properties, although, the paper doesn't report any J values greater than 350 kJ/m$^2$. Franco et. al. [3] state that it is possible to ignore the mismatching and use homogenous weld properties to calculate J if "the distance of the crack tip to the interface is not too small with respect to the ligament size, and if the initiation load is less than the yield limit load." Tregoning [4] showed that when the crack tip is close to the interface, it can cause a significant decrease in the tearing resistance of an under-matched weld. Burstow et. al. [5] found that the constraint of an under-matched weld is a function of mismatch level, specimen geometry, applied load and the weld geometry. The effects of geometry and mismatch on constraint are coupled by the relationship between the crack tip plastic zone and the higher yield base metal. They introduce a normalized load parameter that describes the size of the plastic zone relative to the distance from the crack tip to the weld fusion line. At low normalized load levels, where the plastic zone is contained within the weld metal, constraint effects are due almost entirely to specimen geometry. As normalized load is increased, constraint varies with mismatch level. At high normalized load levels, constraint becomes independent of specimen geometry at high levels of mismatch (40% under-match and above).

All of these studies were concerned with the quasi-static fracture behavior of under-matched welds. Naval ship or submarine structures must be able to survive dynamic loading from underwater explosions (UNDEX). The objective of this study was to examine under-matched weld fracture behavior under dynamic loading. Currently there are no standardized test methods for dynamic fracture toughness testing of ductile materials. Consequently, test procedures and analysis methods had to be developed to measure the dynamic tearing resistance of under-matched weld systems. A new test fixture that provides greater control of specimen deflection during impact testing of SE(B) specimens was developed in the course of this program.

Two under-matched systems were examined in this study, both of which were made from 50.8 mm (2 in.) thick HY steel plate with a yield of about 690 MPa (100 ksi) and MIL 100S-1 weld wire. The welding parameters were varied to achieve different amounts of under-matching. SE(B) specimens were removed from the two weldments in the T-S orientation. Presence of residual stress in the specimens caused some problems with obtaining straight pre-cracks. Procedures used to minimize the effects of residual stress are discussed. The pre-cracked specimens were impact loaded in a drop tower in order to measure the tearing resistance under conditions that simulate UNDEX loading. The Normalization Method [6] was used to generate dynamic J-R curves from the test results.

The practical application of the Normalization Method is discussed, along with an in-depth examination of the problems with the method. A considerable amount of effort went into developing procedures for applying the Normalization Method in order to improve the accuracy of the resulting dynamic J-R curves.

## DESCRIPTION OF MATERIAL

Two GMAW 8ft. x 25 in. weldments were made for this program, designated GOS and GOT. Both welds were made using MIL 100S-1 weld wire. The first weld, designated GOS, was made from a special Ti modified HY-80 plate. The modification resulted in higher strength than is typically obtained with HY-80. The chemical composition of this plate is given in **Table 1** and impact toughness (Charpy and dynamic tear) are given in **Table 2** and **Table 3**. The second weld, designated GOT, was made from a Ti modified HY-100 plate. The chemical composition and impact toughness of this plate are shown in **Table 4, Table 5** and **Table 6**. Note that the chemistries of the GOS and GOT plates meet the specification requirements for HY-80 and HY-100, respectively. Quasi-static and dynamic tensile strengths of the two plates were measured in this program, and will be presented in the section on results. The composition of the MIL-100S-1 weld wire is given in **Table 7**. The Charpy impact energy curves for the two plates are compared in **Figure 1**. It is apparent that the upper transition behavior of the two plates is similar.

The weld geometry for both of these welds was a symmetric double-V with a root gap of 1/8 in. and an included angle of 60° (see **Figure 2**). While the welding procedures met current fabrication requirements for 100S wire, the parameters were selected specifically to maximize the amount of under-matching. The heat input for these welds was just below the maximum allowable value of 100 kJ/in. for production GMA welds of 2 in. thick plate. High heat input tends to lower the yield strength of the weld metal. Both welds had preheat and interpass temperatures of 300°F. The GOS weld was made with a voltage of 29, wire feed speed of 280 in./min., a current of 385 amps, travel speed of 7 inches per minute and a heat input of 95.7 kJ/in. The GOT weld was made with a voltage of 27, wire feed speed of 220 – 240 in./min., a current of 360 – 380 amps, travel speed of 7 inches per minute and a heat input of 94 kJ/in.

**Table 1. Chemical Composition of Ti Modified HY-80 Plate (GOS).**

| | Thick-ness (in.) | Chemical Composition (wt%) | | | | | | | | | | | |
|---|---|---|---|---|---|---|---|---|---|---|---|---|---|
| | | C | Si | Mn | P | S | Ni | Cr | Mo | V | Al | Cu | Ti |
| GOS | 2 | 0.149 | 0.29 | 0.27 | 0.013 | 0.001 | 3.03 | 1.64 | 0.46 | 0.003 | 0.023 | 0.008 | 0.008 |
| HY-80 Specification for 2 in. thick plate | | 0.13 – 0.18 | 0.15 – 0.38 | 0.10 – 0.40 | 0.015 max. | 0.008 max. | 2.50 – 3.50 | 1.40 – 1.80 | 0.35 – 0.60 | 0.03 max. | - | 0.25 max. | 0.02 max. |

**Table 2. Charpy Tests of Ti Modified HY-80 Plate (GOS).**

| Temperature (°F) | Impact Energy (ft-lb) | Lateral Expansion (in.) |
|---|---|---|
| 75 | 126 | 0.078 |
| | 107 | 0.069 |
| | 134 | 0.081 |
| 0 | 103 | 0.060 |
| | 142 | 0.080 |
| | 138 | 0.077 |
| -60 | 136 | 0.078 |
| | 131 | 0.077 |
| | 96 | 0.064 |
| -120 | 58 | 0.036 |
| | 56 | 0.040 |
| | 99 | 0.062 |

HY-80 Specification (average of 3 tests) 35 ft-lb at –120°F and 60 ft-lb at 0°F

**Table 3. Dynamic Tear Tests of Ti Modified HY-80 Plate (GOS).**

| Temperature (°F) | Impact Energy (ft-lb) | % Shear |
|---|---|---|
| -40 | 1132 | 95 |
| | 1251 | 100 |

HY-80 Specification (average of 2 tests) 450 ft-lb at –40°F

**Table 4. Chemical Composition of Ti Modified HY-100 Plate (GOT).**

| | Thick-ness (in.) | Chemical Composition (wt%) | | | | | | | | | | | |
|---|---|---|---|---|---|---|---|---|---|---|---|---|---|
| | | C | Si | Mn | P | S | Ni | Cr | Mo | Va | Al | Cu | Ti |
| GOT | 2 | 0.147 | 0.28 | 0.26 | 0.007 | 0.001 | 3.05 | 1.65 | 0.48 | 0.003 | 0.024 | 0.012 | 0.006 |
| HY-100 Specification for 2 in. thick plate | | 0.14 – 0.20 | 0.15 – 0.38 | 0.10 – 0.40 | 0.015 max | 0.008 max. | 2.75 – 3.50 | 1.40 – 1.80 | 0.35 – 0.60 | 0.03 max. | - | 0.25 max. | 0.02 max. |

**Table 5. Charpy Tests of Ti Modified HY-100 Plate (GOT).**

| Temperature (°F) | Impact Energy (ft-lb) | Lateral Expansion (in.) |
|---|---|---|
| 75 | 125 | 0.074 |
| | 126 | 0.070 |
| | 140 | 0.076 |
| 0 | 113 | 0.071 |
| | 145 | 0.079 |
| | 142 | 0.078 |
| -60 | 140 | 0.080 |
| | 133 | 0.077 |
| | 96 | 0.064 |
| -120 | 112 | 0.065 |
| | 75 | 0.043 |
| | 100 | 0.063 |

HY-100 Specification (average of 3 tests) 40 ft-lb at –120°F and 60 ft-lb at 0°F

**Table 6. Dynamic Tear Tests of Ti Modified HY-100 Plate (GOT).**

| Temperature (°F) | Impact Energy (ft-lb) | % Shear |
|---|---|---|
| -40 | 1177 | 100 |
| | 1206 | 100 |

HY-100 Specification (average of 2 tests) 500 ft-lb at –40°F

**Table 7. Chemical Composition of MIL-100S-1 Weld Wire.**

| | Chemical Composition (wt%) | | | | | | | | | | | | |
|---|---|---|---|---|---|---|---|---|---|---|---|---|---|
| | C | Mn | P | S | Si | Cr | Ni | Mo | Ti | Cu | V | Al | Zr |
| 100S-1 | 0.06 | 1.65 | 0.01 | 0.005 | 0.33 | 0.12 | 1.79 | 0.33 | 0.02 | 0.03 | 0.01 | 0.01 | 0.01 |

Chemical composition provided by wire manufacturer

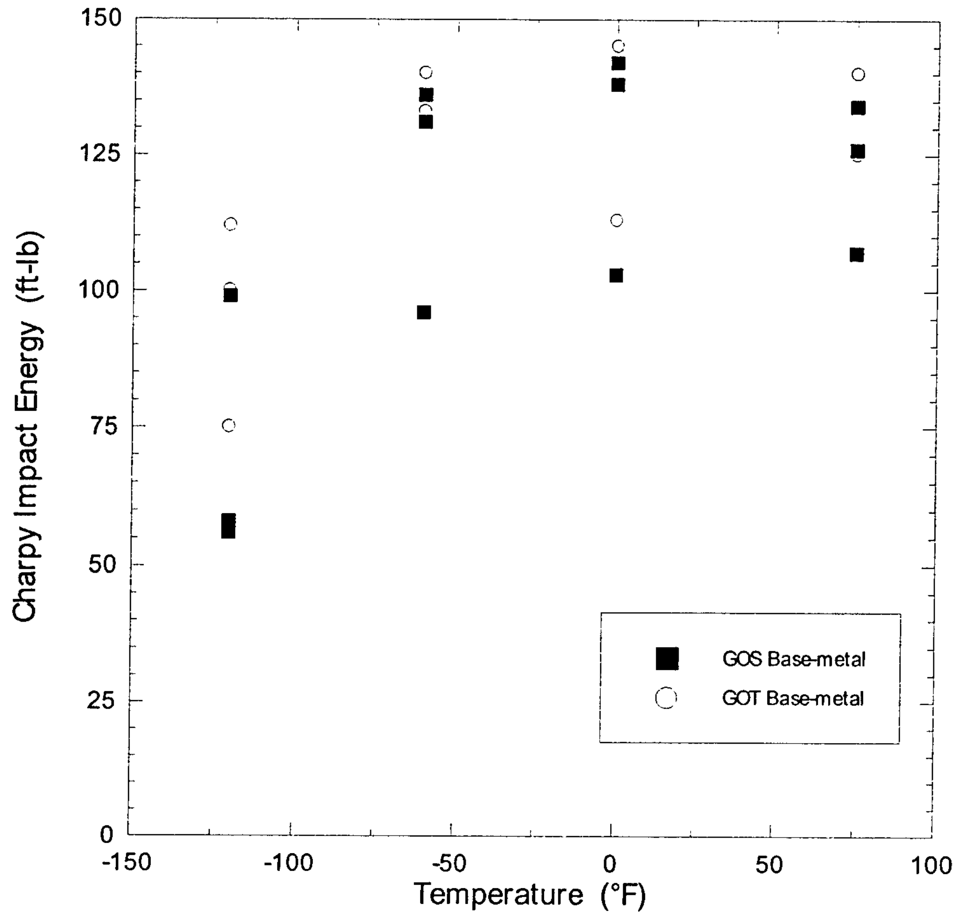


**Figure 1. Charpy Impact Energy for base-metal from GOS and GOT plates.**

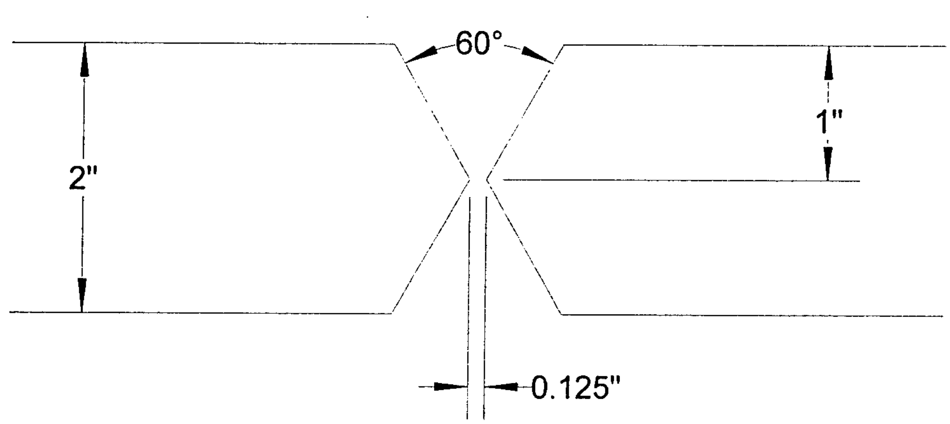


**Figure 2. Geometry of weld preparation**

## SPECIMEN PREPARATION

The weldments were each inspected using radiography to identify flaws in the weld. Areas showing lack of fusion were identified and marked so that no specimens would be removed from those areas. The following specimens were removed from each weldment: 6 Hull Toughness Element (HTE) specimens for explosive load fracture testing, 10 dynamic SE(B)'s, 5 short-crack quasi-static SE(B)'s and 11 tensile specimens. The results of the HTE tests will be presented in a subsequent report.

All of the tensile specimens were machined with the long axis parallel to the weld. Five baseplate specimens were tested for each plate: 3 quasi-statically and 2 dynamically. Six weld metal tensile specimens were tested for GOS and 4 for GOT. The specimens were evenly distributed between the ¼ and ¾ thickness locations, designated as the weld top and weld bottom respectively. Two weld metal specimens were tested dynamically and the remainder were tested quasi-statically. The quasi-static tensile specimens were standard 0.505 in. gage diameter with threaded ends. No special preparation was required for these specimens.

The dynamic tensile specimens were a special design that included a shoulder for direct load measurement, a 0.252 gage diameter, and button-head ends (see **Figure 3**). One strain gage was applied in the center of the gage section and two were applied in the shoulder section on opposite sides of the specimen (180° apart). The shoulder gages were then wired as a half-bridge and the specimen was calibrated quasi-statically so that load could be determined from the shoulder strain readings. The maximum load used in calibration was kept below 1,500 lbs for the GOS specimens and 2,000 lbs for the GOT specimens.

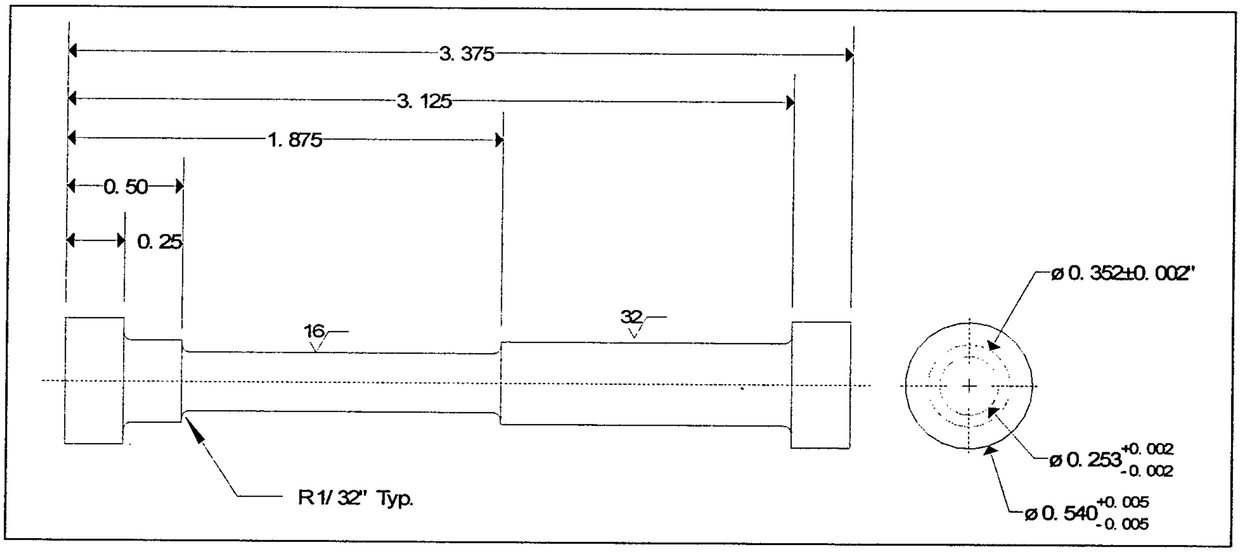


**Figure 3. Dynamic Tensile Specimen (dimensions in inches)**

The SE(B) specimens were all T-S orientation with the notches centered relative to the narrowest part of the weld, as shown in Figure 4. After removing the SE(B) blanks from the weldment, the surfaces were polished and etched using 10% ammonium persulfate to reveal the weld. The initial blanks were cut to 10 in. length to allow for correct placement of the notch in the weld. Once the notch location was marked, the notch was cut and the length was machined to obtain a symmetric specimen relative to the notch.

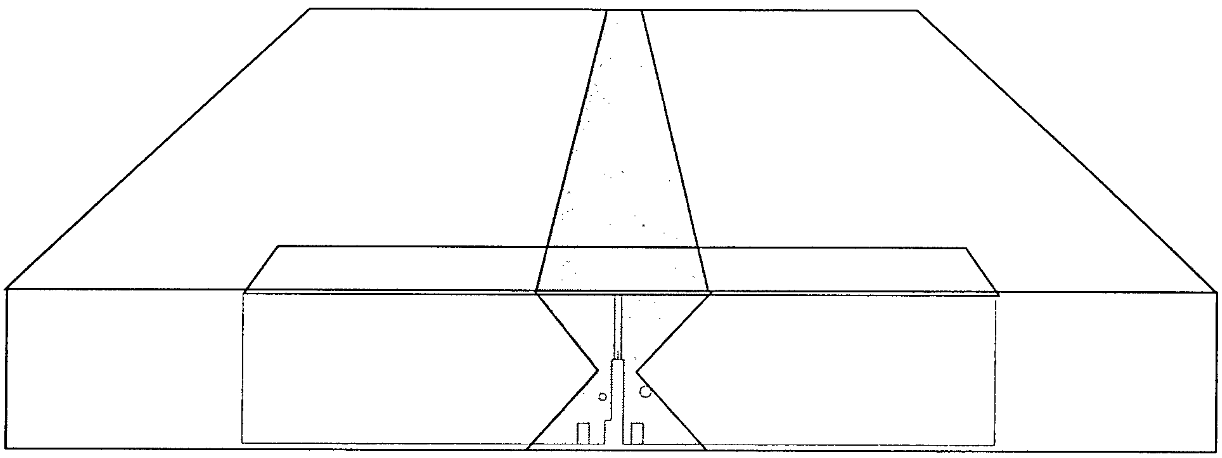

**Figure 4. Orientation of SE(B) specimens relative to weldment.**

When the SE(B) blanks were saw cut from the weldments, residual stresses caused the blanks to bow. In order to make the specimens straight, the width dimension was cut down from 2.000 in. to 1.750 in. The notches were also shortened to maintain notch length to width ($a_n$/W) ratios of 0.114 for the short-crack specimens and 0.486 for the others. The thickness was left at 1.000 in. The geometry of the dynamic SE(B) is shown in **Figure 5** and the quasi-static, short-crack specimen is shown in **Figure 6**.

Residual stresses in the weld also caused problems with pre-cracking of some of the SE(B) specimens. Two different techniques were used in an effort to reduce the effect of residual stress on curvature of the fatigue pre-crack; one was reverse bending and the other was transverse compression. Reverse bending was used on the quasi-static, short crack SE(B)'s. A single cycle of reverse four-point bending was applied at a load equal to 48% of the limit load. For the GOS specimens the reverse bend load was 17,000 lbs and for the GOT specimens it was 19,000 lbs. The magnitude of the load was chosen based on pervious experience [4]. The specimens were then fatigue pre-cracked using standard procedures in E1737 [7].

The straightness of the pre-cracks in the short-crack specimens turned out to be quite good; however, in many cases it still did not meet the requirements in E1737. As seen in **Figure 7**, the curvature for a typical short-crack specimen that is invalid by E1737 does not appear to be unacceptable. This is because the allowable deviation from straightness in E1737 is 5% of the average physical crack length. For short cracks, the average crack length is small, so the allowable deviation is also small. The allowable deviation for a 1 in. thick SE(B) specimen with an average crack length of 1.0 in. (a/W = 0.5) is 0.050 in.

For the same thickness specimen with an average crack length of 0.3 in., the allowable deviation decreases to 0.015 in. This places undue restrictions on short crack tests. A qualitative assessment of curvature is based on not only the amount of deviation from straightness, but also the thickness over which this occurs. The same 0.050 in. deviation would appear much more curved for a 0.5 in. thick specimen than for a 1 in. thick specimen. A 0.050 in. deviation would appear to have the same curvature for two specimens with the same thickness and different crack lengths. Therefore, the allowable deviation in E1737 should be expressed in terms of specimen thickness, not average crack length. A deviation of 5% for a 1 in. thick specimen with a/W = 0.5 in. is approximately equivalent to 6% of the net thickness (20% side-groove). If the straightness requirement were based on 6% of the net thickness, the allowable deviation for the short cracks would be 0.048 in. and all of the pre-cracks would be valid.

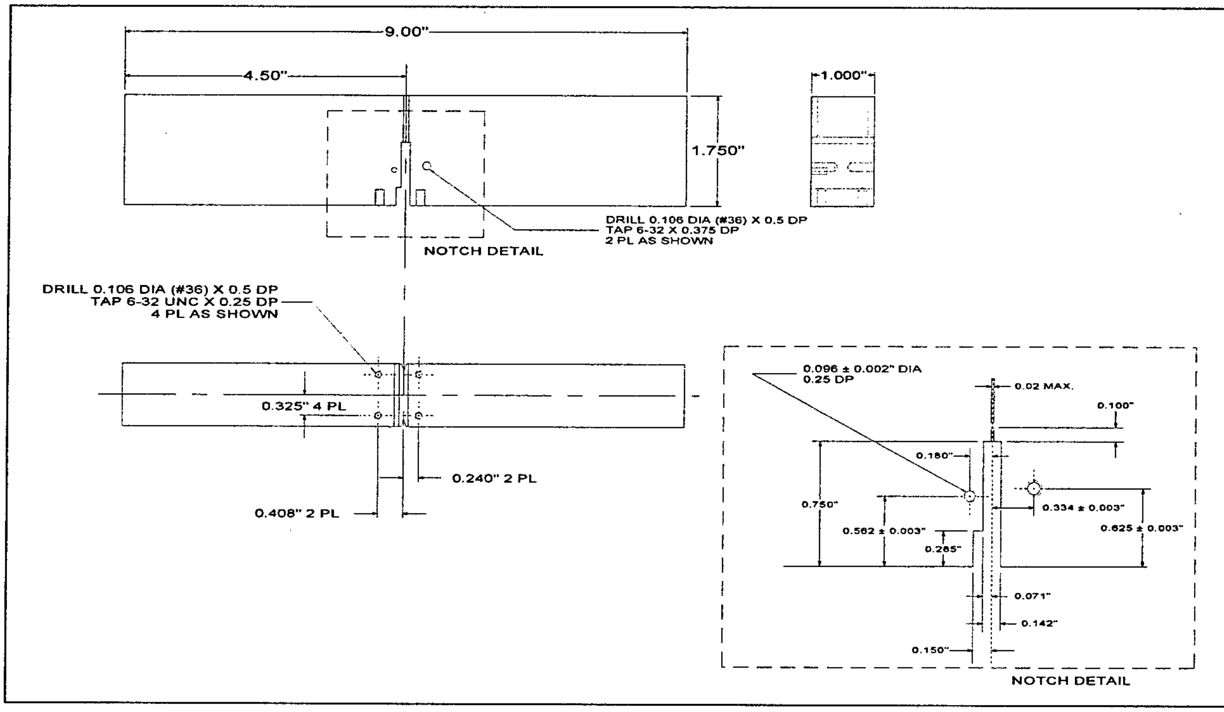


**Figure 5. Dynamic SE(B) specimen (dimensions in inches)**

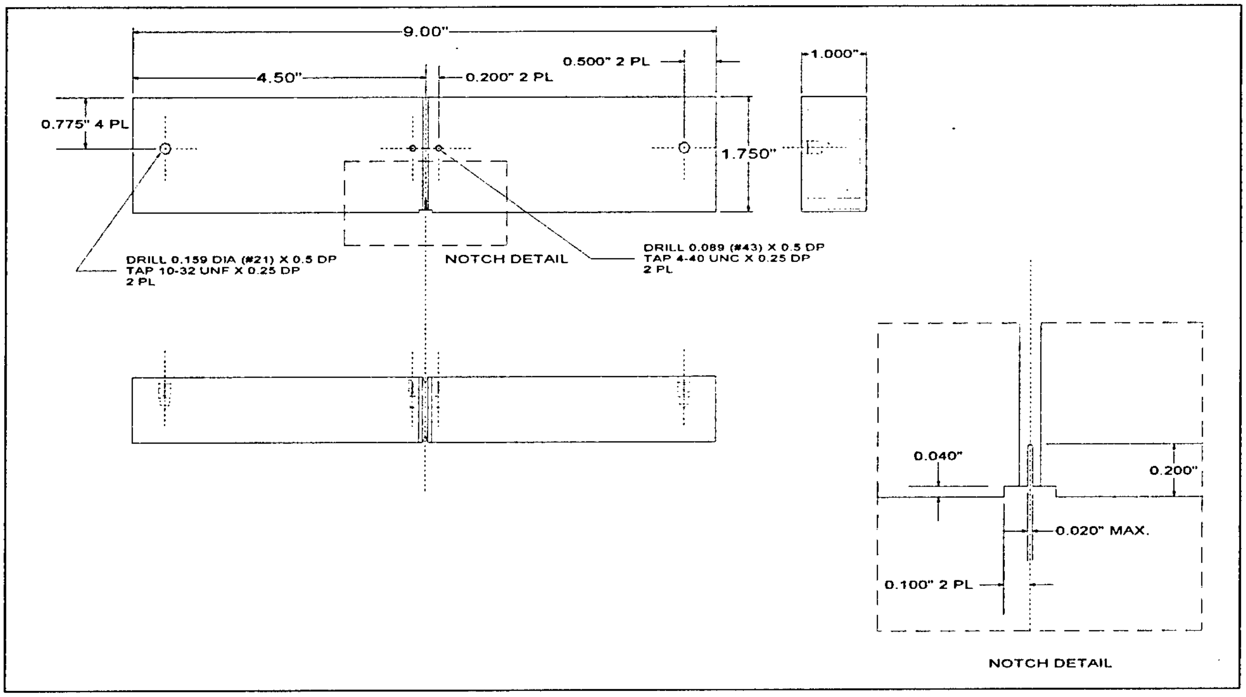


**Figure 6. Short-crack SE(B) specimen (dimensions in inches)**

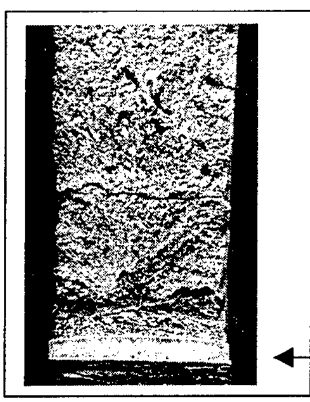


**Figure 7. Typical fatigue pre-crack on short crack SE(B) specimen.**

The dynamic, deep-crack specimens were pre-cracked using a different procedure. One each of the GOS and GOT specimens were pre-cracked using reverse bend pre-compression as above and tested quasi-statically so that crack-front straightness could be checked. The resulting pre-cracks are shown in **Figure 8**. For these initial two specimens, reverse bending was used with a load of 7,000 lbs for GOS and 9,000 lbs for GOT. The straightness on the GOT specimen appeared satisfactory, so the remaining dynamic GOT specimens were pre-cracked the same way. On the other hand, the first GOS specimen had excessive crack-front curvature. Consequently, transverse compression was used on the remaining specimens in conjunction with the previous reverse bending. The procedures given in a draft annex to ASTM E1290 for testing of ferritic steel weldments [8] were followed for the compression. A ½" diameter indentor (Type 3 in the E1290 annex) was used and two overlapping indents were made in the ligament area on each side of the specimen. The compression was done in increasing load steps, each time measuring the residual plastic deformation on the side of the specimen until 0.005 in. was obtained. Typically this took from 2 to 5 load steps. Then the specimen was moved and a second indent was made on the same side, once again with increasing load steps until 0.005 in. residual plastic displacement was obtained. This process was then repeated on the other side. For a 1 inch thick specimen, an indent of 0.005 in. on each side represents 1% plastic strain through the thickness, which is the plastic strain level recommended in [8]. These specimens were then fatigue pre-cracked using standard procedures [7]. The resulting pre-cracks were straighter than without transverse compression, but 4 out of 9 still failed the straightness requirement in E1737. The best and worst pre-cracks where transverse compression was used are shown in **Figure 9**. The tendency for the cracks to trail behind near the surfaces indicates that the compression was not able to fully relieve the compressive residual stresses, or perhaps it induced compressive residual stresses at the surface. Five of the last 6 specimens that were compressed were valid, indicating that the residual stresses may have varied along the length of the weld (consecutive numbered specimens were adjacent in the weldment).

For the deep crack GOT specimens that were reverse bent, only 2 out of 9 pre-cracks were invalid.

After pre-cracking, all specimens were side-grooved 10% on each side. The dynamic specimens had strain gages applied at the quarter points on the front and back faces in order to measure load directly on the specimen (see **Figure 10**). These gages were wired as a full bridge and the specimens were calibrated quasi-statically to obtain a full scale output of 10 volts at 20,000 lbs. The maximum load used in calibrating was limited to about 2,000 lbs (just below the final maximum precracking load) so as not to increase the plastic zone at the crack tip left over from pre-cracking. There is undoubtedly some error introduced by calibrating up to 2,000 lbs and then measuring up to 20,000 lbs. Unfortunately, this error is unavoidable since direct load measurement on the specimen is the only way to measure applied load in an impact test of a SE(B) specimen. There is also some load measurement error introduced by crack growth and plasticity in the ligament. These errors will be discussed further in the section on analysis.

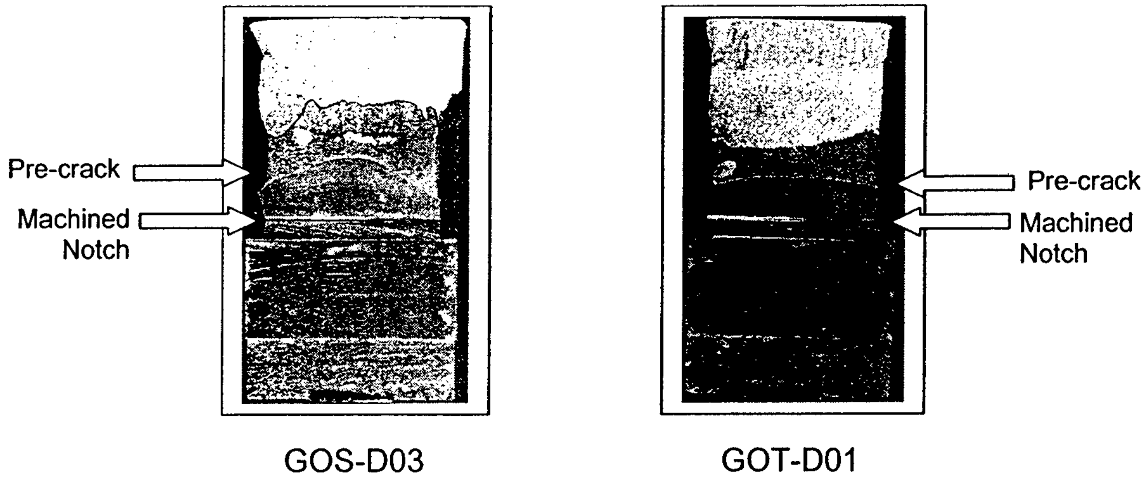


**Figure 8. Fatigue pre-cracks on first two deep crack specimens with only reverse bending.**

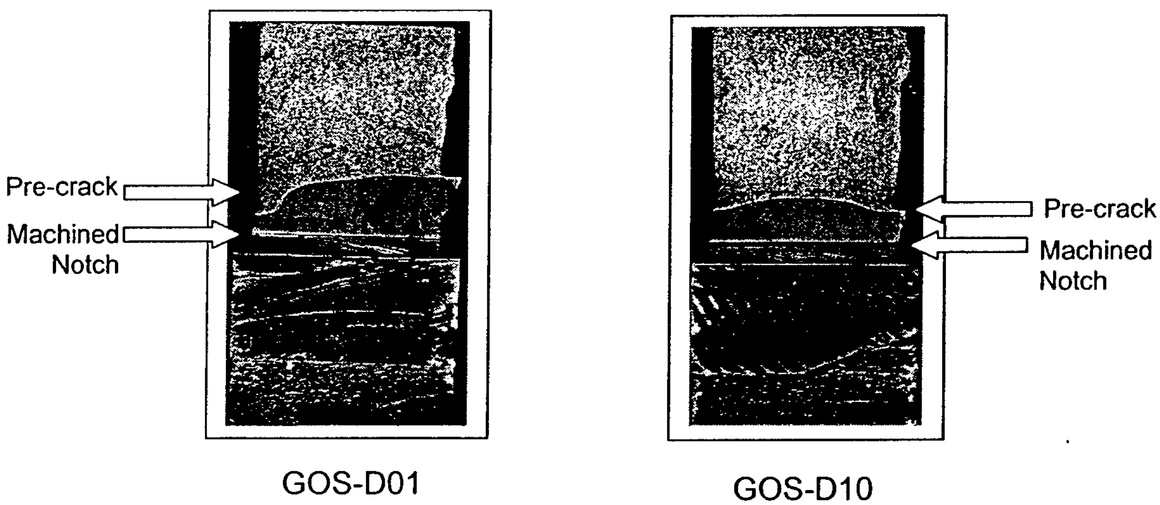


**Figure 9. Fatigue pre-cracks for deep crack specimens with transverse compression showing range from worst to best.**

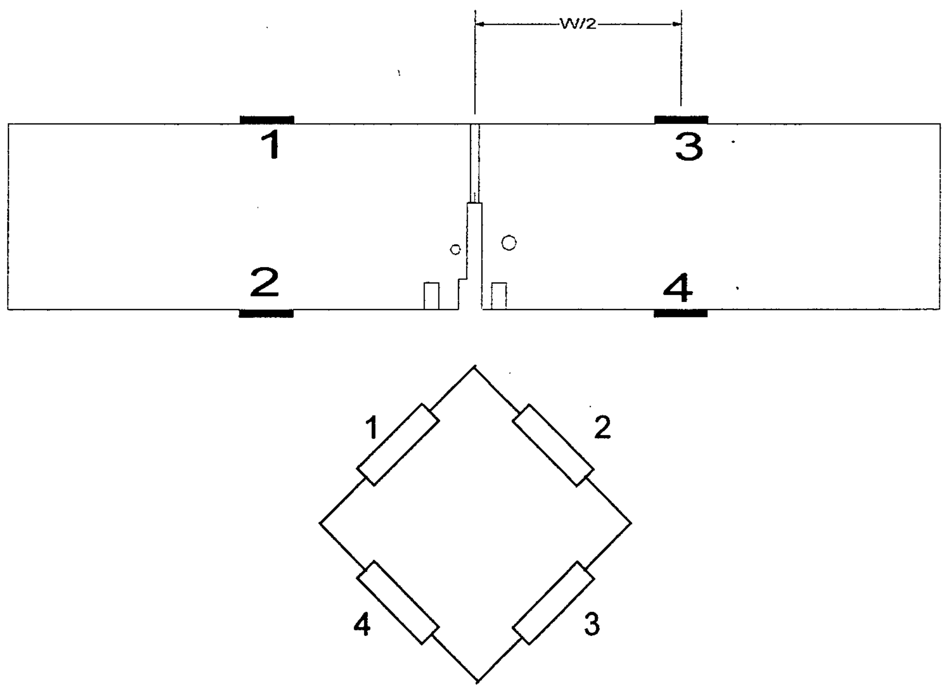


**Figure 10. Strain-gage placement and wiring for dynamic SE(B) specimens.**

## TEST PROCEDURE

### Tensile tests

The quasi-static tensile tests were conducted at 28°F using the standard procedures given in ASTM test method E8 [9].

The dynamic tensile tests were a bit more involved. These were run in a high-rate servo-hydraulic load frame. This frame is capable of actuator displacement rates of up to 200 in./sec when there is no resisting load. When a load is applied to the actuator, the actual displacement rates are lower. A slack grip is used in the load train to allow the actuator to accelerate before load is applied. This grip provides about 0.14 in. of slack in the load train before the specimen sees any load. It is also designed to provide a gradual stiffness increase when the slack is gone, thereby cushioning the impact of load transfer. This load transfer occurs over a small displacement. Use of the slack grip increases the achievable displacement rate during the test considerably. The rate in these tests was about 100 in./sec. A computer controlled digital oscilloscope was used to store two channels of data, load from the shoulder strain gages and strain from the gage section strain gage. Shunt calibration was used to convert voltage readings to axial strain for the gage in the gage section. These tests were also run at 28°F. After the test, measurements of elongation and reduction of area were made. The percent elongation was determined by measuring the distance between the shoulders on the specimen before and after the test. No punch marks were made in the specimens.

### Quasi-static short-crack SE(B) tests

The short-crack SE(B) specimens were all tested at 28°F following the procedures in ASTM 1737 [7] where applicable. The tests were run in a 100 kip capacity servo-hydraulic load frame in actuator displacement control. Actuator control was used instead of clip gage control because pop-ins were considered likely, and when these occur in clip gage control the load frame can jump unexpectedly. Pop-ins do not effect the stability of the frame in displacement control. A clip gage mounted on razor blades spot welded to the front face of the specimen was used to measure crack opening displacement. A flex bar mounted to the side of the specimen was used to measure load line displacement. The flex bar eliminates the need to correct measured load line displacement for brinnelling and load train compliance. After the tests, the specimens were heat tinted to mark the final crack and then cooled in liquid nitrogen and broken open.

In addition to the short crack specimens, two dynamic specimens were tested quasi-statically in order to obtain baseline data and to check the straightness of the pre-cracks. These specimens were also tested at 28°F using the same procedures at the short-crack specimens.

### Dynamic SE(B) tests

The objective of these tests was to measure the dynamic tearing resistance curve for stable ductile tearing. In order to do this, it was necessary to prevent the fracture mode transition to cleavage. Therefore, the test temperature was varied initially to determine the lowest temperature where the fracture would not trip to cleavage. Once this temperature was determined, the remaining tests were conducted at that temperature. For the GOS specimens this turned out to be 110°F and for the GOT it was 100°F. The impetus for using the lowest temperature was to minimize the difficulties with subsequent testing of HTE specimens, which were to be tested at the same temperature as part of a follow-on program. It is difficult to conduct elevated temperature HTE tests, and the difficulties increase as the temperature increases. The dynamic tearing resistance data would be used to predict the outcome of the HTE tests, so it was important that the fracture mode be the same for the two tests.

The dynamic loading in these tests was intended to simulate the rates typical of Underwater Explosion (UNDEX) events, where peak pressure is reached in 1 to 3 milliseconds. This requires very high loading rates, which are difficult to attain in conventional servo-hydraulic load frames. These high rates can be achieved through impact loading in a drop tower. The impact velocity, and the corresponding loading rate, is determined by the height of the cross-head while the available energy is determined by the weight of the cross-head. Weight can be added to the cross-head to increase the energy at impact. For these tests the cross-head height was 30 in. and the weight was 625 lbs. The corresponding impact velocity was 152 in./sec. At this velocity, the specimen would theoretically be deflected 0.152 in. in 1 millisecond, which is more than enough to induce tearing. The actual deflection rate of the specimen was lower, as will be discussed in a later section. The loading rate for these tests was approximately 3 x $10^6$ lb/sec, which translates into a stress intensity factor rate for the linear part of the load-time record of 3.6 x $10^4$ ksi√in/sec (for SE(B) with a/W = 0.58).

The three-point bend fixture used for these tests is shown in **Figure 11**. This fixture is designed to limit the deflection of specimen in order to indirectly control the amount of crack extension. The specimen rests on fixed supports rather than rollers because there was concern that rollers would fly out on impact. Teflon tape was placed between the specimen and the supports to minimize friction. The specimen is prevented from bouncing on impact by bounce restraints attached to the supports. Without these restraints, the specimen ends would bounce off the supports and the deflection could not be controlled. The restraints allow the specimen to pivot, but not to lift off the supports. Load is applied to the specimen through impact of the cross-head tup with the tower. An aluminum cone placed between the tower and the tup damps out much of the ringing that occurs on impact. There is some reduction in loading rate, but this is more than offset by the improved quality of the measurements. The cone is made from 1100 Aluminum (O temper), which has a very low yield strength and low strain hardening. The tower and stop-blocks are designed to limit the deflection of the specimen.

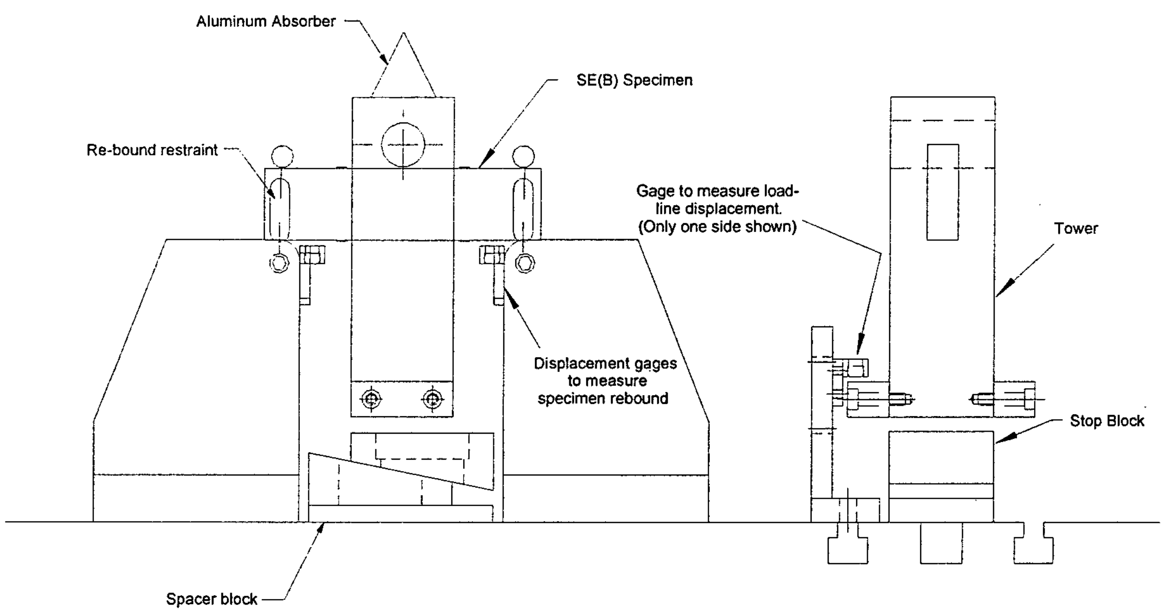


**Figure 11. Bend fixture with displacement limits for drop tower testing.**

The stop block consists of three pieces, a flat spacer block and two tapered blocks. The tapered blocks have a finely serrated surface to allow small, precise adjustments in the height and to prevent them from slipping when hit. Each serration represents approximately 0.004 in. vertical displacement. The tapered blocks are adjusted to achieve the desired load-line displacement between the tower and the stop block. A bolt (not shown) attaches the tapered blocks to the spacer plate to hold the tapered blocks in place during the test.

There are 5 measurements made during the test; specimen load, two load-line (LL) displacements and two support-point displacements. Displacements were measured using capacitive gages with a 0.2 in. full scale range and amplifiers with a 3.5 kHz cut-off frequency (-3 db). Data was recorded on a digital oscilloscope at a sampling rate of 4 micro-seconds per point (250 kHz). This sampling rate was more than adequate to ensure fidelity of the captured signals.

The LL displacement of the specimen is recorded remotely, that is, at a location not directly on the specimen. The tower on the right side of **Figure 11** shows a pair of wings on the bottom of the tower. These are the target surfaces used to measure LL displacement. The LL gages (only one is shown on left side of tower in **Figure 11**) are mounted on separate fixtures attached to the base of the drop tower. The gages are positioned away from the specimen and on the base, rather than the tower, to isolate them from the acceleration and shock of impact. The displacement being measured is actually that of the tower, and not the specimen. However, the tower is designed to fit tightly around the specimen so that the two move together. Since the width dimension for all the specimens was not exactly the same, provisions had to be made to adjust the slot width to accommodate the dimensional tolerance. This was done by machining flats on the loading pin of various depths ranging from 0.005 in. to 0.020 in. To obtain a tight fit, the specimen was placed in the slot and the pin was rotated to find the flat providing the tightest fit.

Ideally, the specimen and the various fixture parts will be square, parallel and perpendicular so that the bottom surface of the tower is parallel to the stop block surface, and the tower will travel straight down without tilting. In reality, the tower does tilt, so two LL gages are used to determine the average LL displacement. With careful alignment, the difference between the two measurements can be kept quite small.

While the remote location of the LL cap gages is necessary to protect the gages, it can also be a source of error in the measured LL displacement. This error is mostly a result of load train compliance and brinnelling of the specimen at the loading point. Load train compliance error comes from deformation of the supports and the tower. The dimensions of the tower and supports were designed to make them very stiff, and thereby minimize this error. Also, the deformation of the tower tends to cause a negative error, while support deformation causes a positive error, so the two tend to cancel each other out. The other source of error, brinnelling, is caused by the contact stresses at the loading point causing local plastic deformation in the specimen. This deformation causes the measured deflection to be slightly larger than the actual specimen LL displacement. This error was minimized somewhat by using a loading pin with a flat contact surface, thereby reducing the contact stresses and the amount of plastic deformation. The error involved in measuring LL displacement remotely was not quantified in this study.

Another problem that was found during testing was overshoot. The actual maximum displacement of the tower was consistently higher than the set LL displacement (determined by measuring the gap between the tower and the stop block). The difference is illustrated in **Figure 12.** In the figure, the data for each weldment are fit with a straight line using linear regression. For the GOS tests, the overshoot was fairly constant at about 0.008 in. It did not vary much with set displacement, as is indicated by the slope of nearly one. The offset for the GOT tests was higher, at about 0.015 in. Although the slope of the GOT line is also higher, this is probably a result of scatter in the data at large displacement, and therefore is not considered significant. The overshoot may be partly due to difficulties in measuring the gap height, and partly due to settling of the stop block under load. The higher overshoot in the GOT specimens may be related to the higher maximum loads obtained in those tests. During the course of testing, this overshoot was accounted for by estimating the amount of overshoot from previous tests.

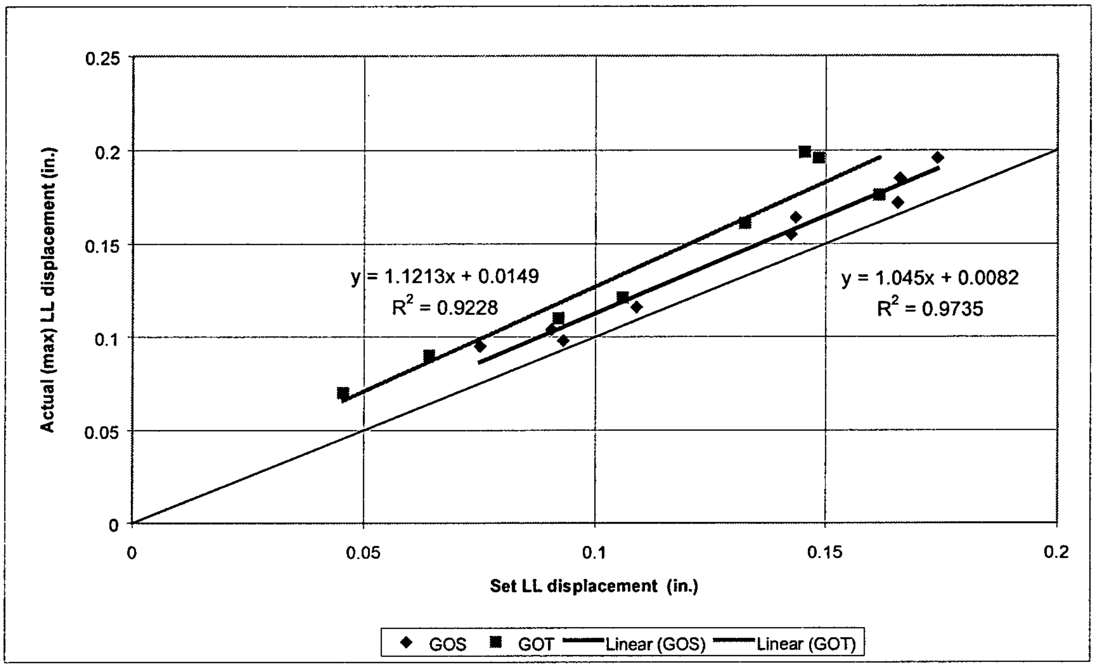


**Figure 12. Actual maximum load-line displacement versus set load-line displacement for GOS and GOT dynamic SE(B) tests**

## DATA ANALYSIS PROCEDURE

### Quasi-static short-crack SE(B) tests

The analysis procedures in ASTM E1737 [7] cover homogeneous specimens with pre-crack lengths in the range of 0.45 <= a/W <= 0.70. The specimens for these tests were from under-matched welds, which are not homogeneous, and the initial a/W ranged from 0.167 to 0.188. Therefore, new equations had to be obtained for determining compliance and J.

Various studies have shown that the yield strength mismatch between base metal and weld can have an influence on the plastic part of J when the crack tip is located in the weld metal. This influence has been quantified in terms of the weld fusion line margin, which is the perpendicular distance from the crack tip to the fusion line divided by the crack length ($L_{crack}$/a, see **Figure 13**). Mercier [11] found that for fusion line margins of greater than 1.5 in short-crack specimens, the influence of the neighboring base metal is negligible, and the specimen may be analyzed as though it were homogeneous with weld metal properties. At smaller margins, the error in J calculated using the homogeneous J equation increases as the margin decreases. The error also varies with crack growth, reaching a maximum at about $\Delta a/W = 0.025$. For margins ranging from 1.3 to 0.6, which covers the specimens tested in this study, the homogeneous J equation underestimates J by a maximum of about 4 to 16%, respectively, at $\Delta a/W = 0.025$. The error is much less near initiation, which is the focus of this study, therefore the following analysis does not consider the effect of fusion line margin in calculating J. The specimens are treated as though they are homogeneous with weld metal properties.

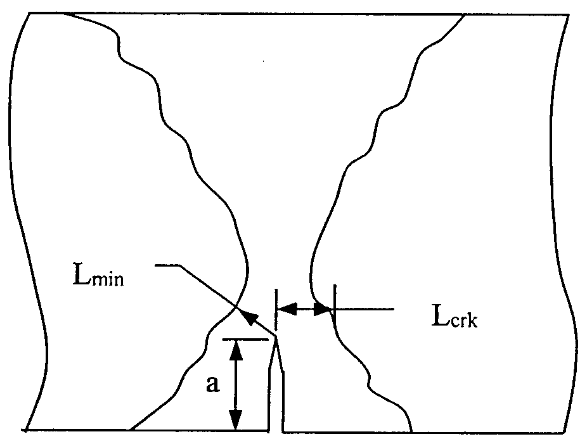


**Figure 13. Cross-section of double-V weld showing definition of $L_{crk}$ and a.**

Equations for homogeneous short-crack specimens have been developed by Sumpter [12] and Joyce [13]. These equations do not consider the influence of the weld on J. Joyce developed the following equation for crack length estimation from compliance by reverse fitting the equation by Tada [14] that gives compliance as a function of crack length.

$$\frac{a}{W} = \left[1.01878 - 4.5367u + 9.0101u^2 - 27.333u^3 + 74.4u^4 - 71.489u^5\right] \qquad (1)$$

where:

$$u = \frac{1}{1 + \sqrt{\frac{BWE'C}{S/4}}}$$ and C is the compliance measured at the notched edge.

This equation is accurate to within ±0.06% for a/W values from 0.05 to 0.45. For a/W greater than 0.45 the equation in ASTM E1737 is used.

Sumpter developed the following equation for the eta factor for SE(B) specimens with a/W < 0.282.

$$\eta = 0.32 + 12\left(\frac{a}{W}\right) - 49.5\left(\frac{a}{W}\right)^2 + 99.8\left(\frac{a}{W}\right)^3 \tag{2}$$

This $\eta$ is used along with the plastic area under the load vs. load line displacement curve to calculate the plastic part of J. The following equation from E1737 is used to calculate J.

$$J_{pl(i)} = \left[J_{plk(i-1)} + \left(\frac{\eta_{(i-1)}}{b_{(i-1)}}\right)\left(\frac{A_{pl(i)} - A_{pl(i-1)}}{B_N}\right)\right] \cdot \left[1 - \gamma_{(i-1)}\left(\frac{a_{(i)} - a_{(i-1)}}{b_{(i-1)}}\right)\right] \tag{3}$$

where:

$$\gamma_i = \left[\eta_i - 1 - \frac{b_i}{W}\frac{\eta_i'}{\eta_i}\right] \quad \text{and} \quad \eta_i' = \frac{d\eta_i}{d(a_i/W)} \tag{4}$$

For a/W ≥ 0.282, $\eta = 2.0$ and $\gamma = 1.0$. The only modifications made to the E1737 analysis procedures were in the equations for calculation of crack length and $\eta$. In all other respects the procedures given in E1737 were followed in the analysis.

**Dynamic SE(B) tests**

The analysis of the dynamic tests was much more complicated than the quasi-static tests because there is no real-time measurement of crack extension during a dynamic test. Crack extension must be inferred from other measurements. The following sections discuss the procedures used to infer crack extension using the Normalization Method, and the problems associated with that method.

As mentioned previously, the displacements were measured using capacitive displacement transducers. The operating principal of these transducers is based on converting the capacitance of a variable air gap into a 0 to 10 volt dc signal. Since generation of capacitance requires an ac current, the gages are excited with a 15 kHz carrier wave. This carrier frequency is removed from the return signal by a demodulation filter in the signal conditioner. This filter has a –3 db cut-off frequency of 3.5 kHz, consequently, signals with frequency components above 3.5 kHz will be attenuated. The main signal of interest in these tests has a rise time of about 3 ms. This translates into a frequency of about 83 Hz, which is well below the cut-off frequency. Therefore, the frequency response of the signal conditioner is sufficient for this application, and the main signal of interest will not be attenuated by the demodulation filter.

Unfortunately, the demodulation filter introduces a frequency dependent phase shift into the demodulated signal. This phase shift shows up in the data as a time delay. When the data is plotted as load versus displacement, the time delay in the displacement causes a curvature in the initial part of the plot, which should be linear, and loops in any rebounds. The initial loading should be linear because compliance is constant for fixed crack length, and crack length is not changing early in the test. Rebounds should also be linear because they are a partial elastic unloading. By time-shifting the data, it is possible to correct for this delay. The amount of time shift is determined based on what is required to make the initial loading linear. After some trial and error, a value of -100 micro-seconds was found to work well with all of the tests (The negative value indicates that displacement is being shifted back in time). A typical example is shown in **Figure 14**. The uncorrected data shown in (a) has a high initial slope and a loop when the tower contacts the stop block. A –100 micro-second time shift eliminates the initial high slope and makes the rebound almost linear.

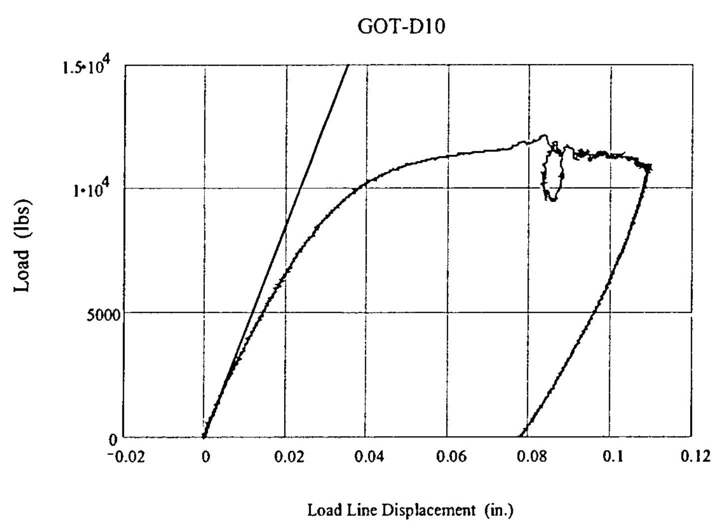


(a)

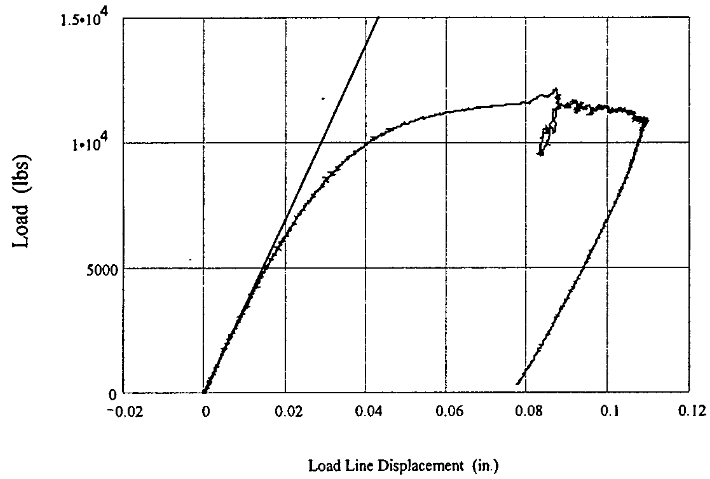


(b)

**Figure 14. Effect of time delay on Load-Displacement trace. (a) Before correction for delay. (b) After correction for time delay.**

Once the displacement data is time shifted, the next step is to extract crack extension from the load-displacement data. One way to do this is to use a method called Normalization. According to this method, the load for a particular specimen geometry can be expressed as a separable function of crack length and plastic displacement.

$$P(a, v_{pl}) = G\left(\frac{a}{W}\right)H\left(\frac{v_{pl}}{W}\right) \tag{5}$$

The crack length function, G, accounts for specimen geometry and is different for each specimen type. The plasticity function, H, is a function of the material flow behavior (yield strength and strain hardening characteristics). The dependence on crack length can be removed by defining a normalized load.

$$P_N = \frac{P}{G} = H\left(v_{plN}\right) \tag{6}$$

Where $v_{plN}$ is the normalized plastic displacement. The curve defined by H is a function of material flow properties and is independent of geometry or crack length. Load-displacement curves can be generated for fixed crack lengths using equation 5 if the plasticity function and the geometry functions are known. As shown in **Figure 15**, any deviation of the load-displacement behavior in a test from the fixed crack length curve is an indication of crack extension. The premise of this method is that the amount of deviation can be used to infer crack extension. At the point where the dashed curve crosses the curve for crack length $a_1$, the crack length is equal to $a_1$.

There are practical limits to the application of this method that result from the assumption of separability. For instance, the plasticity function does not account for net section yielding. This places an upper limit on the plastic displacement of the specimen. This would not impose a restriction as long as crack extension begins well before limit load (net section yielding). There are other more restrictive limitations that will be presented in the ensuing discussion.

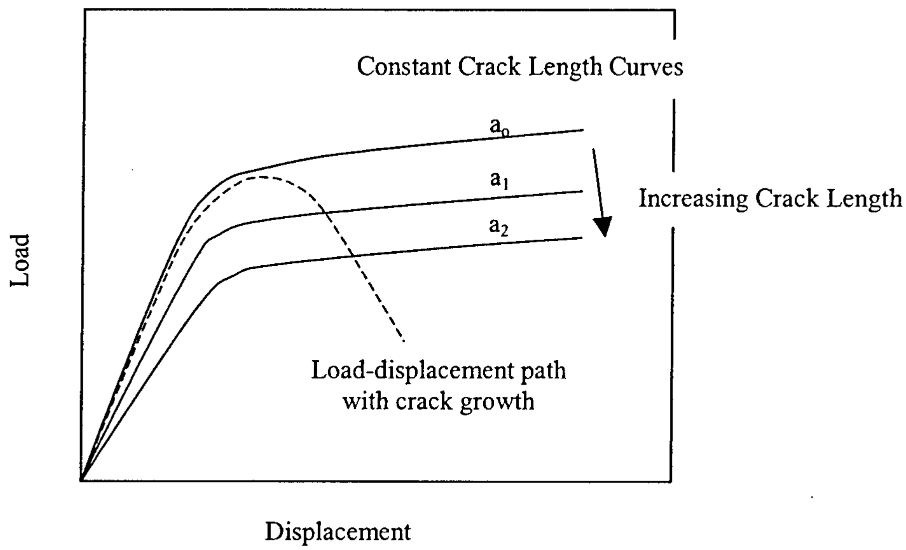


**Figure 15. Illustration of crack length prediction using method of Normalization**

*Procedure used for Normalization Analysis*

The data for dynamic specimen GOT-D06 will be used to illustrate the analysis procedure. A printout of the MathCAD worksheet used for the analysis is included in Appendix A.

**1. Data Sampling** – A typical load-displacement record from a test is shown in **Figure 16**. The sampling rate of the data acquisition system was such that the data records from the tests typically had 3,000 to 4,000 points. This was a cumbersome amount of data for this analysis, so the record was sampled using a displacement increment of 0.001 in. to reduce the amount of data to about 100 or 200 points. The sampling algorithm searches the data set sequentially and selects the point that exceeds the displacement threshold. The threshold is then incremented by 0.001 in. and the process is continued. Because the algorithm selects only points with increasing displacement, all unloadings are removed from the sampled data set. The point of maximum load-line displacement is retained in the sampled data set as the last point. The load-displacement record for GOT-D06 after sampling is shown in **Figure 17.**

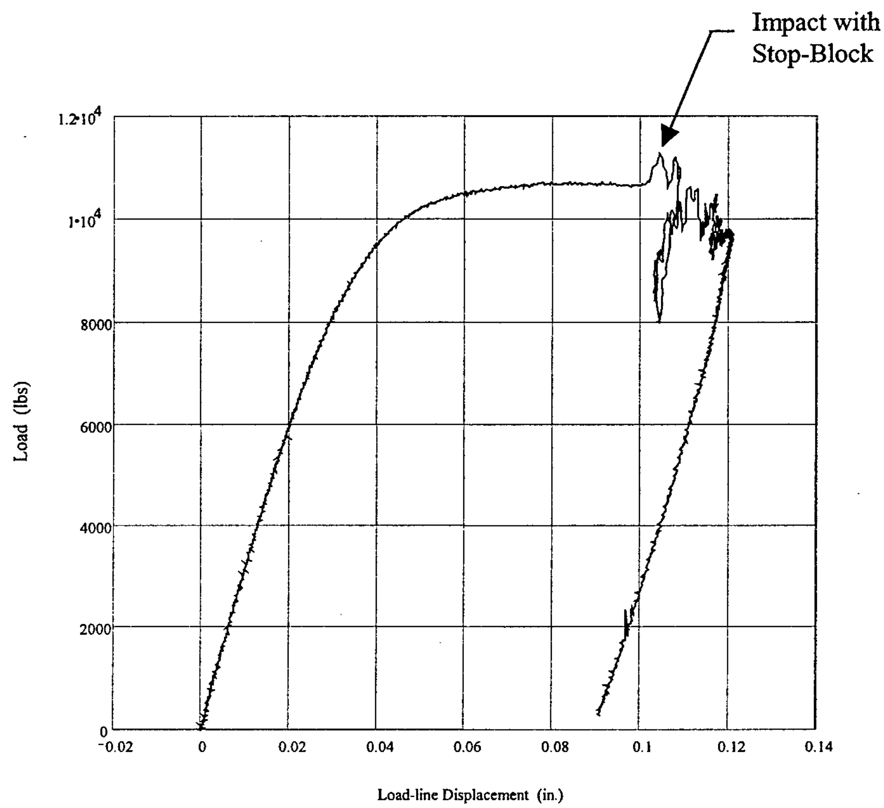


**Figure 16. Load-displacement data for GOT-D06.**

**2. Crack Extension Estimate** – Crack length for each point in the data file is estimated assuming only blunting occurs.

$$a = a_o + \frac{J}{2\sigma_Y} \quad (7)$$

where $a_o$ is the measured initial crack length and $\sigma_Y$ is the flow strength (average of yield and ultimate). For this estimate, J was calculated using the equation:

$$J = \frac{K^2}{E'} + \frac{\eta A_{pl}}{Bb} \tag{8}$$

where $K$, $\eta$ and $b$ are calculated using $a_o$ and $A_{pl}$ is calculated using:

$$A_{pl} = A_{total} - \frac{C\left(\frac{a_o}{W}\right) \cdot P^2}{2} \tag{9}$$

where $A_{total}$ is the total area under the load-displacement trace up to the point being evaluated, $C$ is the compliance for the initial measured crack length and $P$ is the load.

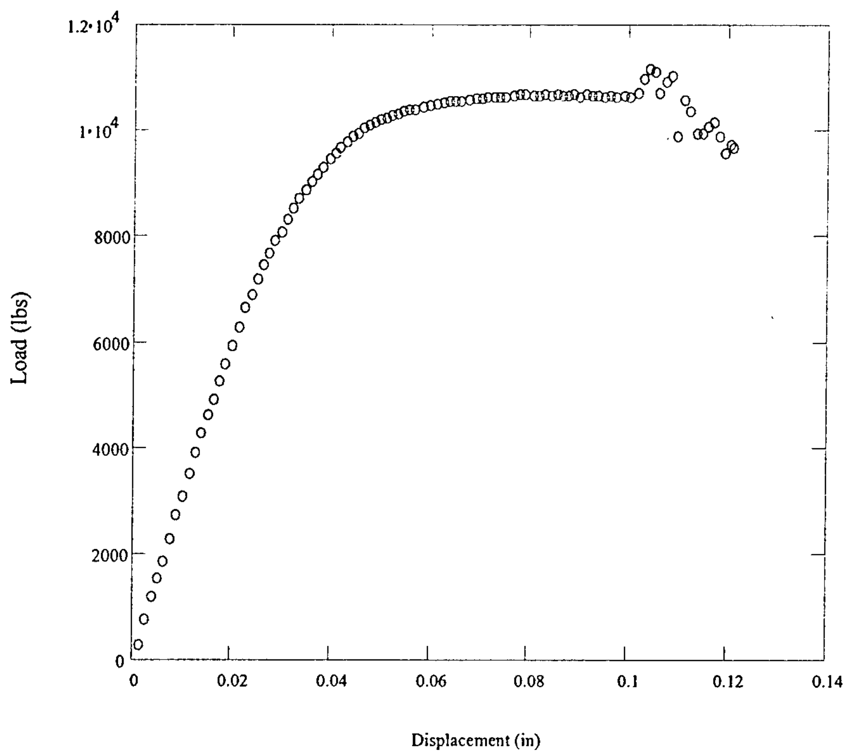


**Figure 17. Load-displacement data for GOT-D06 after sampling.**

3. **Normalize load and displacement** – Once the crack length is estimated, the data is normalized using equation 6, where:

$$G = WB\left(\frac{W-a}{W}\right)^{\eta} \tag{10}$$

$$v_{plN} = \frac{v - P \cdot C\left(\frac{a}{W}\right)}{W} \tag{11}$$

$a$ - Estimated crack length from step 2.

The final point (maximum load-line displacement) is normalized using the measured final crack length. This point becomes the anchor point for the next step.

4. **Data selection for fit** – A tangent is drawn from the anchor point to the normalized load-displacement curve, as shown in **Figure 18**. The point of tangency defines the upper limit on the data selected for the plasticity (H) function fit. The lower limit is somewhat arbitrarily set at $v_{plN} = 0.001$. The reason for the lower limit is to eliminate data where $P_N$ is increasing with little or no increase in $v_{plN}$. These points tend to bias the fit by forcing it to be nearly vertical at low $v_{plN}$. This is also the region where the plastic displacement is very small compared to the total displacement, and large errors can result from small errors in estimating compliance. It is best to avoid this region. The anchor point is then added to the selected data to be fit.

5. **Fitting the Plasticity Function** – The data selected in step 4 is then fit with an equation of the form:

$$P_N = \frac{O + Lv_{plN} + Mv_{plN}^2}{N + v_{plN}} \tag{12}$$

This functional form is referred to as the LMNO function. It was originally proposed by Landes [6] as the LMN function. The fourth coefficient, O, was added by Joyce [16] to account for the fact that $P_N$ is not zero at zero plastic displacement. When $v_{plN}$ is large relative to N and O, the equation becomes nearly linear. This is consistent with observations of true stress-true strain curves at large strain. The fit was done using TableCurve from Jandel Scientific [15]. The selected data and the resulting fit are shown in **Figure 19**.

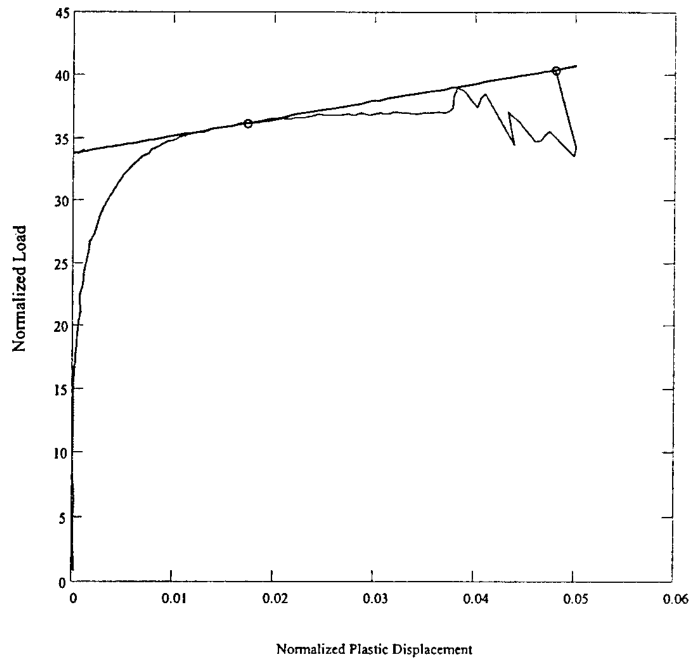


**Figure 18. Normalized load-displacement data showing tangent construction for determining upper selection limit.**

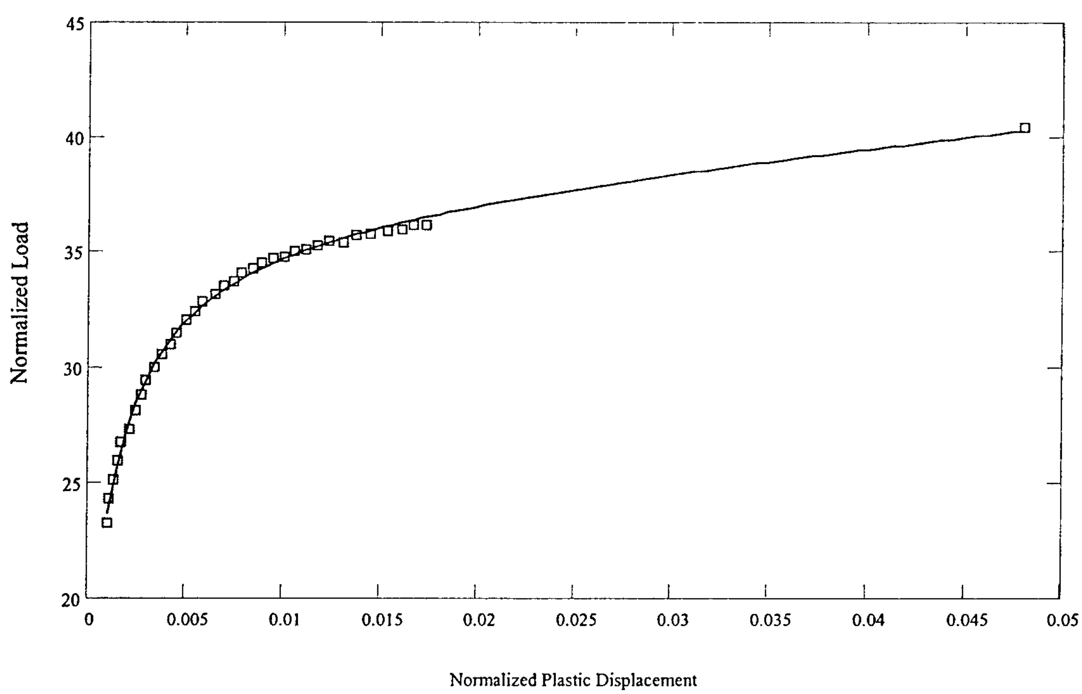


**Figure 19. Normalized data and Plasticity function fit.**

6. **Calculation of Crack Length** – The next step is to move the normalized load-displacement points onto the H function by adjusting the crack length. This is done using an error minimization algorithm where the error is the difference between the normalized load and the H function at the $v_{plN}$ of the point in question. Crack lengths are calculated in this way for points with $v_{plN} > 0.001$. The adjusted points are shown along with the data selected for the fit in **Figure 20**.

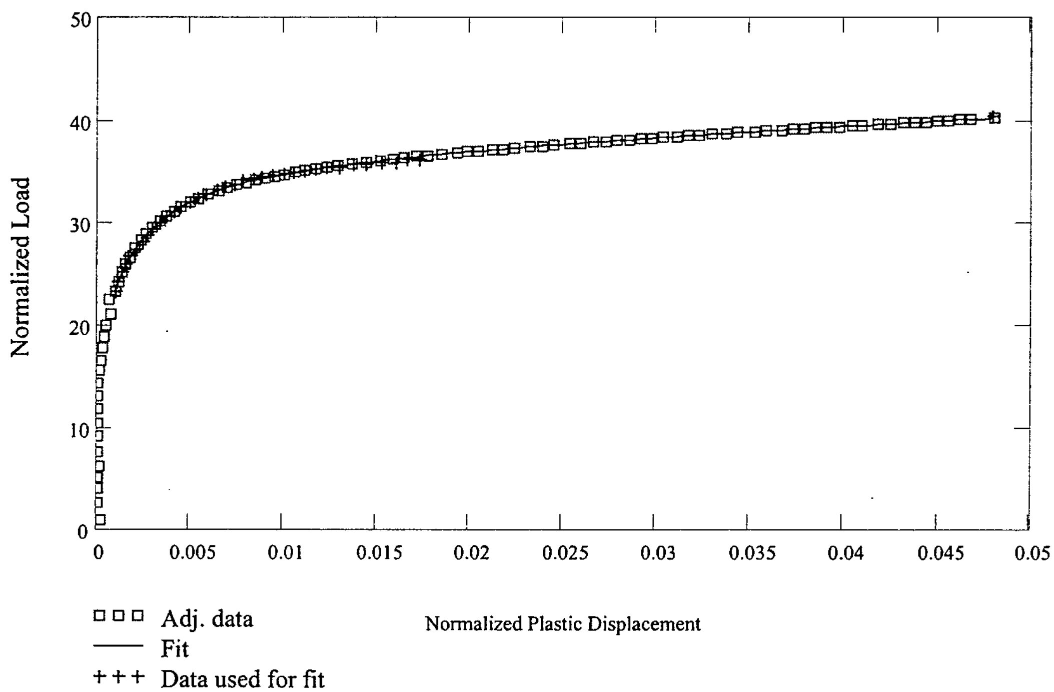


**Figure 20. Normalized data adjusted to the Plasticity Function.**

7. **Calculation of J** – Once the load, displacement and crack length are known, then J and Δa can be calculated for every point. J is calculated using equation 3. The use of the η for a homogenous specimen is justified based on the work of Kirk and Dodds [2], where it was shown that the presence of the weld does not effect the calculation of J for 20% mismatch and a/W = 0.5. The resulting J-R curve is shown in **Figure 21**. The calculated J and Δa at the anchor point is indicated in this graph with a "+".

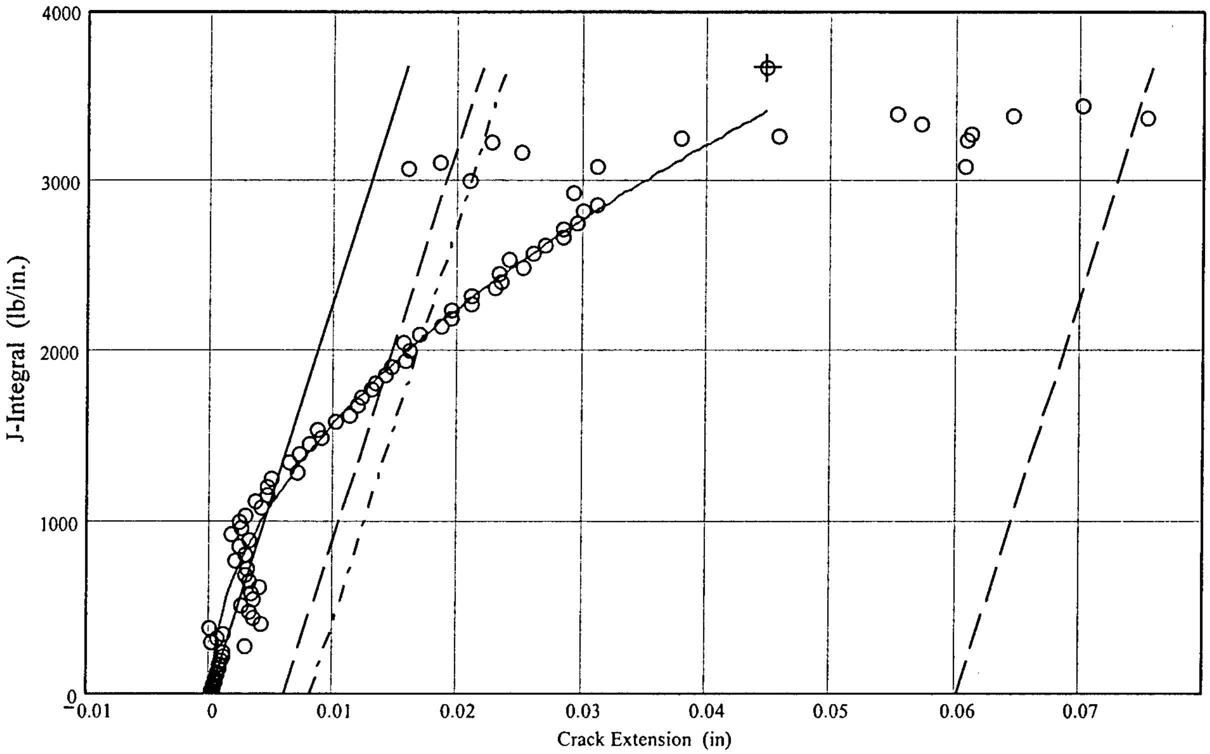


**Figure 21. Dynamic J-R curve from Normalization.**

Note that the crack length for points with $v_{plN} < 0.001$ are not corrected, so they lie right on the blunting line. Note also the large amount of scatter in the data above a J of about 3,000 lb/in. This scatter is due to high frequency noise in the load-displacement signal at the point of impact with the stop block (see **Figure 16**).

*Observations on Normalization Method*

The Normalization Method is not particularly robust because there are many variables involved, and the results are very sensitive to the values chosen for those variables. The basic problem is that data from the early part of a test, and the end point, are used to interpolate what happened during the test. The results are only as good as the function used for the interpolation. The appropriate functional form for the interpolation is not known, and the coefficients of the fit are based on sparse data at the ends of the data range. The following discussion will focus on specific parts of the process and how they influence the final result.

The first challenge in performing the interpolation is to select the data to be used in the interpolation. Ideally, points should be chosen where the load, displacement and crack length are known so that the calculated normalized loads and displacement are correct.

However, the only points where crack length is known for certain are at the beginning and end of the test. An attempt is made to increase the amount of data available for the fit by assuming that early in the test the only crack growth is due to blunting. Consequently, for materials where crack growth starts with little or no blunting or plastic deformation, the Normalization Method will not work. Experience indicates that ductile tearing starts at or before maximum load. As ductility decreases or specimen size (constraint) increases, the point of ductile tearing initiation occurs earlier in the test relative to maximum load. The challenge is to estimate the point of ductile tearing initiation so that only data up to this point is used in the fit. After initiation, the crack length is not known and the normalized data is not accurate. Using this data biases the fit since the actual crack extension is greater than the assumed blunting. The net result is that crack extension is under-estimated and $J_{Ic}$ increases.

In this analysis, the point of ductile tearing initiation is estimated by drawing a line from the final point (where load, displacement and crack length should be known) tangent to the normalized load-displacement curve (Refer to steps 2 and 3 and **Figure 18** above). Initiation is assumed to correspond to the point of tangency. This point is very sensitive to the position of the final point, especially when the normalized load-displacement curve is almost parallel to the tangent.

The final point is often referred to as the anchor point because the crack length is known and the plasticity function should go through this point. The accuracy of the final point is only as good as the measurements of final load, displacement and crack length. In dynamic testing load and displacement are not so easily measured. In these tests, load was measured directly on the specimen and displacement was measured remotely. Each of these measurements has some error associated with it. For the load, the specimen is calibrated up to the maximum pre-cracking load, which is well below the maximum load in the test. Extrapolation of the load calibration is one potential source of error. Another potential source of error in specimen load measurement is crack growth and plasticity. Earlier studies have shown that these effects tend to cause load to be under-estimated. The error from a quasi-static test of a compact tension specimen where load was measured with a conventional load cell and using strain gages on the specimen is shown in **Figure 22**. In this figure, the percent error is the difference between the load cell and specimen load divided by the load cell, therefore, a positive percent error indicates the specimen load is under-estimating the true load. The maximum error approaches 4% at 0.21 in. of crack extension, so this is not expected to be a large source of error.

These tests had the additional complication that when the tower hit the stop-block it caused ringing in the load signal (see **Figure 16**). This ringing also tended to cause under-estimation of the final load. Consequently, in the analysis of these tests, the anchor point sometimes fell below the normalized load-displacement curve, as shown in **Figure 23** (Compare with **Figure 18**). This is clearly not accurate because the plasticity function should be monotonically increasing, and should always fall on or above the estimated curve based on crack growth by blunting alone. Some judgement was required in determining final load for these tests. An example of this is given in **Figure 24**. In this case, the final load was estimated to be 8% higher than measured based on extrapolation of the loading and unloading portions of the curve before and after the impact. It would be preferable to minimize the errors in load measurement, and thereby eliminate the need to correct the final measured load.

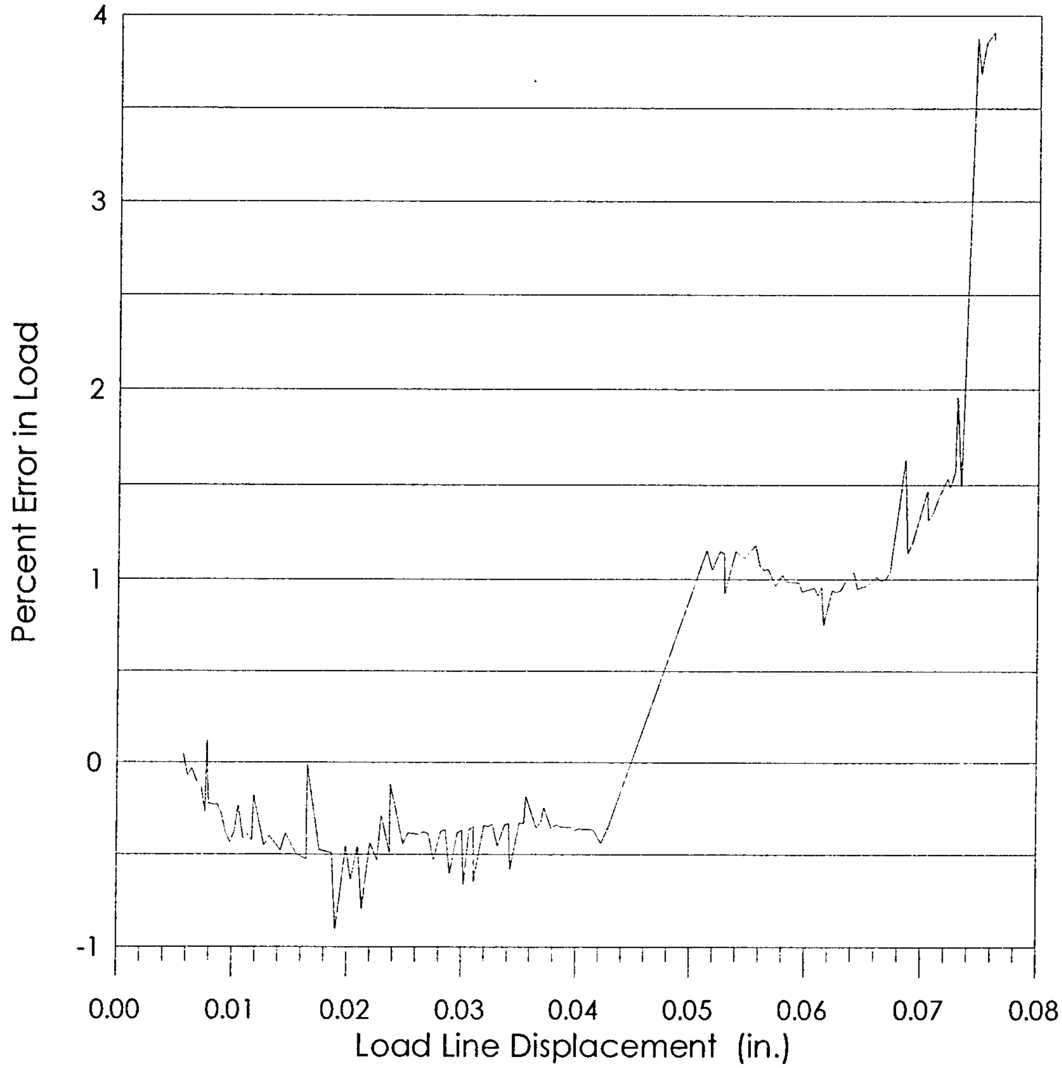


**Figure 22. Effect of crack growth and plasticity on error in specimen load measurement using strain gages for Compact Tension specimen (ductile crack growth during test was 0.21 in.)**

Another variable that has a significant influence on the analysis is initial specimen compliance. If the initial load-displacement slope is not very close to the theoretical compliance, the resulting initial plastic displacements will either be negative, or they will be too large. Since one of the selection criteria for the fit is $v_{pIN} > 0.001$, errors in estimated compliance can significantly influence the resulting fit. Displacement offsets in the data (non-zero displacement at zero load) have a similar effect. In this analysis, the initial slopes did not consistently match the theoretical compliance. A compliance adjustment factor, $\lambda$, was used to match the initial slope. The discrepancy in slope may be due to slight errors in calibration or time-shifting.

As mentioned previously, the functional form used for the plasticity function in this analysis was the LMNO function. There is no general agreement on what the form of the plasticity function should be, or whether there is a universal form that works for all materials. Landes and Donoso [17] showed that the plasticity function can be related to the tensile true stress-true strain behavior of the material. If this is the case, then it should be possible to determine the appropriate functional form from the true stress-true strain curve. However, in this study the LMNO function was found to work pretty well for the HY welds, so no attempt was made to find an alternative functional form. It is worth noting that there are many forms that could have been used to fit the data, some of which provided better fits based on correlation coefficients or F-statistics. Previous experience has shown that the form can have a significant effect on the resulting J-R curve, so the LMNO form should not be "forced" to fit the data if it is not appropriate.

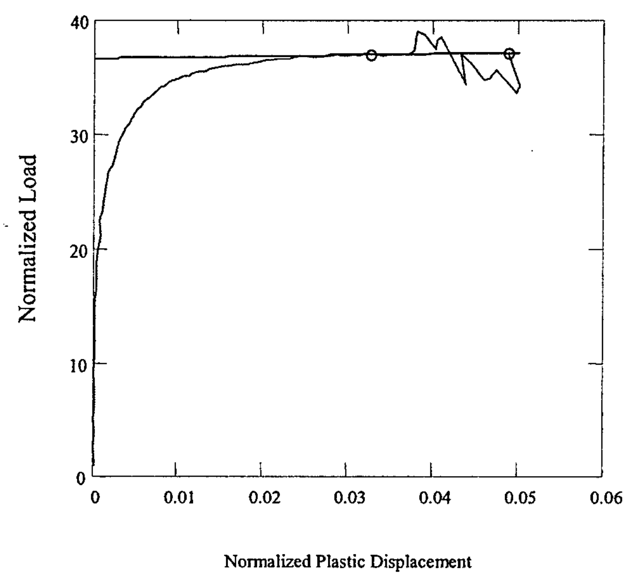


**Figure 23. Anchor point for GOT-D06 without final load correction.**

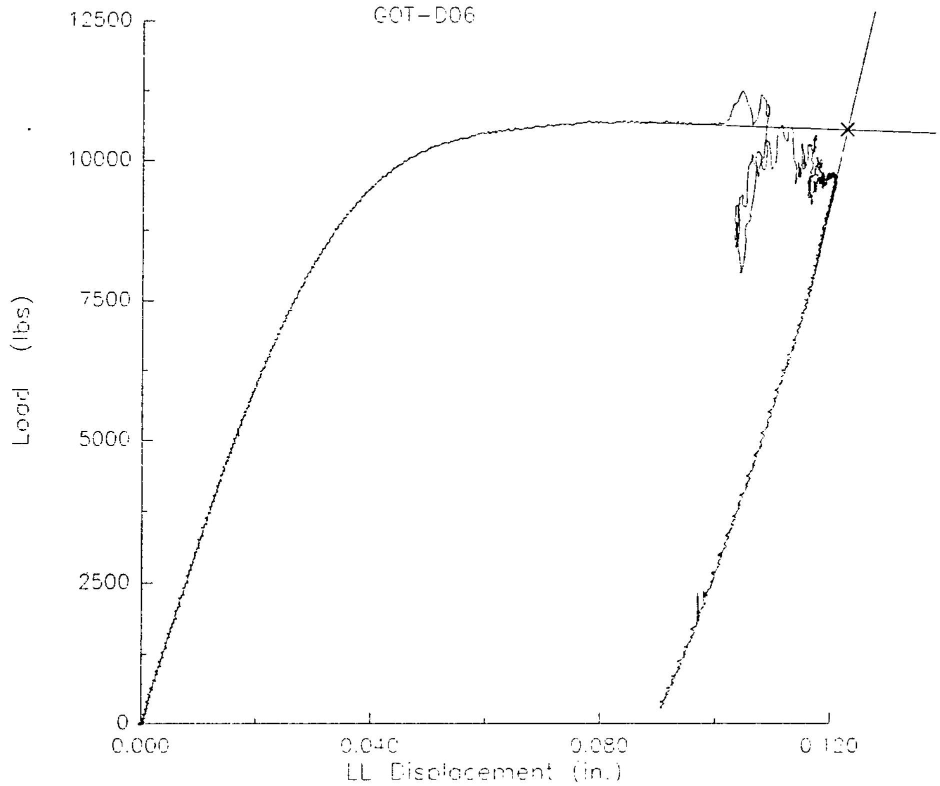


**Figure 24. Estimation of final load and displacement for GOT-D06.**

This naturally leads to the question, what constitutes a good fit? In general, the plasticity function should fit the data very closely, it should go through the anchor point, and it should not cut under the data in the vicinity of the "knee". The normalized load and displacement equations are not very sensitive to crack length, so large changes in crack length are required to make small changes in $P_N$ and $v_{plN}$. Increasing crack length increases $P_N$ and decreases $v_{plN}$, so shifting a point down and right decreases the crack length. Therefore, if the fit cuts below the data, the resulting crack length will be less than the initial crack length + blunting. This moves the J-Δa points to the left, thereby either moving them off the blunting line or under-estimating crack extension beyond blunting. This effect can be seen to a small degree in **Figure 19** and **Figure 21**. The data points that fall to the left of the blunting line in **Figure 21** are the ones that fall below the fitted curve in **Figure 19**. It is particularly important that the fit be close to the data when the curve is steep. This is because crack length has more effect on $P_N$ than $v_{plN}$. Increasing crack length moves a point more up than left. When the curve is steep, a point may appear close but will require a relatively large increase in crack length to shift it onto the curve.

With all of these reservations about the application of the method, one might question the usefulness of Normalization. Without any additional information, it is questionable how accurately one can determine J-R curves using this method. However, there are ways to improve the accuracy of the method by introducing additional information. If the correct shape of the plasticity function were known, this would lend confidence in the resulting J-

R curve. If it were possible to obtain intermediate points where load, displacement and crack length were all known, then the shape of the function could be verified by checking that it goes through these known points. These intermediate points can be obtained by conducting multiple tests with different final crack lengths/displacements on otherwise identical specimens. The test technique is similar to the traditional multi-specimen R-curve, where multiple specimens with different final crack extensions are used to determine $J_{Ic}$. However, in this case, multiple specimens are used to generate multiple J-R curves, and the anchor points for each test serve to verify the shape of the plasticity function. It is also possible to combine the anchor points for all of the tests and use this anchor point set, along with the selected data for each test, to perform the fit provided the true plasticity function is the same for all of the specimens. Weighting could be applied to improve the fit to the anchors. An example of this is shown in **Figure 25** for dynamic specimen GOT-D04. The normalized load-displacement data is combined with the anchor points from 4 other tests before fitting. The anchor points have been given a weight of 5 while the other points have a weight of 1. The fact that all of the anchor points fall within the 90% prediction interval for the fit gives confidence that the LMNO function is an appropriate form for this material.

The work of Landes and Donoso [17] indicates that there exists a true plasticity function for a particular material. Ideally, the plasticity functions derived from a series of replicate tests would all fall on top of one another. Practically speaking, this is not the case. There are slight variations from test to test, or specimen to specimen, which cause the fitted plasticity functions to be slightly different. The sensitivity of crack length to $P_N$ and $v_{plN}$ prevents one true plasticity function from being used to analyze all the tests. However, if there are large differences in the plasticity functions for replicate tests, this would be cause to start looking for other contributing factors, such as orientation, microstructure or temperature, that could effect the plasticity function. A comparison of the plasticity functions for the dynamic GOT specimens is given in **Figure 26**. Most of the tests were conducted close to 100°F except for D02, which was tested at 140°F. The plasticity functions for the lower temperatures all fall fairly close together, while the curve for the higher temperature is noticeably below the others. For this material, temperature appears to have an effect on the plasticity function. Other factors may also effect the plasticity function, such as microstructure and residual stress. Shown in **Figure 27** are the plasticity functions for 5 dynamic GOS tests conducted between 100°F and 110°F. Variations in local weld properties may be responsible for the difference between the curve for D07 and the others.

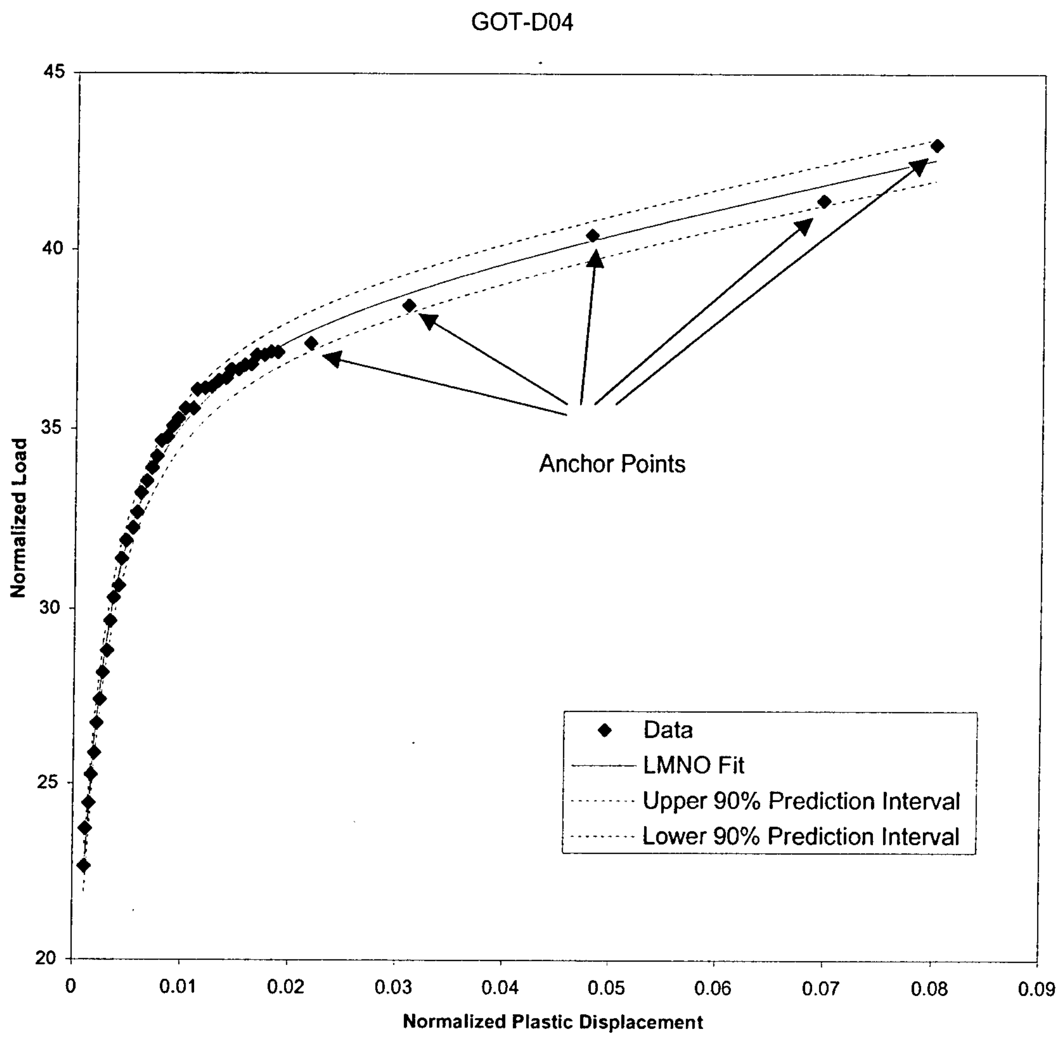


**Figure 25. LMNO fit of GOT-D04 with anchor points and prediction intervals.**

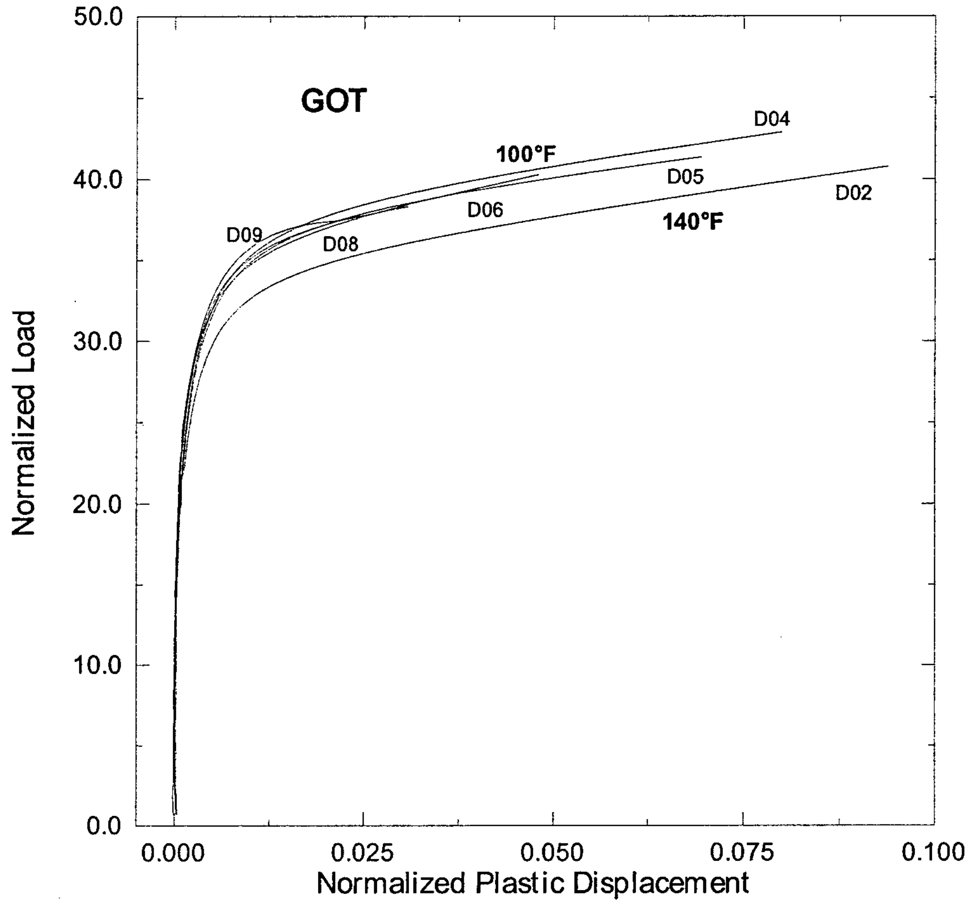


**Figure 26. Plasticity functions for dynamic GOT tests.**

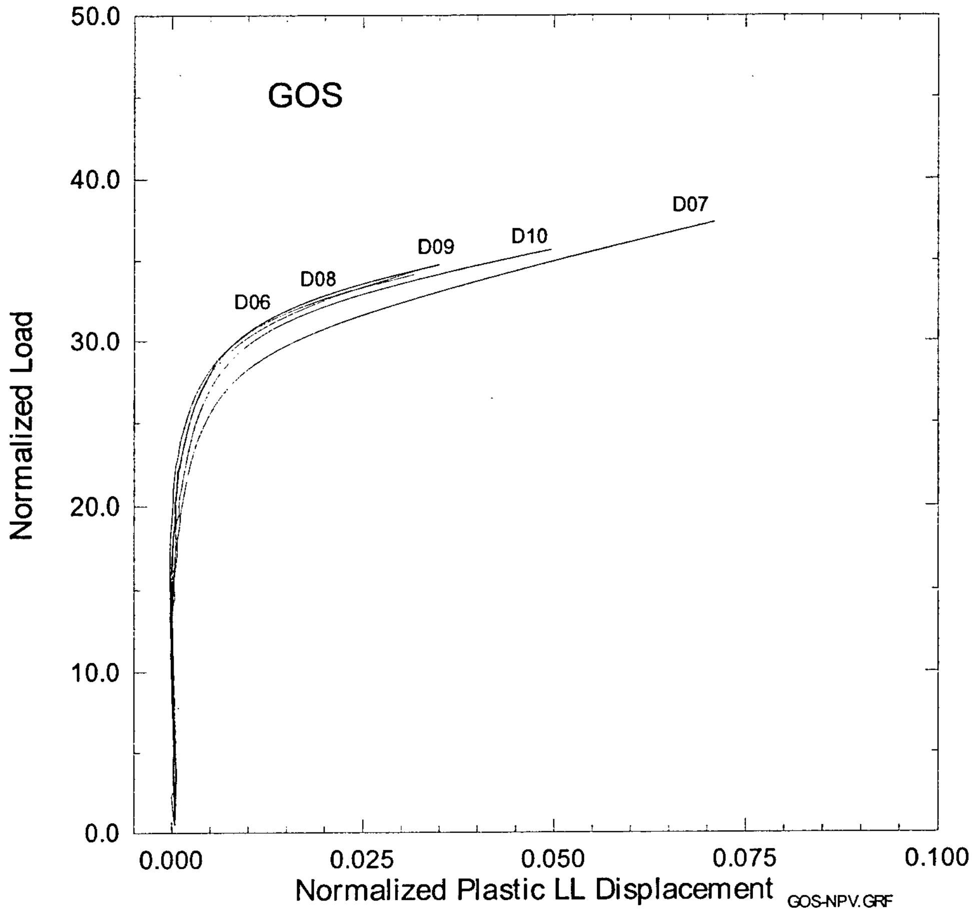


**Figure 27. Plasticity functions for dynamic GOS tests.**

## TEST RESULTS

### Tensile Tests

The results of the quasi-static and dynamic tensile tests are presented in Table 8. The effect of loading rate on yield strength, and the resulting under-matching percentages, are presented in Table 9 and Table 10. For the GOS weld there is about a 16% increase in yield strength under dynamic loading for both the base metal and the weld metal. Therefore, the under-matching percentage is about 20% and is insensitive to loading rate. For the GOT weld, the base metal yield is more sensitive to loading rate (+20%) than the weld metal yield (+12%). Consequently, increasing the rate increases the under-matching from 5% to 12% for this weld.

# Table 8. Tensile test results for GOS and GOT welds.

### BASE METAL

**GOS HY-80 Ti Mod, 20% Under-matched**

Quasistatic Tensiles

| ID | Modulus | $\sigma_{ys}$ (ksi) | $\sigma_{uts}$ (ksi) | %Elongation | %RA |
|---|---|---|---|---|---|
| **Baseplate** | | | | | |
| GOS-BP1 | 2.90E+07 | 102.9 | 120.1 | 25.1 | 74.0 |
| GOS-BP3 | 2.82E+07 | 99.1 | 117.6 | 25.1 | 71.0 |
| **Average=** | 2.86E+07 | 101.00 | 118.85 | 25.08 | 72.48 |

Dynamic Tensiles

| ID | Modulus | $\sigma_{ys}$ (ksi) | $\sigma_{uts}$ (ksi) | %Elongation | %RA |
|---|---|---|---|---|---|
| **Baseplate** | | | | | |
| GOS-BP4 | 2.92E+07 | 117.1 | 131.0 | 20.5 | 74.0 |
| GOS-BP5 | 3.05E+07 | 117.5 | 132.2 | 18.4 | 72.1 |
| **Average=** | 2.99E+07 | 117.30 | 131.60 | 19.45 | 73.05 |

### WELD METAL

Quasistatic Tensiles

| ID | Modulus | $\sigma_{ys}$ (ksi) | $\sigma_{uts}$ (ksi) | %Elongatioı | %RA |
|---|---|---|---|---|---|
| **Weld Top** | | | | | |
| GOS-WT1 | 3.04E+07 | 85.2 | 100.1 | 25.1 | 68.3 |
| GOS-WT2 | 3.03E+07 | 79.0 | 94.7 | 23.9 | 68.6 |
| **Average=** | 3.04E+07 | 82.09 | 97.41 | 24.47 | 68.45 |

Quasistatic Tensiles

| ID | Modulus | $\sigma_{ys}$ (ksi) | $\sigma_{uts}$ (ksi) | %Elongatioı | %RA |
|---|---|---|---|---|---|
| **Weld Bottom** | | | | | |
| GOS-WB1 | 3.03E+07 | 81.5 | 96.1 | 25.0 | 70.2 |
| GOS-WB2 | 2.80E+07 | 78.9 | 95.7 | 29.7 | 71.2 |
| **Average=** | 2.92E+07 | 80.16 | 95.91 | 27.34 | 70.70 |
| | | | | | |
| **All Weld** | | | | | |
| **Average=** | 2.98E+07 | 81.13 | 96.66 | 25.90 | 69.58 |

Dynamic Tensiles

| ID | Modulus | $\sigma_{ys}$ (ksi) | $\sigma_{uts}$ (ksi) | %Elongatioı | %RA |
|---|---|---|---|---|---|
| **Weld** | | | | | |
| GOS-WT3 | 2.33E+07 | 89.7 | 105.2 | 19.3 | 65.5 |
| GOS-WB3 | 3.17E+07 | 98.9 | 109.7 | 23.3 | 68.3 |
| **Average=** | 2.75E+07 | 94.30 | 107.45 | 21.30 | 66.90 |

**GOT HY-100 Ti Mod, 5% Under-matched**

### BASE METAL

Quasistatic Tensiles

| ID | Modulus | $\sigma_{ys}$ (ksi) | $\sigma_{uts}$ (ksi) | %Elongation | %RA |
|---|---|---|---|---|---|
| **Baseplate** | | | | | |
| GOT-BP1 | 2.88E+07 | 106.5 | 123.5 | 22.2 | 71.3 |
| GOT-BP2 | 2.92E+07 | 106.1 | 122.8 | 23.9 | 72.9 |
| GOT-BP3 | 2.90E+07 | 106.7 | 121.4 | 23.9 | 75.8 |
| **Average=** | 2.90E+07 | 106.43 | 122.54 | 23.32 | 73.34 |

Dynamic Tensiles

| ID | Modulus | $\sigma_{ys}$ (ksi) | $\sigma_{uts}$ (ksi) | %Elongation | %RA |
|---|---|---|---|---|---|
| **Baseplate** | | | | | |
| GOT-BP4 | 3.21E+07 | 129.6 | 139.2 | 19.1 | 72.5 |
| GOT-BP5 | 2.73E+07 | 127.6 | 137.6 | 17.7 | 71.3 |
| **Average=** | 2.97E+07 | 128.60 | 138.40 | 18.40 | 71.90 |

### WELD METAL

Quasistatic Tensiles

| ID | Modulus | $\sigma_{ys}$ (ksi) | $\sigma_{uts}$ (ksi) | %Elongatioı | %RA |
|---|---|---|---|---|---|
| **All Weld** | | | | | |
| GOT-WT1 | 2.87E+07 | 96.5 | 115.8 | 20.1 | 67.7 |
| GOT-WB1 | 2.88E+07 | 105.6 | 125.3 | 17.7 | 61.4 |
| **Average=** | 2.88E+07 | 101.03 | 120.55 | 18.89 | 64.52 |

Dynamic Tensiles

| ID | Modulus | $\sigma_{ys}$ (ksi) | $\sigma_{uts}$ (ksi) | %Elongatioı | %RA |
|---|---|---|---|---|---|
| **Weld** | | | | | |
| GOT-WT2 | 2.75E+07 | 110.2 | 120.2 | 20.7 | 69.6 |
| GOT-WB2 | 2.72E+07 | 115.3 | 120.2 | 25.5 | 71.9 |
| **Average=** | 2.74E+07 | 112.75 | 120.20 | 23.10 | 70.75 |

**Table 9. Summary of yield strengths for GOS Weld**

| | Quasi-Static Yield (ksi) | Dynamic Yield (ksi) | % Increase |
|---|---|---|---|
| Base Metal | 101.0 | 117.3 | 16.1 |
| Weld Metal | 81.1 | 94.3 | 16.3 |
| % Under-matching | 19.7 | 19.6 | |

**Table 10. Summary of yield strengths for GOT Weld**

| | Quasi-Static Yield (ksi) | Dynamic Yield (ksi) | % Increase |
|---|---|---|---|
| Base Metal | 106.4 | 128.6 | 20.9 |
| Weld Metal | 101.0 | 112.8 | 11.7 |
| % Under-matching | 5.1 | 12.3 | |

## Quasi-static Fracture Toughness Test Results

The results of the quasi-static fracture toughness tests on the GOT weld at 28°F are summarized in **Table 11**. The analysis records are provided in Appendix B. A "Q" in the specimen ID (GOS-Qxx) denotes a short-crack specimen and a "D" (GOS-Dxx) denotes a deep crack specimen. All but two of the tests ended with fracture instability (GOT-Q05 and –D01). The crack extension at instability varied from as small as 0.004 in. to 0.238 in. This is a large variation, but is not uncommon in welds. None of the J values at instability were valid $J_c$'s, either because they did not meet the size requirements, or there was too much ductile crack growth preceding instability. Only one valid $J_{Ic}$ was obtained, although based on the earlier discussion about the overly restrictive validity criteria for short cracks, GOT-Q03 could also be considered valid. The variation in $J_{Ic}$ is also quite large, although this too is common in welds. The last column in the table is the minimum distance from the crack tip to the fusion line, $L_{min}$ (see **Figure 13**). $L_{min}$ was not measured for GOT-D01 because fusion line margin has little effect on constraint of deeply cracked specimens.

The J-R curves for the 6 tests are shown in **Figure 28**. The J-R curve for specimen GOT-Q01 deviates from the rest because it exhibited an early instability followed by ductile crack growth. Otherwise, the J-R curves fall fairly close together. The large variation in $J_{Ic}$ is seen to be due in part to the steep slope in the initial part of the J-R curves.

In homogeneous SE(B) specimens deep cracks have higher constraint, and consequently exhibit lower J-R curves, than short cracks of the same material [10]. However, in these tests the short-crack specimens fall right in with the deep-crack specimen. This may be partly due to under-estimation of J for the short-crack specimens as a result of neglecting the effect of the weld fusion margin. It may also be due to the narrow fusion margin (Lcrk/a = 0.6 to 0.8) elevating the constraint of the short crack specimens [5]. The two specimens with the smallest $L_{min}$ (Q01 and Q02) cleaved early in the test, thereby indicating a condition of high constraint. The $L_{min}$ values for Q03 and Q05 are the same, and the J-R curves are close. The one specimen that clearly does not fit the trend is Q04, which has an $L_{min}$ close to Q03 and Q05, and yet the J-R curve is noticeably lower. Examination of the fracture surface on this specimen revealed a large amount of porosity in the weld. It is likely that the porosity decreased the tearing resistance, thereby lowering the J-R curve below that of the deep-crack specimen D01.

**Table 11. Results of Quasi-Static Fracture Toughness Tests at 28°F of GOT Weld.**

| Specimen | $a_o/W$ | $J_{Ic}$ (lb/in.) | Invalidity Codes[1] | $J_c$ (lb/in.) | Invalidity Codes[2] | Δa at Instability (in.) | $L_{min}$ (in.) |
|---|---|---|---|---|---|---|---|
| GOT-Q01 | 0.169 | | | 889 | i | 0.004 | 0.195 |
| GOT-Q02 | 0.175 | | | 1427 | i | 0.007 | 0.173 |
| GOT-Q03 | 0.171 | 3318 | a | 7491 | ii | 0.169 | 0.218 |
| GOT-Q04 | 0.167 | 1876 | *Valid* | 7119 | ii | 0.238 | 0.235 |
| GOT-Q05 | 0.188 | 2050 | a, b, c | | | *No instability* | 0.218 |
| GOT-D01 | 0.587 | 2428 | a, d | | | *No instability* | |

[1]Invalidity codes for $J_{Ic}$
(a) Initial crack curvature exceeds 5% of average
(b) Final crack curvature exceeds 5% of average
(c) Variation in crack extension exceeds 50% of average extension
(d) Error in crack extension prediction exceeds allowable limits
(e) Unacceptable data spacing for power-law fit
(f) Thickness or initial ligament < 25 $J_Q/\sigma_Y$

[2]Invalidity codes for $J_c$
(i) $B, b_o < 200\ J_{Qc}/\sigma_Y$
(ii) $\Delta a > 0.008 + J_{Qc}/(2\ \sigma_Y)$

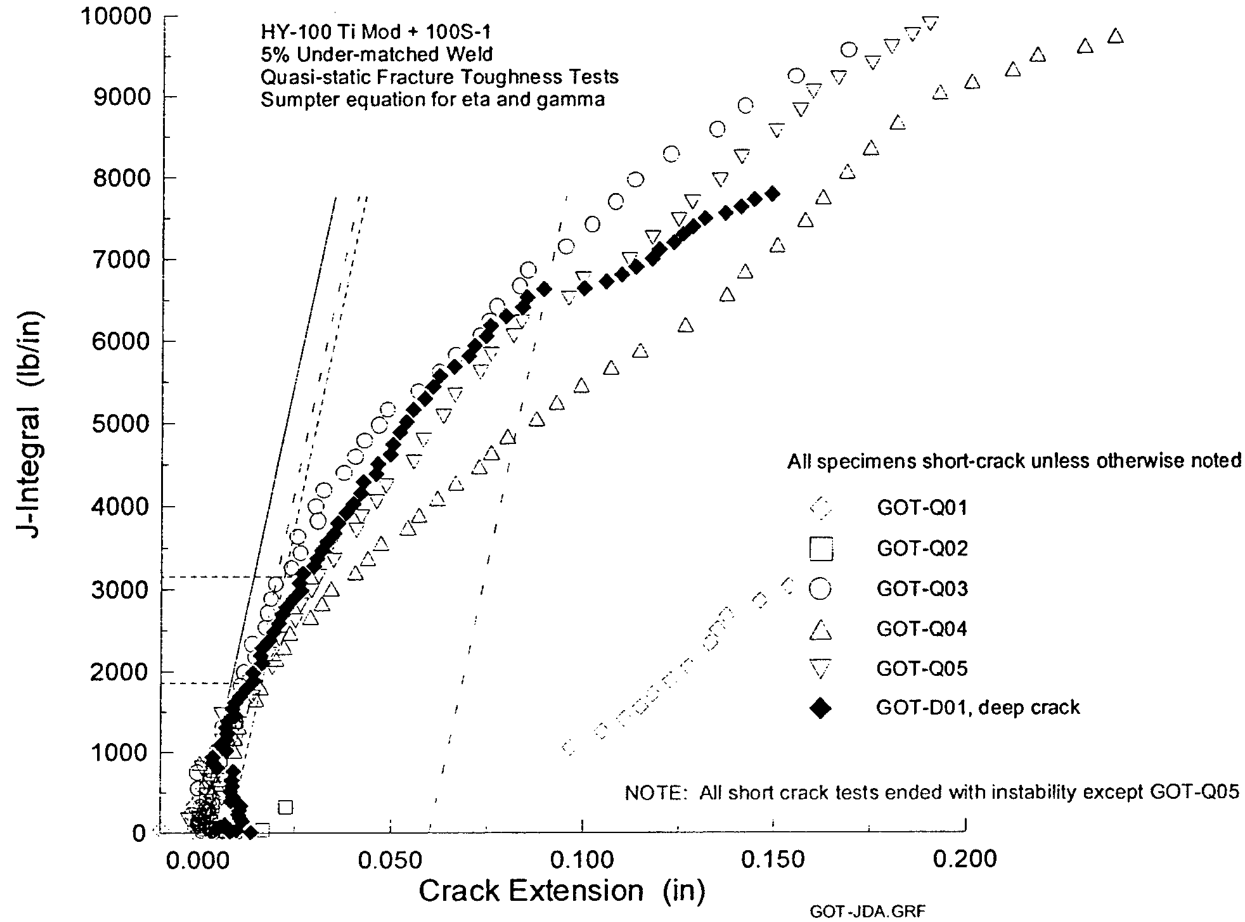


**Figure 28. J-R curves from quasi-static fracture toughness tests of GOT weld.**

The results of the quasi-static fracture toughness tests on the GOS weld are summarized in **Table 12**, and the J-R curves are shown in **Figure 29**. Only one valid $J_{Ic}$ was obtained, although based on the earlier discussion, GOS-Q03 and –Q04 could also be considered valid. Tests GOS-Q02 and –Q05 are invalid largely because of the instability that occurred early in the test, thereby limiting the amount of data available for the power-law fit. The J-R curves for these two specimens (refer to Appendix B for test records) show that the data up to the point of instability is sufficient to determine $J_{Ic}$, and therefore should not be discarded. Considering all of the marginally valid tests, the range in $J_{Ic}$ is from 1798 lb/in. to 3284 lb/in., which is close to the range obtained from the GOT weld. There is no obvious effect of under-matching on quasi-static initiation toughness for these tests.

Even though the initiation toughnesses are about the same, beyond initiation the J-R curves for the GOS weld are somewhat lower than the GOT weld. The lowest curve for GOS is the deep crack specimen, which is consistent with the expected higher constraint (based on homogeneous specimen behavior). It appears that the higher $L_{min}$ values ($L_{crk}/a = 0.8$ to 1.3) of the GOS weld may be causing less under-estimation in J and less increase in constraint. It is also interesting to note that the position of the J-R curves for the GOS weld correlates reasonably well with the value of $L_{min}$. Constraint appears to increase with decreasing $L_{min}$, thereby lowering the J-R curve. This observation is consistent with similar observations in [4].

In ferritic steels the propensity for fracture instability (cleavage) increases as temperature is decreased in the transition regime. The large number of quasi-static tests that transitioned to cleavage, along with the large variation in ductile crack growth preceding cleavage, indicates that these welds are probably in mid to upper transition at 28°F. The combined effects of micro-structural variations in the welds, and variations in constraint due to weld geometry, could be contributing to the wide variation in ductile crack growth preceding cleavage.

The tearing resistance of a metal is expressed in terms of the tearing modulus, which is:

$$T = \frac{E}{\sigma_{ys}^2}\frac{dJ}{da} \tag{13}$$

The tearing resistance can be compared by looking at the slope of normalized J-R curves, where J is multiplied by the modulus and divided by the weld metal yield strength squared. Examination of **Figure 30** shows that the GOS weld has higher tearing resistance, even though the GOS J-R curves are lower than the GOT curves. It is not clear how under-matching may be influencing the tearing resistance because the effects of microstructure, as indicated by the different yield strengths, and degree of under-matching cannot be separated. The lower tearing resistance of the GOT weld may also be due to the higher constraint caused by the closer proximity of the weld fusion line.

**Table 12. Results of Quasi-Static Fracture Toughness Tests at 28°F of GOS Weld.**

| Specimen | $a_o/W$ | $J_{Ic}$ (lb/in.) | Invalidity Codes[1] | $J_c$ (lb/in.) | Invalidity Codes[2] | $\Delta a$ at Instability (in.) | $L_{min}$ |
|---|---|---|---|---|---|---|---|
| GOS-Q01 | 0.175 | 1897 | *Valid* | 3885 | ii | 0.076 | 0.290 |
| GOS-Q02 | 0.177 | 1798 | b, e | 2232 | ii | 0.027 | 0.225 |
| GOS-Q03 | 0.167 | 1910 | a | 5747 | ii | 0.104 | 0.285 |
| GOS-Q04 | 0.176 | 2853 | a | 5826 | ii | 0.132 | 0.260 |
| GOS-Q05 | 0.173 | 3284 | e | 3621 | ii | 0.038 | 0.300 |
| GOS-D03 | 0.613 | 1492 | a, b | | | *No instability* | |

[1]Invalidity codes for $J_{Ic}$
(a) Initial crack curvature exceeds 5% of average
(b) Final crack curvature exceeds 5% of average
(c) Variation in crack extension exceeds 50% of average extension
(d) Error in crack extension prediction exceeds allowable limits
(e) Unacceptable data spacing for power-law fit
(f) Thickness or initial ligament < 25 $J_Q/\sigma_Y$

[2]Invalidity codes for $J_c$
(i) B, $b_o$ < 200 $J_{Qc}/\sigma_Y$
(ii) $\Delta a > 0.008 + J_{Qc}/(2\,\sigma_Y)$

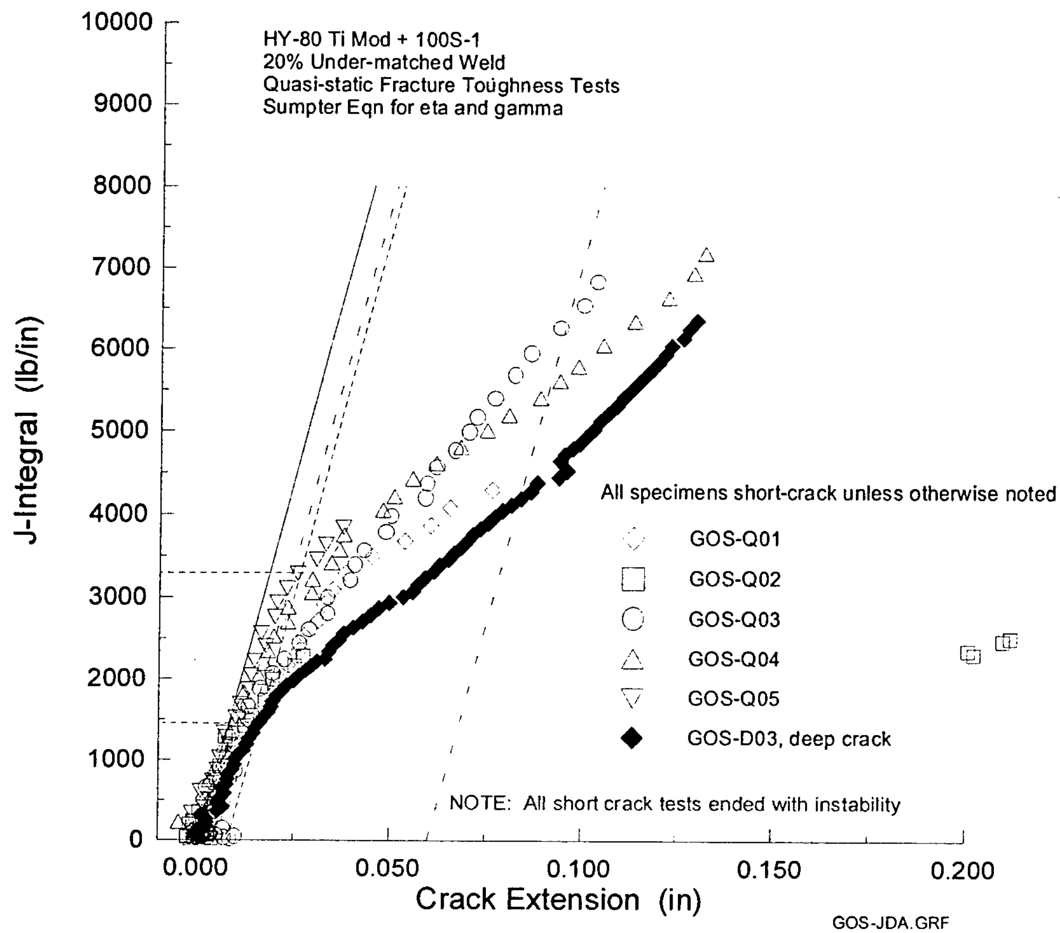


**Figure 29. J-R curves for Quasi-static fracture toughness tests of GOS weld.**

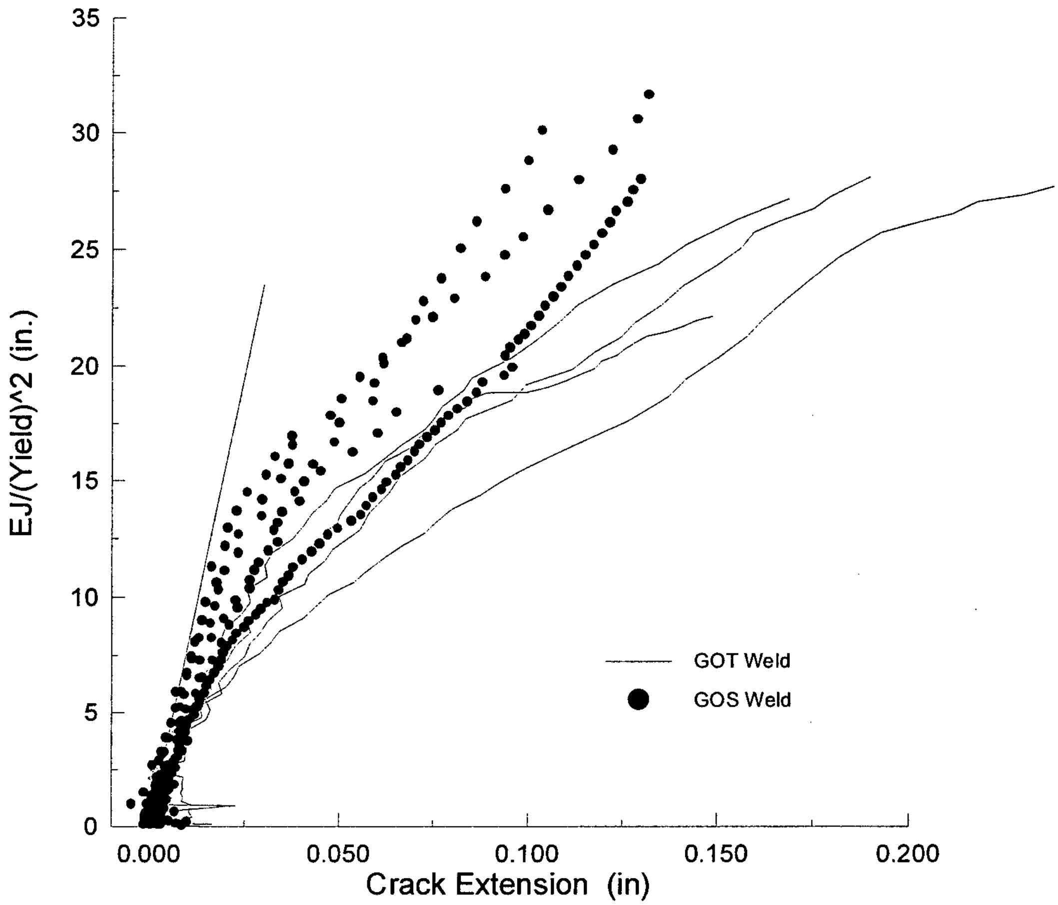


**Figure 30. Comparison of quasi-static tearing resistance of GOS and GOT welds.**

## Dynamic Fracture Toughness Test Results

The results of the dynamic fracture toughness tests on the GOT weld are summarized in **Table 13** and the J-R curves are shown in **Figure 31**. Also shown in the figure are the highest and lowest J-R curves from the quasi-static tests of the GOT weld. Note that all of the dynamic data falls within the bounds of the 28°F quasi-static data. Comparison of the initiation toughness ($J_{Ic}$) values in **Table 13** with those in **Table 11** indicates that there is no net effect of rate or temperature on initiation toughness for the range of loading rates and temperatures investigated. Recall that the dynamic tests were run at various elevated temperatures in an effort to get ductile tearing without transition to cleavage. The quasi-static initiation toughness at 28°F ranges from 1876 to 3318 lb/in. while the dynamic value at 100°F ranges from 1616 to 3159 lb/in. The approximately 200 lb/in. shift in the upper and lower values is much less than the spread, which is about 1500 lb/in., thereby making it difficult to conclude that there is a difference between the initiation toughness at the two rates and temperatures. Increases in loading rate push the transition curve to higher temperatures in ferritic steels. For these tests, the competing effects of rate and temperature appear to be canceling each other out. For quasi-static loading 28°F appears to be near upper shelf. Increasing the loading rate shifts the transition curve to higher temperatures and consequently decreases the toughness, but increasing the temperature to 100°F increases the toughness to the point where there appears to be no net result.

The earliest method for determining $J_{Ic}$, prior to the development of compliance for real-time measurement of crack length, was to test multiple specimens with monotonic loading to varying amounts of crack extension. The J at maximum load-line displacement, and the corresponding measured crack extension, for a test became a single point on a J vs. $\Delta a$ plot. A linear fit through the data was used to determine $J_{Ic}$. Since these specimens were also tested to different amounts of crack extension, a multi-specimen J-R curve can be created from this data. J at maximum load-line displacement was calculated using the non-crack growth corrected formula (equation 14). The resulting multi-specimen J-R curve is shown in **Figure 32**. Note that $J_{Id}$ predicted from a linear fit through this data is very close to the estimates made using Normalization. This lends some confidence to the Normalization analysis.

$$J_{pl} = \frac{\eta A_{pl}}{bB} \tag{14}$$

**Table 13. Results of Dynamic Fracture Toughness Tests of GOT Weld.**

| Specimen | $a_o/W$ | Temp (°F) | $J_{Id}$ (lb/in.) | Invalidity Codes[1] | Crack Extension (in.) | J @ max. Load-line Disp. (lb/in.) |
|---|---|---|---|---|---|---|
| GOT-D02 | 0.578 | 140 | 2057 | *Valid* | 0.096 | 6183 |
| GOT-D03 | Bad Test – Data Acquisition Problems | | | | | |
| GOT-D04 | 0.587 | 100 | 2295 | *Valid* | 0.079 | 5812 |
| GOT-D05 | 0.586 | 90 | 2509 | *Valid* | 0.063 | 5228 |
| GOT-D06 | 0.587 | 100 | 2070 | *Valid* | 0.046 | 3698 |
| GOT-D07 | 0.540 | 100 | 3159 | *Valid* | 0.114 | 7115 |
| GOT-D08 | 0.585 | 100 | 2087 | *Valid* | 0.026 | 2542 |
| GOT-D09 | 0.590 | 100 | 1616 | a, b | 0.011 | 1879 |
| GOT-D10 | 0.571 | 100 | 2285 | *Valid* | 0.038 | 3307 |

[1]Invalidity codes for $J_{Id}$
(a) Initial crack curvature exceeds 5% of average
(b) Final crack curvature exceeds 5% of average
(c) Variation in crack extension exceeds 50% of average extension
(d) Thickness or initial ligament < 25 $J_Q/\sigma_Y$

The dynamic fracture toughness tests of the GOS weld are summarized in **Table 14** and the J-R curves are given in **Figure 33**. Some of the dynamic tests were run at 28°F to compare with the quasi-static tests. At this temperature, dynamic loading significantly decreases the initiation toughness and the ductile crack growth prior to cleavage.

Consequently, there was not enough plasticity or ductile crack growth at instability to perform the normalization analysis or to obtain a measurement of $J_{Id}$. This is consistent with the earlier discussion of rate effects. For these tests, the dynamic fracture initiation toughness at the onset of cleavage ($J_{cd}$) was calculated and is presented in **Table 15.** $J_{cd}$ was also calculated for tests D05 and D07 where cleavage followed significant ductile crack growth.

The dynamic J-R curves for GOS fall approximately within the bounds of the quasi-static J-R curves, with the exception of GOS-D05 and –D07, once again indicating that the effects of rate and temperature are canceling each other out. Specimen GOT-D05 was tested at 72°F, which may partly explain why it falls outside the bounds of the quasi-static tests. Specimen D07 had a longer precrack than the others, therefore the crack tip was sampling a different microstructure. Consequently, the lower curve for D07 may be caused by microstructural variations in the weld.

A multi-specimen J-R curve was created for the tests between 72°F and 110°F. The J-$\Delta a$ pairs used for the curve are shown in **Table 16** and the Normalization and multi-specimen curves are compared in **Figure 34**. There appears to be two resistance curves for this weld. The higher curve, represented by specimens D08, D09 and D10, has a $J_{Id}$ of about 2,100 lb/in. The lower curve, represented by specimens D05 and D07, has a $J_{Id}$ of about 1,550 lb/in. When considered as two curves, the multi-specimen $J_{Id}$'s agree very well with the Normalization J-R curves. The appearance of two resistance curves may also be due to microstructural variations in the weld.

No cleavage was observed at 140°F, so this temperature appears to be on upper shelf for both welds. Instabilities occurred at 72°F and 100°F for the GOS weld, so 110°F appears to be just on the upper shelf for the loading rate of these tests. By comparison, GOT exhibited ductile behavior at 90°F, so GOT appears to have a slightly lower transition temperature. The toughness versus temperature behavior of the two welds is compared in **Figure 35**. The ranges in ductile initiation toughness ($J_{Id}$) for the two welds are so close that it is difficult to differentiate between them. Once again it is not possible to separate the effects of under-matching from microstructure in the interpretation of these tests. The original intent was to produce two identical welds using base plates with different yield strengths so that one weld would be matched and the other under-matched. However, the yield strength of the Ti Mod HY-80 was higher than expected, and therefore it was not possible to make the two welds the same.

The load versus time, load-line displacement versus time and load versus load-line displacement traces for all of the dynamic GOT and GOS tests are shown in **Figure 36** through **Figure 41**. Referring to the load-time traces for GOT, the point of impact with the stop block is identified by the sudden, high frequency oscillation in the load. As mentioned previously in the discussion on problems with the normalization method, this oscillation made determination of load at a critical point in the test difficult. In an effort to alleviate this, a thin (0.118 in. thick) sheet of rubber (75 Shore A durometer) was placed on the stop block for the test of GOT-D07. Comparison of the load-time traces in **Figure 36** shows that the rubber reduced the oscillation in the load signal at impact. The improvement can also be seen in the load-displacement trace (**Figure 38**). The rebound that occurs right after impact is clearer. Note that the load is higher for GOT-D07 that for the other tests, which is partly due to the shorter pre-crack. The pre-cracks for most of the specimens fell between 1.018 and 1.031 in., but D07 was 0.946 in. It is interesting to note that the rubber did not increase the difference between set and maximum load-line deflection by much. For D02 the set deflection was 0.146 and the max. was 0.199 in. while for D07 the set was 0.149 and the max. was 0.196. (Set deflection did not include the thickness of the rubber). Apparently the rubber compresses to only a few mils thick at impact.

**Table 14. Dynamic Ductile Fracture Initiation Toughness ($J_{Id}$) of GOS Weld.**

| Specimen | $a_o/W$ | Temp. (°F) | $J_{Id}$ (lb/in.) | Invalidity Codes[1] | Ductile Crack Ext. (in.) |
|---|---|---|---|---|---|
| GOS-D04 | 0.607 | 140 | 2606 | a | 0.065 |
| GOS-D05 | 0.599 | 72 | 1647 | c | 0.052 |
| GOS-D06 | 0.606 | 100 | 2257 | a | 0.063 |
| GOS-D07 | 0.673 | 100 | 1457 | *Valid* | 0.070 |
| GOS-D08 | 0.576 | 110 | 2093 | *Valid* | 0.022 |
| GOS-D09 | 0.579 | 110 | 2170 | *Valid* | 0.025 |
| GOS-D10 | 0.579 | 110 | 2011 | *Valid* | 0.069 |

[1]Invalidity codes for $J_{Id}$

(a) Initial crack curvature exceeds 5% of average
(b) Final crack curvature exceeds 5% of average
(c) Variation in crack extension exceeds 50% of average extension
(d) Thickness or initial ligament < 25 $J_Q/\sigma_Y$

**Table 15. Dynamic Cleavage Fracture Initiation Toughness ($J_{cd}$) of GOS Weld**

| Specimen | $a_o/W$ | Temp. (°F) | $J_{cd}$ (lb/in.) | Invalidity Codes[2] | $\Delta a$ at Instability (in.) |
|---|---|---|---|---|---|
| GOS-D01 | 0.611 | 28 | 892 | ii | 0.019 |
| GOS-D02 | 0.607 | 28 | 632 | i | 0.006 |
| GOS-D05 | 0.599 | 72 | 2834 | ii | 0.052 |
| GOS-D07 | 0.673 | 100 | 3464 | ii | 0.070 |

[2]Invalidity codes for $J_{cd}$
(i) B, $b_o < 200\ J_{Qcd}/\sigma_Y$
(ii) $\Delta a > 0.008 + J_{Qcd}/(2\ \sigma_Y)$

**Table 16. Data Used for Multi-specimen J-R Curve for GOS Weld.**

| Specimen | Temperature (°F) | J@ max. Load-line Disp. (lb/in.) | J@ Instability (lb/in.) | Crack Extension (in.) |
|---|---|---|---|---|
| GOS-D05 | 72 | | 2834 | 0.052 |
| GOS-D07 | 100 | | 3464 | 0.070 |
| GOS-D08 | 110 | 2375 | | 0.022 |
| GOS-D09 | 110 | 2501 | | 0.025 |
| GOS-D10 | 110 | 4351 | | 0.069 |

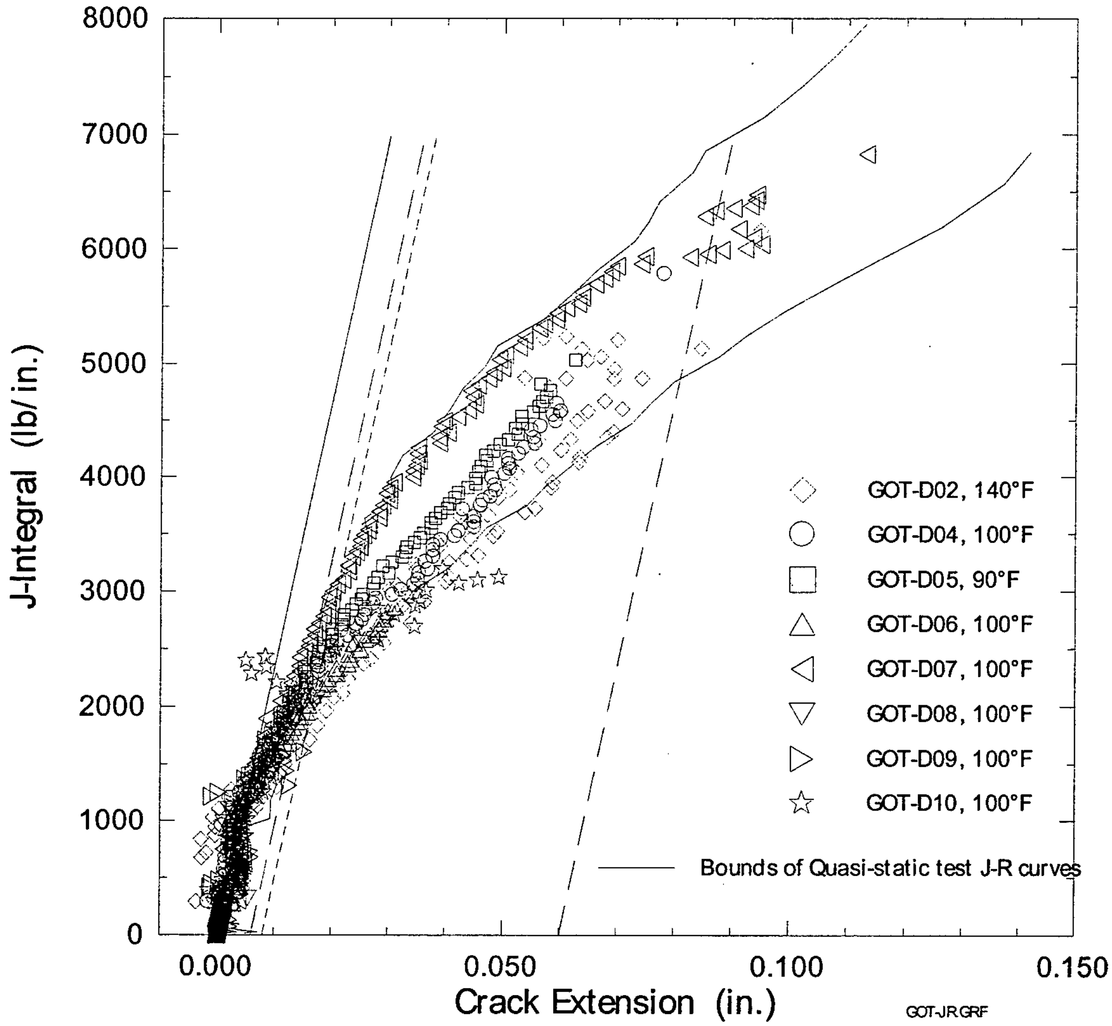


**Figure 31. Dynamic J-R curves for GOT weld.**

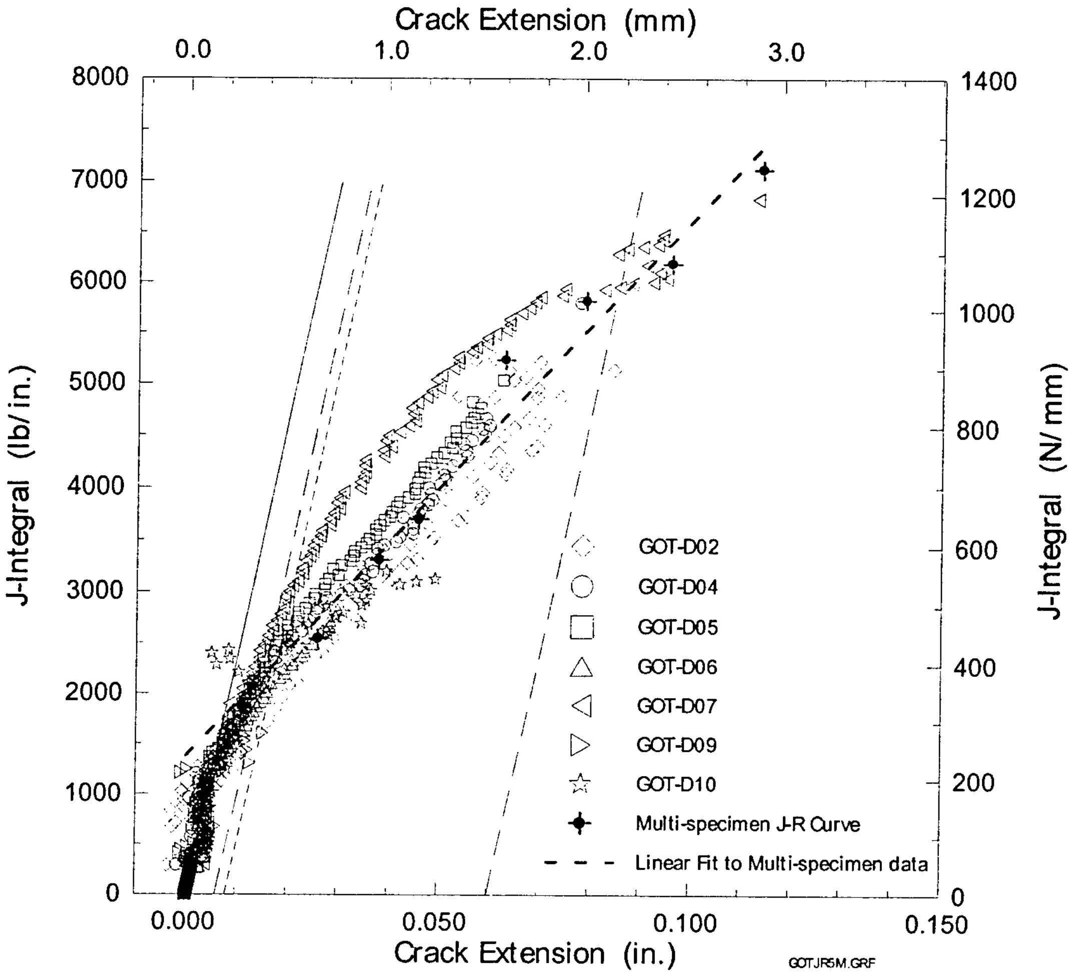


**Figure 32. Comparison of J-R curves predicted by Normalization and Multi-Specimen methods for GOT weld.**

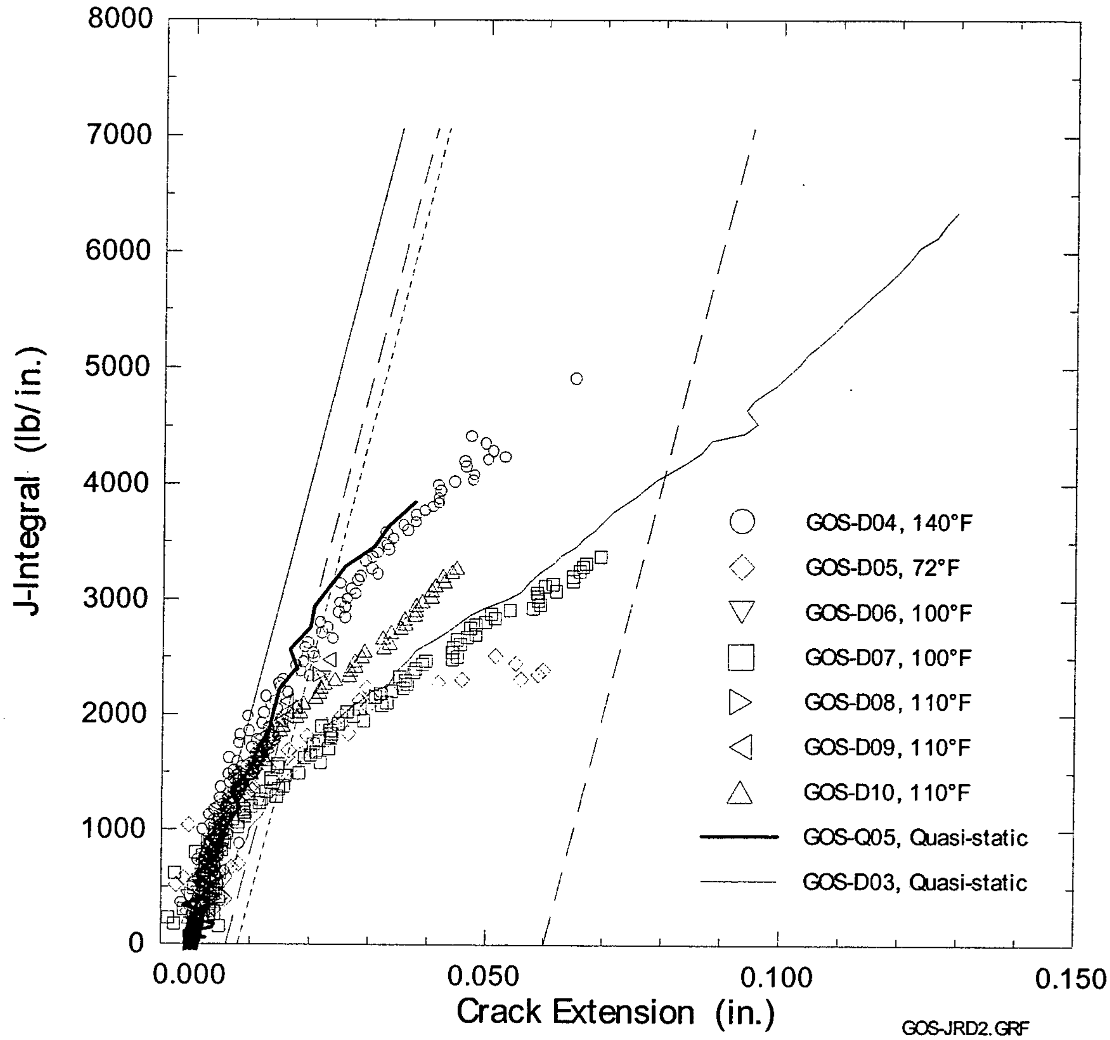


**Figure 33. Dynamic J-R curves for GOS weld.**

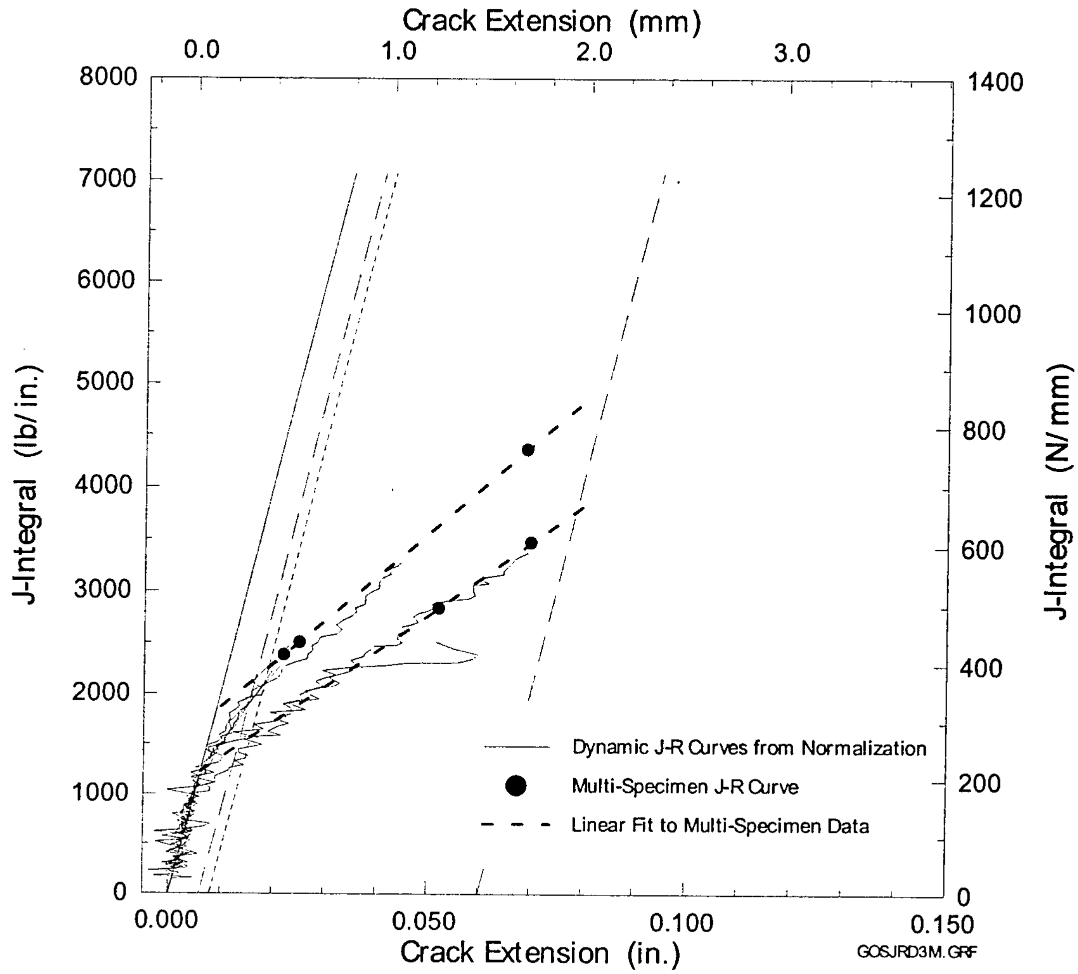


**Figure 34. Comparison of Normalization and Multi-Specimen dynamic J-R curves for GOS weld.**

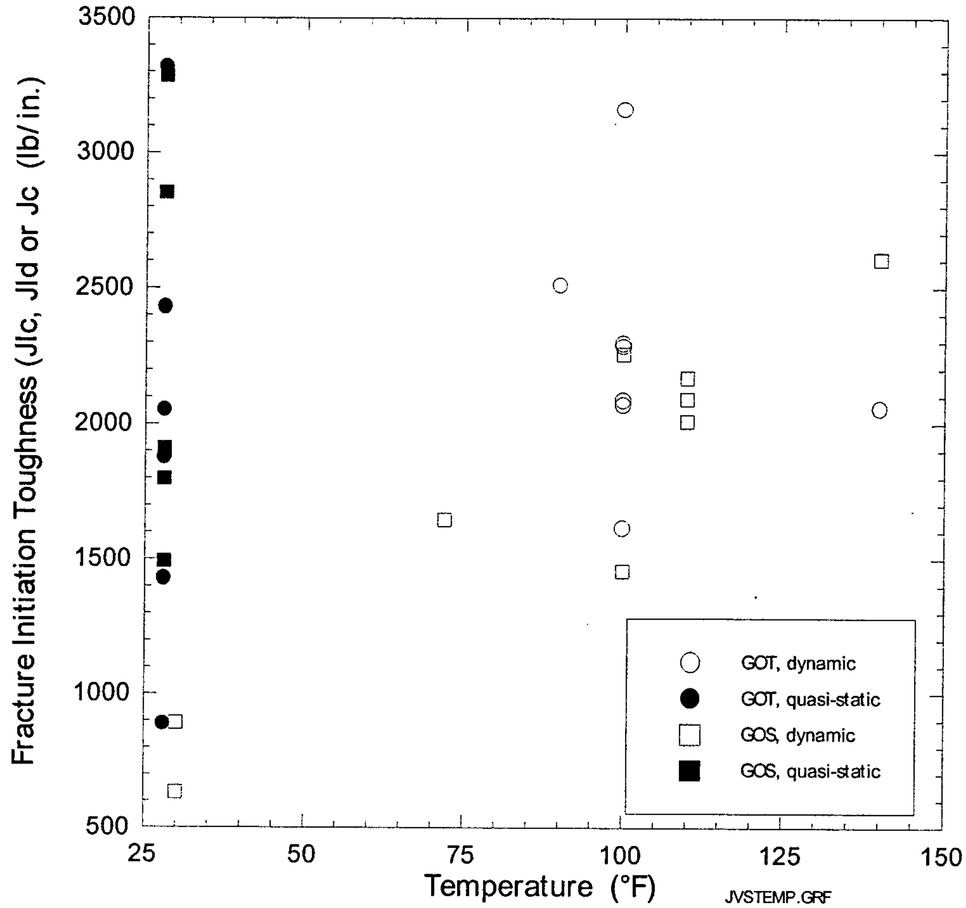


**Figure 35. Dynamic Initiation Toughness versus Temperature for GOS and GOT Welds.**

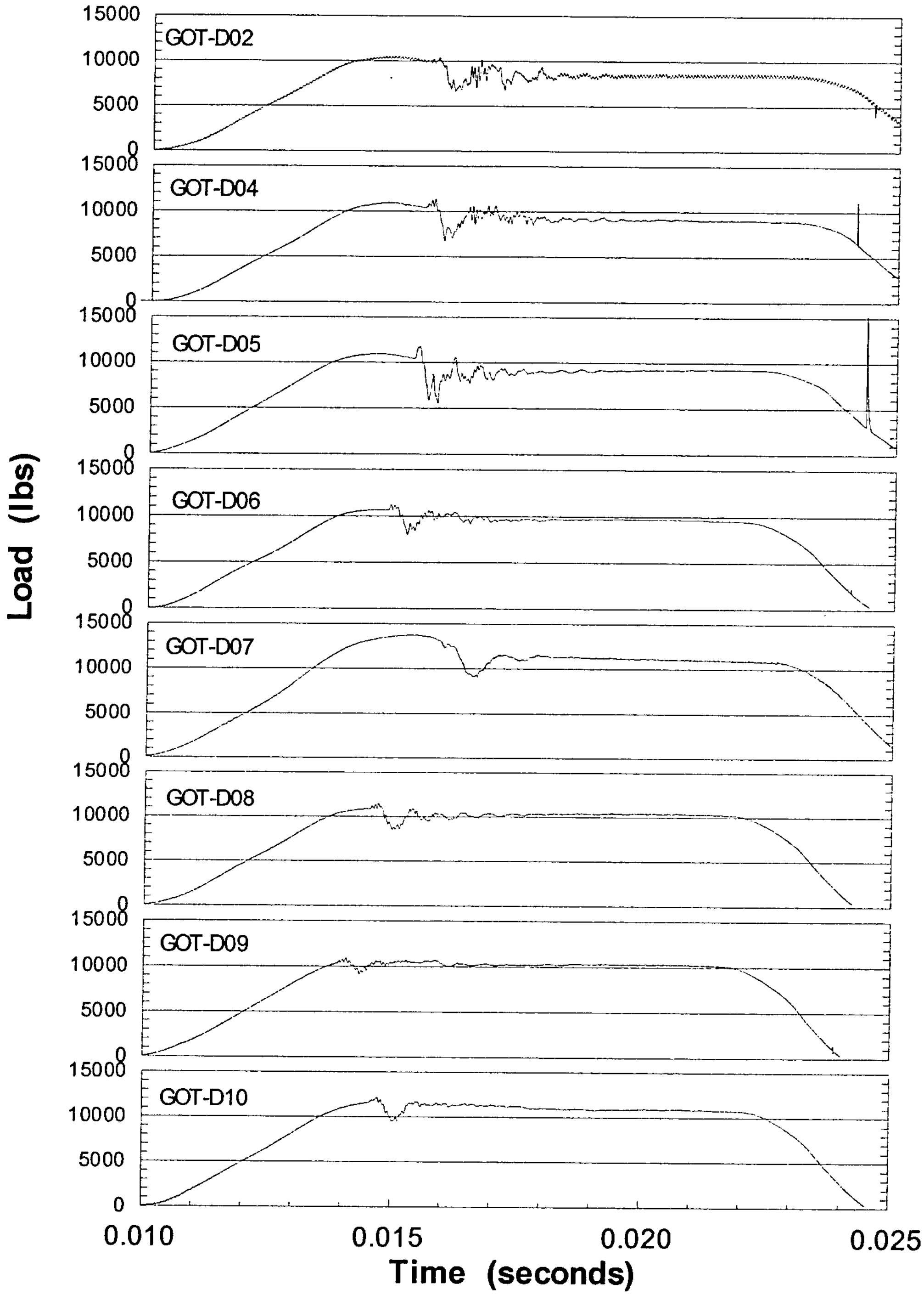


**Figure 36. Load vs. time traces for dynamic fracture toughness tests of GOT weld.**

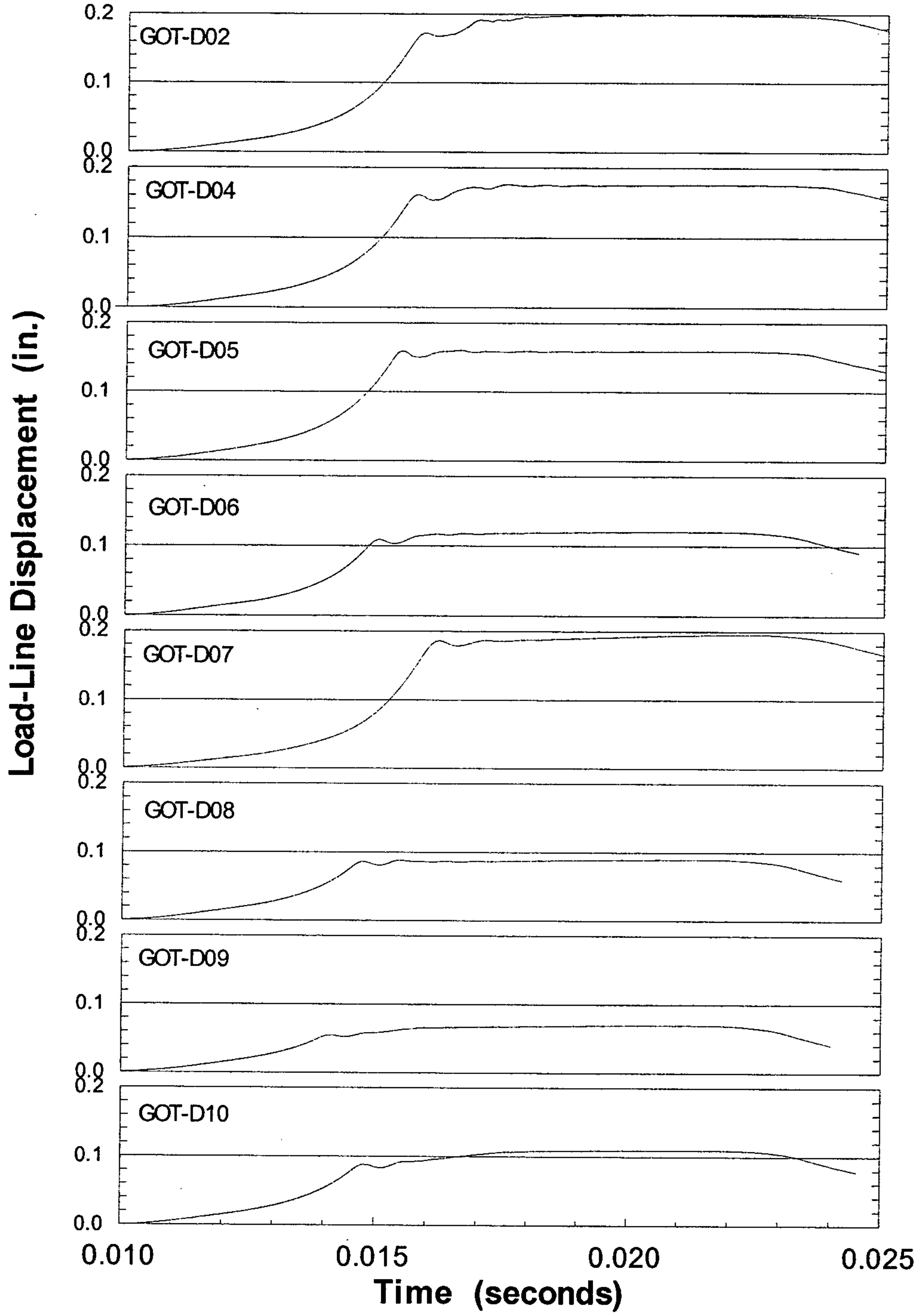


**Figure 37. Load-line displacement vs. time traces for dynamic fracture toughness tests of GOT weld.**

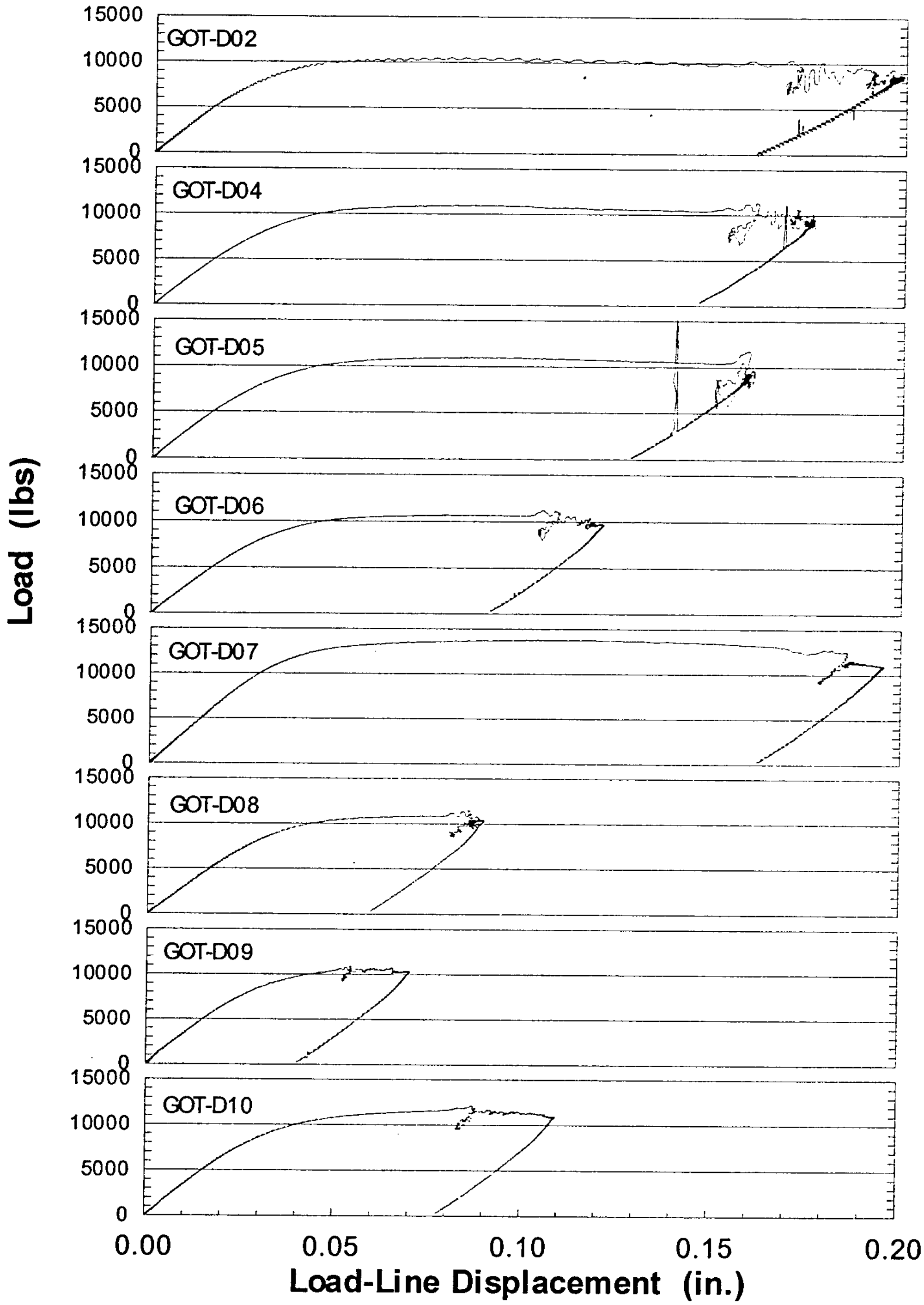


**Figure 38. Load vs. Load-line displacement traces for the dynamic fracture toughness tests of the GOT weld.**

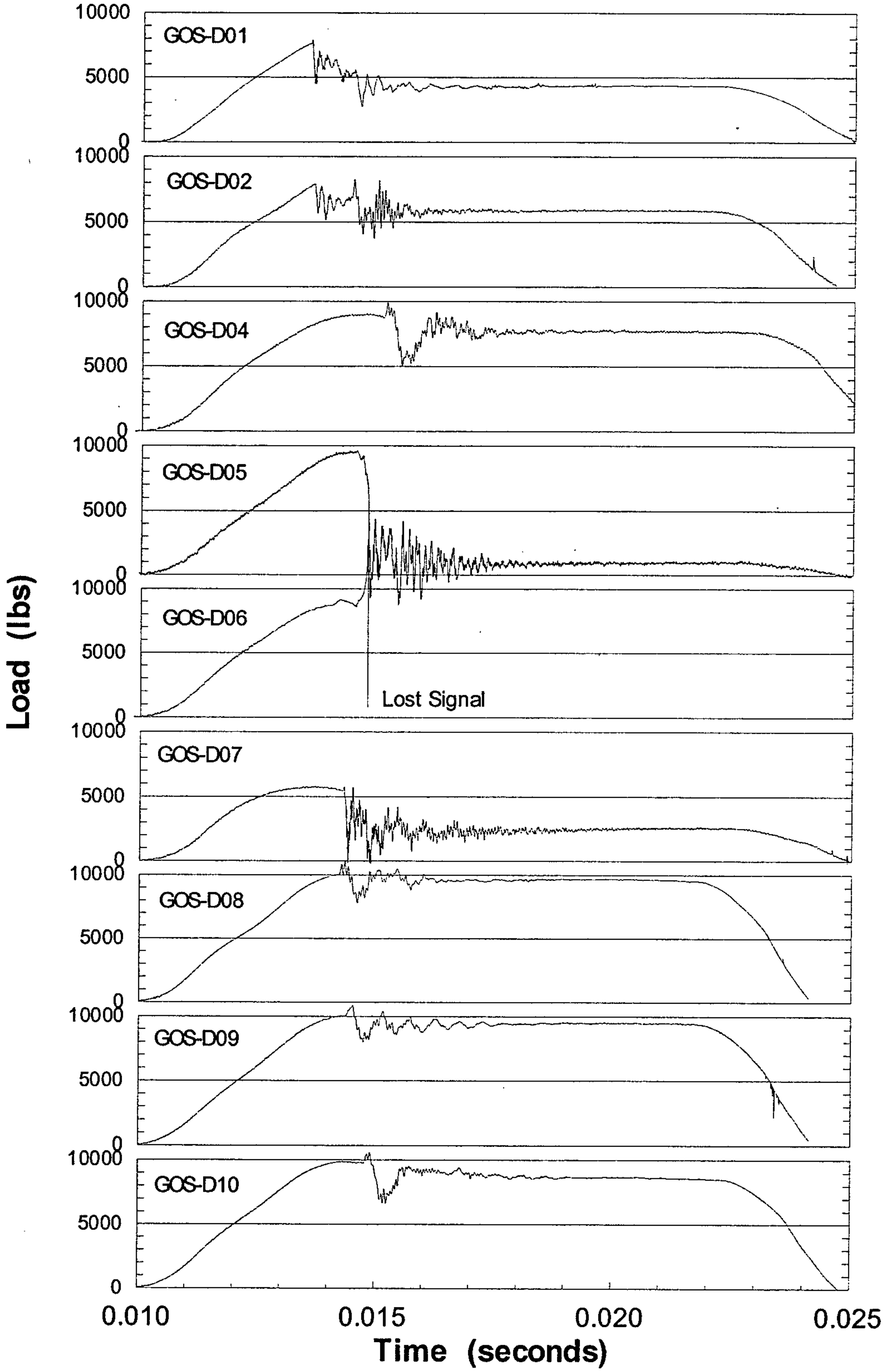


**Figure 39. Load vs. Time Traces for dynamic fracture toughness tests of GOS weld.**

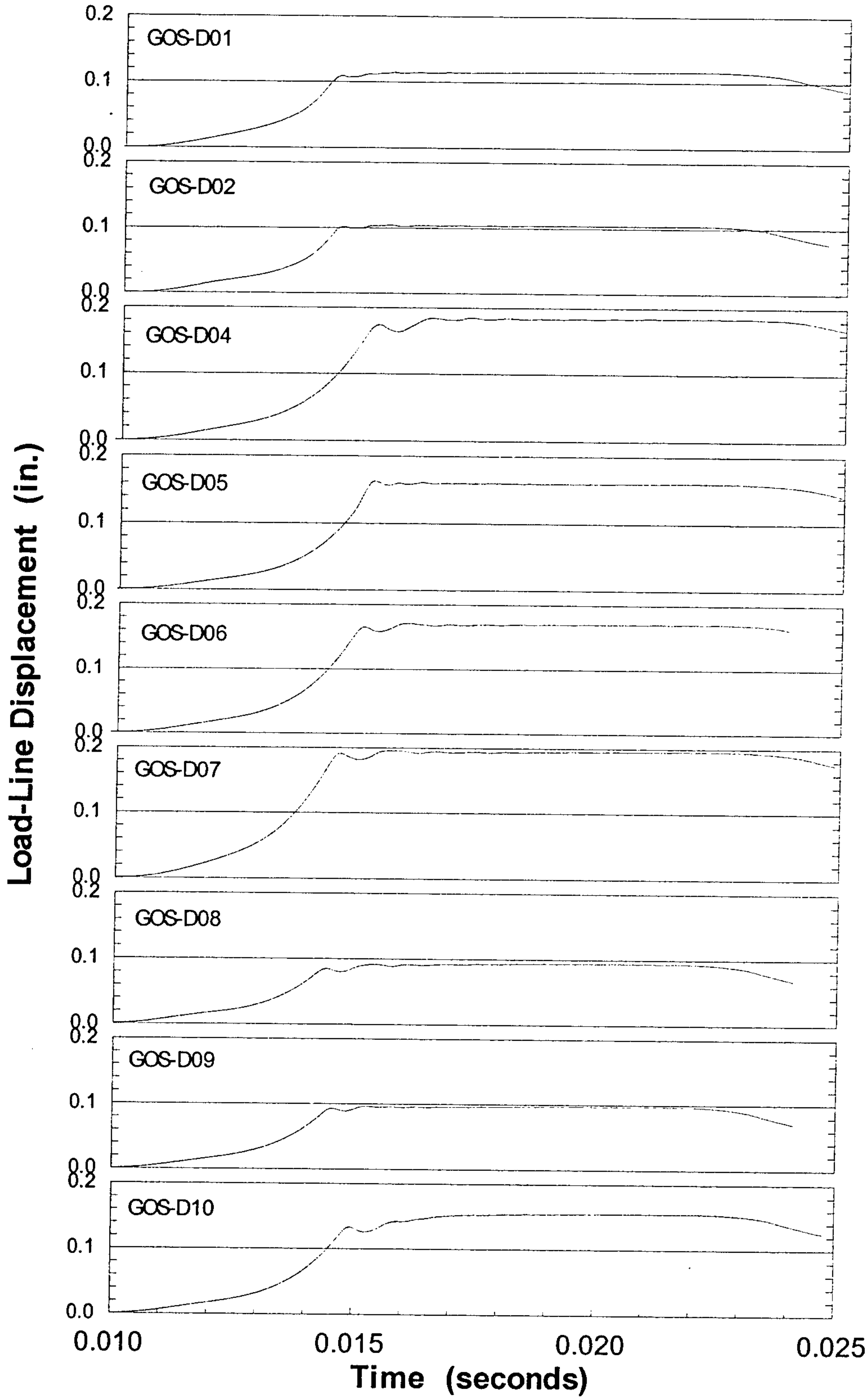


**Figure 40. Load-line displacement vs. time traces for dynamic fracture toughness tests of GOS weld.**

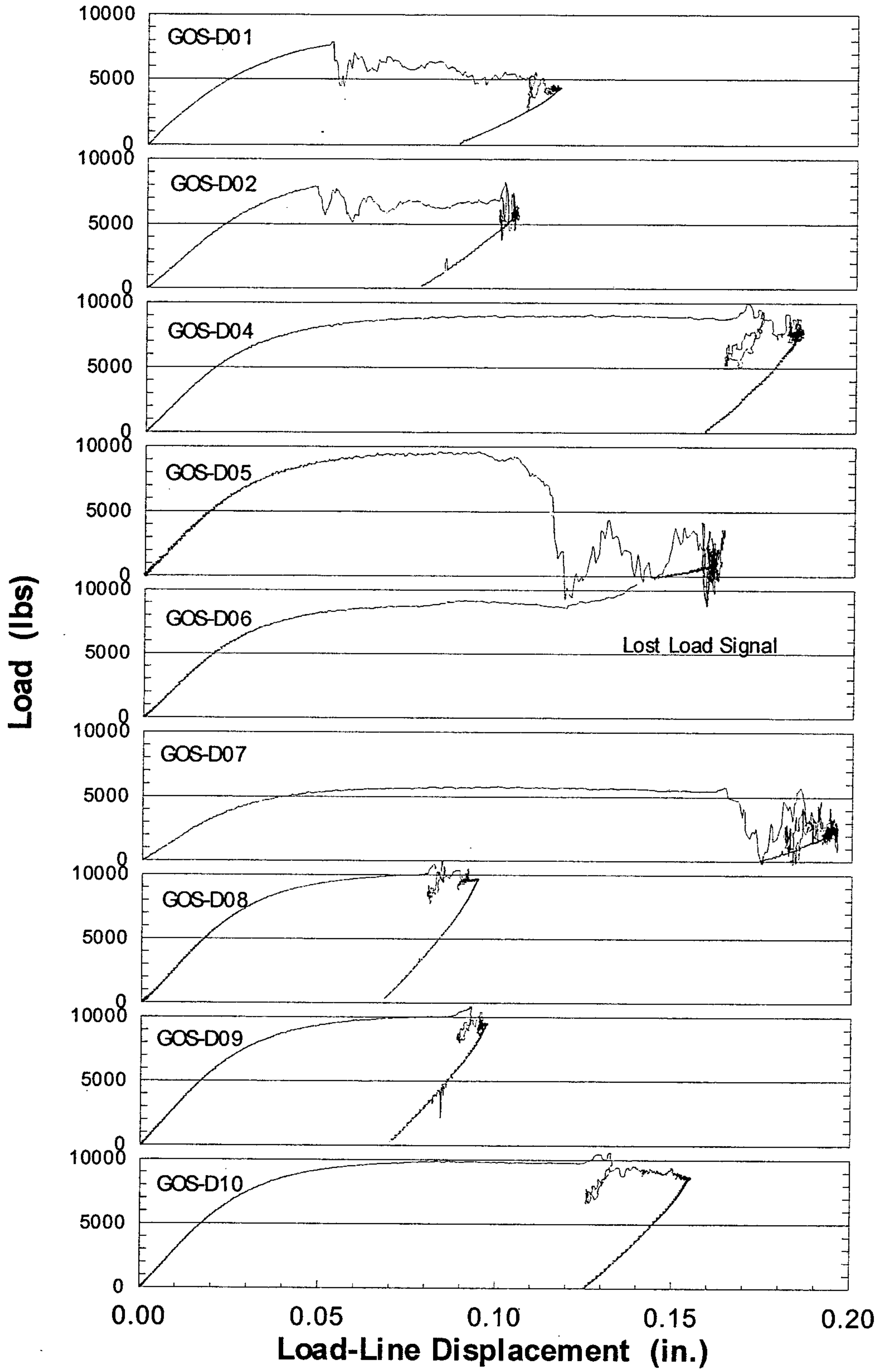


**Figure 41. Load vs. Load-line displacement traces for dynamic fracture toughness tests of GOS weld.**

The source of the "bounce" in the dynamic SE(B) tests is not known for certain. This bounce is commonly seen in impact testing, and is thought to be caused by rebound of the tower off the stop block. The displacement versus time traces show that the tower starts out at a low velocity initially, and then accelerates. The low initial velocity is caused by deformation of the aluminum absorber. As the absorber crushes, it gradually increases the force transmitted to the tower. When the absorber reaches maximum deformation, the tower velocity reaches the cross-head velocity. A sudden deceleration occurs when the tower impacts the stop block. This would be expected to occur at the maximum load line displacement, but the traces show that it does not. The tower impacting the stop block with a slight tilt may cause the early bounce. In this case, the tower would tend to rattle on the stop block until it comes to rest at the maximum load line displacement. This rattling may cause the average displacement and load to oscillate, thereby causing the observed bounce. The position of this bounce relative to maximum displacement would depend on extent of tilt in the tower. This may explain why the bounce occurs at different places in each test. The bounce is not observed when unstable fracture occurs in the test. This is consistent with the tilt theory since there is no more load on the specimen after fracture instability. The rubber sheet used in the test of GOT-D07 reduces the high frequency ringing around the bounce, but does not eliminate the rebound.

The impact of the tower with the stop block may also be exciting natural modes of vibration in the specimen other than the first mode (simple bending). The resulting deformation would appear in the strain readings used to determine load. This would cause some error in the load measurement, and may account for the small rise in load just before the bounce.

## CONCLUSIONS

Fixtures, instrumentation and procedures for dynamic fracture toughness testing of SE(B) specimens were developed that allowed control of load-line deflection in order to obtain varying amounts of ductile crack extension. A procedure for applying the Normalization Method to the analysis of dynamic fracture toughness tests was also developed. The key to making this procedure work was using multiple specimens with varying ductile crack growth to establish the correct form for the plasticity function. The accuracy of the procedure for determining $J_{Id}$ was verified by comparing the Normalization dynamic J-R curves with multi-specimen dynamic J-R curves.

It is difficult to make a direct comparison of under-matching effects because the microstructures of the two welds were not the same. Results of the short-crack quasi-static tests were in agreement with previous work on the influence of fusion line margin on constraint and tearing resistance. Narrower fusion line margins led to lower tearing resistance and a greater propensity for fracture instability.

The combined effects of dynamic loading and constraint can be very detrimental in the transition regime, as is evidenced by the decrease in $J_c$ for the GOS weld at 28 °F from over 2,200 lb/in. for the quasi-static tests to less than 900 lb/in. for the dynamic tests. Constraint effects may also be responsible for the low quasi-static $J_c$ values of the GOT weld at 28 °F. The lowest $J_c$ values occur for $L_{min}$ of 0.173 to 0.195. When $L_{min}$ is increased to 0.218 there is a dramatic increase in $J_c$.

On the upper shelf, rate and constraint have less effect, as evidenced by the similarities in the quasi-static $J_{Ic}$ and dynamic $J_{Id}$ values for the two welds. The variability in the measured $J_{Id}$ and $J_{Ic}$ is so large that it may be obscuring any rate, mis-match or constraint effect. This magnitude of variability is not unusual for welds because of the different microstructures at the crack tip in a T-S specimen taken from a multi-pass weld.

## RECOMMENDATIONS FOR FUTURE WORK

Calculation of dynamic J-R curves by the Normalization Method requires accurate measurements of load and displacement during the test. Several sources of error in load measurement were identified in this study. Additional effort is required to quantify the errors in on-specimen load measurement due to limited calibration range, crack growth and plasticity in the remaining ligament.

Impact of the tower on the stop block caused high-frequency oscillation in the load signal, thereby further complicating the determination of the final load. Some effort was made in this study to reduce the oscillation by cushioning the impact of the tower on the stop block. Further evaluation of different cushioning methods should be pursued in an effort to improve the accuracy of the "anchor" point.

The accuracy in load measurement could also be improved through re-design of the bend fixture to add rollers at support points. The use of rollers would eliminate friction between the specimen and the supports, and allow free bending of the specimen.

The measurements taken during a dynamic test of a SE(B) specimen, and the subsequent analysis, assume that the specimen is loaded in simple three-point bending. The impact loading may be exciting vibration modes in the specimen that violate this assumption. Additional insight into the impact response of the specimen could be obtained by conducting dynamic finite element analysis.

The tilting of the tower after impact may cause the bounce observed in these tests. The fixture could be modified to incorporate guides for the tower so that it cannot tilt. This would also improve the accuracy of the final load measurement.

## REFERENCES


1. Mark T. Kirk, "The Effect of Weld Metal Strength Mismatch on the Deformation and Fracture Behavior of Steel Butt Weldments," *DTRC-SME-91/06*, Naval Surface Warfare Center technical report, January 1991.
2. Kirk, M. T. and Dodds, R. H., "Experimental J Estimation Formulas for Single Edge Notch Bend Specimens Containing Mismatched Welds," *Proceedings of the 11th International Conference on Offshore Mechanics and Arctic Engineering*, Vol. 3, part B, American Society of Mechanical Engineers, 1992, pp. 439-448.
3. Franco, C. et. al., "Constraint Effects on the Upper Shelf in Cracked Welded Specimens," Constraint Effects in Fracture, Theory and Applications: Second Volume, ASTM STP 1244, Mark Kirk and Ad Bakker, Eds., American Society for Testing and Materials, Philadelphia, 1995, pp. 363-391.
4. R. L. Tregoning, "Strength and Crack Resistance Behavior of Mismatched Welded Joints," *CDNSWC/TR-61-95-17*, Naval Surface Warfare Center technical report, July 1995.
5. Burstow, M. C., Howard, I. C. and Ainsworth, R. A., "The Influence of Constraint on Crack Tip Stress Fields in Strength Mismatched Welded Joints," *Journal of the Mechanics and Physics of Solids*, Vol. 46, 1998, pp. 845-872.
6. J.D. Landes, Z. Zhou, K. Lee and R. Herrera, "Normalization Method for Developing J-R Curves with the LMN Function," *Journal of Testing and Evaluation*, JTEVA, Vol 19, No. 4, July 1991, pp. 305 – 311.
7. "Standard Test Method for J-Integral Characterization of Fracture Toughness," E1737-96, Volume 03.01, *Annual Book of ASTM Standards*, American Society for Testing and Materials, 1998, pp. 957 – 980.
8. "Annex A1. Special Requirements for Testing of Ferritic Steel Weldments," *Draft Annex to E1290*, Revision 6, ASTM Sub-committee E08.08.07, August 10, 1998.
9. "Standard Test Method for Tension Testing of Metallic Materials," E8-98, Volume 03.01, *Annual Book of ASTM Standards*, American Society for Testing and Materials, 1998, pp. 57 – 77.
10. J.A. Joyce and R.E. Link, "Application of Two Parameter Elastic-Plastic Fracture Mechanics to Analysis of Structures," *Engineering Fracture Mechanics*, Vol. 57, No. 4, July 1997, pp. 431 – 446.
11. Gerard P. Mercier, "The Influence of Localized Plasticity and Crack Tip Constraint in Undermatched Welds," *NSWCCD-61-TR-1999/07*, Naval Surface Warfare Center, Carderock Division, West Bethesda Maryland, March 1999.
12. Sumpter, J.D.G., "$J_c$ Determination for Shallow Notch Welded Bend Specimens," *Fatigue and Fracture of Engineering Materials and Structures*, Vol. 10 (6), 1987, pp. 479 – 493.
13. Joyce, J.A., Hackett, E.M. and Roe, C., "Effects of Crack Depth and Mode of Loading on the J-R Curve Behavior of a High-Strength Steel," *Constraint Effects in Fracture*, ASTM STP 1171, American Society for Testing and Materials, Philadelphia, 1993, pp. 239 – 263.
14. Tada, H., Paris, P.C., and Irwin, G.R., *The Stress Analysis of Cracks Handbook*, Paris Productions, Inc. St. Louis, MO, 1985.

15. *TableCurve 2D: Automated Curve Fitting & Equation Discovery*, Version 4, Jandel Scientific Corporation, San Rafael CA, 1996.
16. J. A. Joyce, "Technical Report: High Rate J Integral Test Development," *Vector Research Technical Report*, Vector Research Company, June 1996.
17. J. R. Donoso and J. D. Landes, "The Common Format Equation Approach for Developing Calibration Functions for Two-Dimensional Fracture Specimens From Tensile Data," *Engineering Fracture Mechanics*, Vol. 54, No. 4 1996, pp. 499 – 512.

# APPENDIX A

Normalization Analysis of Dynamic Fracture Toughness Test

Normalization Data Reduction Technique for SE(B) specimen GOT-D06

Analysis using TableCurve2D to perform curve fit

Ref.: Proposed Appendix to ASTM E1820

Specimen Parameters:

$W \equiv 1.748$ $a_o \equiv 1.026$

$B \equiv 0.998$ $a_f \equiv 1.072$ $aW_f = \frac{a_f}{W}$

$B_N \equiv 0.791$

$S \equiv 7.00$ $a_f - a_o = 0.046$ $B_e \equiv B - \frac{(B - B_N)^2}{B}$ $b_o = W - a_o$

Material Parameters:

$\nu \equiv 0.3$ Compliance adjustment factor:

$E \equiv 27.0 \cdot 10^6$ $E_p \equiv \frac{E}{(1 - \nu^2)}$ $\lambda \equiv 0.999$

$\sigma_Y \equiv 116500$

Read Test Data (Raw data was sampled to reduce number of points and truncated at the max. load-line displaceme

$A := \mathrm{READPRN}(\text{"gotd06\_FINAL.dat"})$ $\mathrm{NumDataPoints} := \mathrm{length}\left(A^{\langle 0 \rangle}\right)$

$k := 0 .. \mathrm{NumDataPoints} - 1$ $\mathrm{NumDataPoints} = 99$

$P_k := A_{k,0}$ $v_k := A_{k,1}$

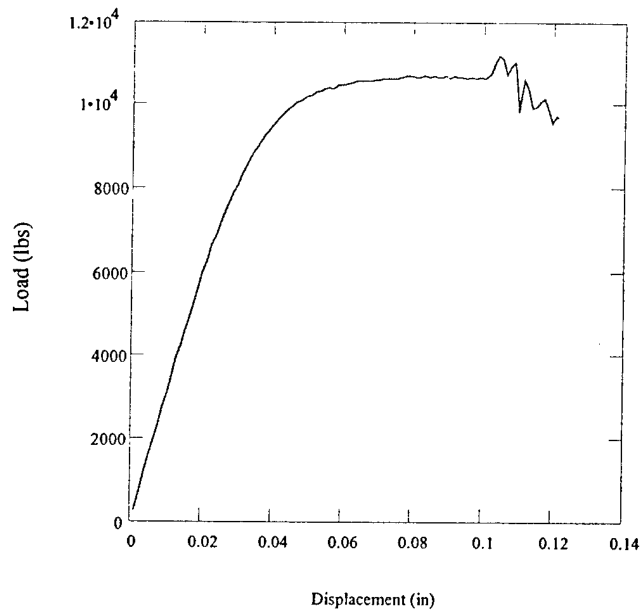


If necessary, LL Displacement is adjusted through "vCorrection" so that plastic displacements don't come out negative

$v_0 = 1.3 \cdot 10^{-3}$

$\mathrm{vCorrection} := 0.0$

$v_k := v_k - \mathrm{vCorrection}$

Calculate Total Area under load-displacement curve (elastic + plastic):

$$\mathrm{Area}_0 := \frac{P_0}{2}\cdot v_0 \qquad kk := 1 .. \mathrm{NumDataPoints} - 1$$

$$\mathrm{Area}_{kk} := \mathrm{Area}_{kk-1} + \frac{P_{kk} + P_{kk-1}}{2}\cdot\left(v_{kk} - v_{kk-1}\right)$$

Find index of array entry corresponding to maximum load and load line displacement

$$\mathrm{Index}(v, \mathrm{thres}) := \left| \begin{array}{l} j \leftarrow 0 \\ \text{while } v_j < \mathrm{thres} \\ \quad j \leftarrow j + 1 \\ j \end{array} \right.$$

$I_{pmax} := \mathrm{Index}(P, \max(P))$ $\qquad$ $I_{pmax} = 83$ $\qquad$ $\max(P) = 1.118\cdot 10^4$

$\mathrm{NumPoints} \equiv \mathrm{NumDataPoints} - 1$ $\qquad$ $I_{lldmax} := \mathrm{Index}(v, \max(v))$ $\qquad$ $\max(v) = 0.121$

$i := 0 .. \mathrm{NumPoints}$ $\qquad$ $I_{lldmax} = 98$ $\qquad$ $P_{I_{lldmax}} = 9.693\cdot 10^3$

Define Functions for Normalization:

$$\mathrm{LLCompliance}(aW) \equiv \left(\frac{\frac{S}{W}}{1 - aW}\right)^2 \cdot \frac{(1.193 + aW\cdot(-1.98 + aW\cdot(4.478 + aW\cdot(-4.443 + aW\cdot(1.739)))))}{\lambda\cdot E\cdot B_e}$$

$$\mathrm{faW}(aW) \equiv \frac{3\cdot\sqrt{aW}\cdot\left[1.99 - aW\cdot(1 - aW)\cdot\left(2.15 - 3.93\cdot aW + 2.7\cdot aW^2\right)\right]}{2\cdot(1 + 2\cdot aW)\cdot(1 - aW)^{1.5}}$$

$$\mathrm{StressIntensity}(P, a) \equiv \frac{\frac{S}{W}\cdot P}{\sqrt{B\cdot B_N\cdot W}}\cdot \mathrm{faW}\left(\frac{a}{W}\right)$$

$$\mathrm{PlArea}(P, \mathrm{Area}, a) \equiv \mathrm{Area} - \frac{\mathrm{LLCompliance}\left(\frac{a}{W}\right)\cdot P^2}{2} \qquad \gamma(a) \equiv 1.0$$

$$\eta(a) \equiv 2$$

$$\mathrm{Jplastic}(P, \mathrm{Area}, a) \equiv \frac{\eta(a)\cdot \mathrm{PlArea}(P, \mathrm{Area}, a)}{B_N\cdot(W - a)}$$

$$\mathrm{Jelastic}(P, a) \equiv \frac{\mathrm{StressIntensity}(P, a)^2}{E_p}$$

$$\text{NormalizedP}(P,a) \equiv \frac{\frac{P}{1000}}{W \cdot B \cdot \left(\frac{W-a}{W}\right)^{\eta(a)}}$$

$$\text{NormalizedVpl}(v,P,a) \equiv \frac{v - P \cdot \text{LLCompliance}\left(\frac{a}{W}\right)}{W}$$

Estimate crack lengths by adding blunting

$$J_i := \text{Jplastic}\left(P_i, \text{Area}_i, a_o\right) + \text{Jelastic}\left(P_i, a_o\right)$$

$$J_{final} := J_{NumPoints}$$

$$\Delta a_{final} := a_f - a_o$$

$$\Delta a_{blunt_i} := \frac{J_i}{2 \cdot \sigma_Y}$$

$$a_i := a_o + \Delta a_{blunt_i}$$

Calculate Normalized P and $v_{pl}$ using estimated crack lengths

$$P_{N_i} := \text{NormalizedP}\left(P_i, a_i\right) \qquad v_{plN_i} := \text{NormalizedVpl}\left(v_i, P_i, a_i\right)$$

Normalize last point using final measured crack length, $a_f$

$$f := \text{NumDataPoints} - 1$$

$$P_f = 9692.54 \qquad v_f = 0.121$$

Over-ride final point to correct for load measurement error:

$$P_f := 10550 \qquad v_f := 0.1227$$

$$P_{N_f} := \text{NormalizedP}\left(P_f, a_f\right) \qquad v_{plN_f} := \text{NormalizedVpl}\left(v_f, P_f, a_f\right)$$

$$P_{N_f} = 40.436 \qquad v_{plN_f} = 0.04798$$

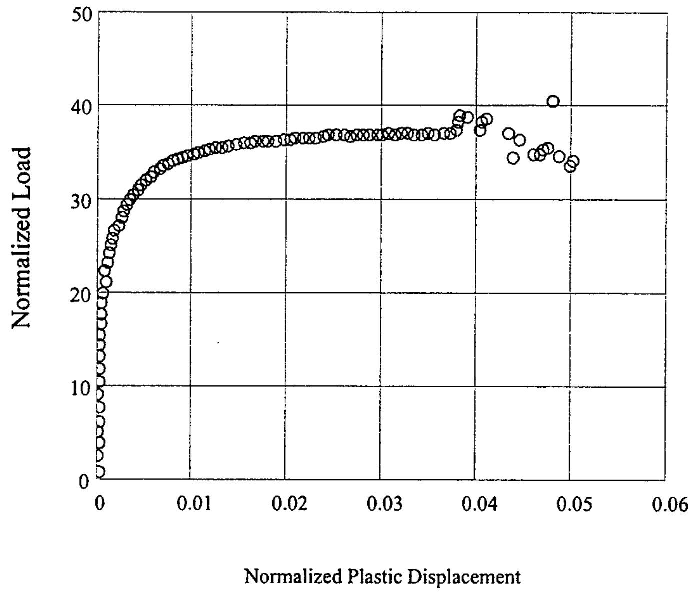


Create data file for export to non-linear fitting program:

Exclude initial points where vplN is less than 0.001

$startpoint := Index\left(v_{plN}, 0.001\right)$ $\qquad startpoint = 18$

Manually select point of tangency: $t := 52$

Draw line between anchor point and point of tangency:

$Point2y := P_{N_f}$ $\qquad Point2x := v_{plN_f}$ $\qquad Point1y := P_{N_t}$ $\qquad Point1x := v_{plN_t}$

$m := \dfrac{Point2y - Point1y}{Point2x - Point1x}$ $\qquad b := Point2y - m \cdot Point2x$ $\qquad Tangent_i := m \cdot v_{plN_i} + b$

Select points between start point and point of tangency:

$endpoint := t$

$ii := startpoint..endpoint$

$vx_{ii - startpoint} := v_{plN_{ii}}$

$vy_{ii - startpoint} := P_{N_{ii}}$

$vx_{endpoint - startpoint + 1} := v_{plN_f}$

$vy_{endpoint - startpoint + 1} := P_{N_f}$

$iii := 0 .. \mathrm{length}(vx) - 1$

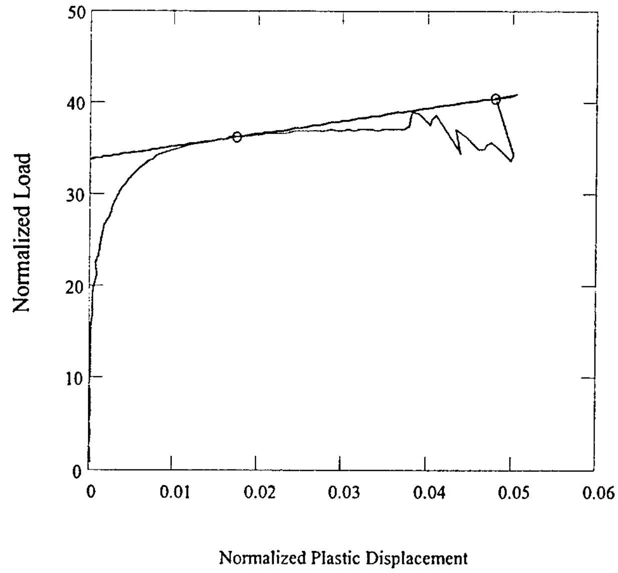


$\mathrm{length}(vx) = 36$

$PNvplN^{\langle 0 \rangle} := vx$

$PNvplN^{\langle 1 \rangle} := vy$

WRITEPRN("fitfile.dat") := PNvplN

Data used in fit ----->:

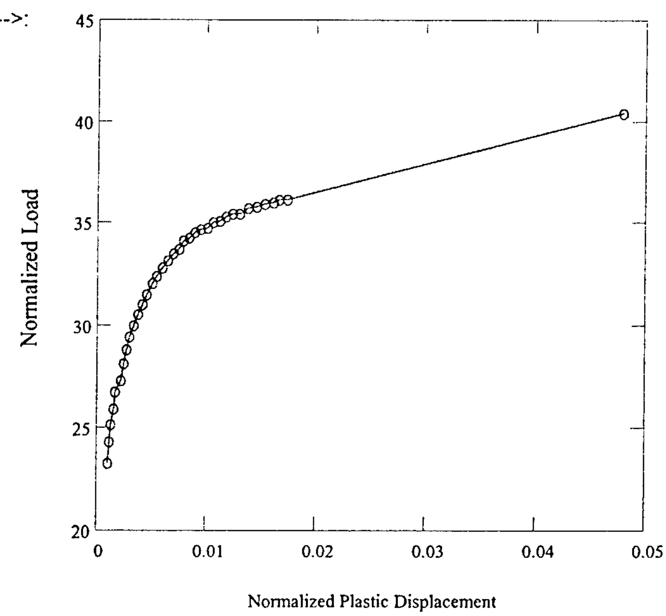


Fitting function:

Joyce LMNO function

$$F(x,u) := \frac{u_3 + u_0 \cdot x + u_1 \cdot x^2}{u_2 + x}$$

Enter fitting function coefficients from Curve Fit program:

$$u := \begin{bmatrix} 37.0377 \\ 84.6854 \\ 0.00155075 \\ 0.0224568 \\ 0 \end{bmatrix}$$

$j := 0 .. 100$

$$r_j := vplN_{startpoint} + j \cdot \frac{vplN_f - vplN_{startpoint}}{100}$$

$$Fit_j := F(r_j, u)$$

Plot of data and curve fit:

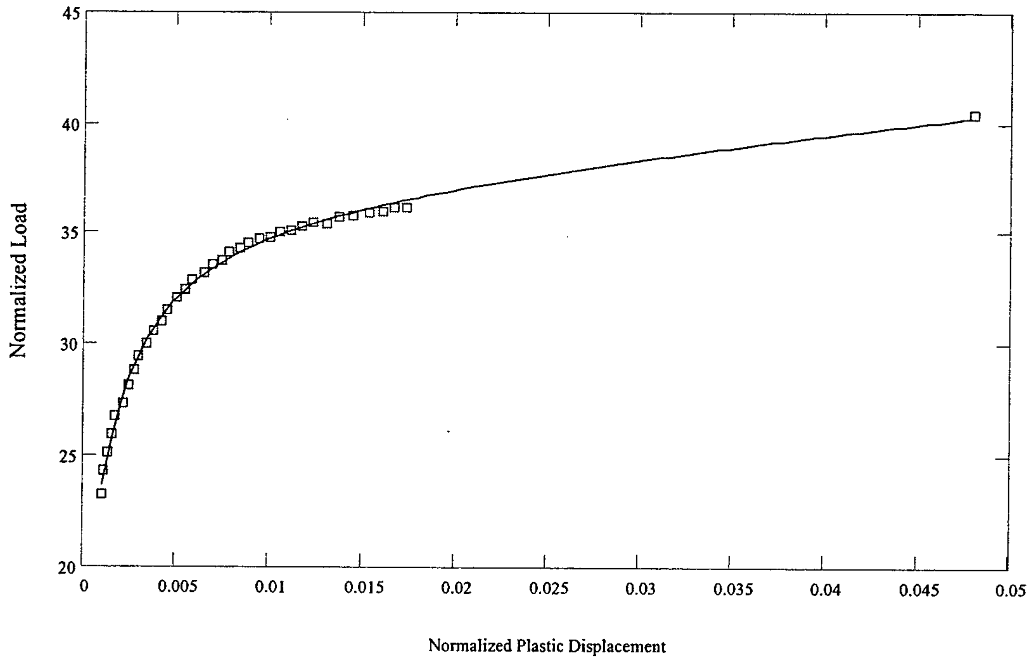


In order for the curve fit to be acceptable, there must be at least 7 points, and it is desireable for the curve to fit the data with a maximum deviation of less than 0.5% of $P_N$ at the final point.

$P_N$ at final point:

$$P_{N_f} = 40.436$$

$$0.005 \cdot P_{N_f} = 0.202$$

$$Err_{ii} := \left| P_{N_{ii}} - F\left(v_{plN_{ii}}, u\right) \right|$$

$$\max(Err) = 0.433$$

$$\mathrm{mean}(Err) = 0.115$$

Note that even though the fit looks good, the maximur deviation exceeds the desired limit.

Do not adjust initial points on blunting line:

$$jj := startpoint - 0 .. NumPoints$$

Interatively solve for each crack length such that points fall on fitted curve

$$Error(u, v, P, a) \equiv NormalizedP(P, a) - F(NormalizedVpl(v, P, a), u)$$

$$a_{pred_i} := a_i$$

$$x := a_o$$

$$a_{pred_{jj}} := \mathrm{root}\left(Error\left(u, v_{jj}, P_{jj}, x\right), x\right)$$

$$P_{N_{jj}} := NormalizedP\left(P_{jj}, a_{pred_{jj}}\right)$$

$v_{plN_{jj}} := \text{NormalizedVpl}\left(v_{jj}, P_{jj}, a_{pred_{jj}}\right)$

$\Delta a_{pred_k} := a_{pred_k} - a_o$

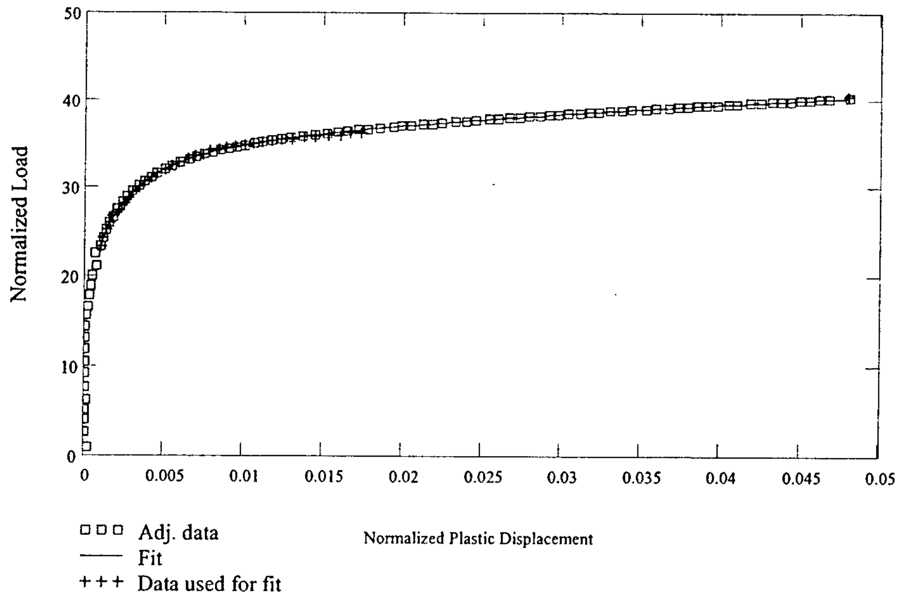


Calculate $v_{el}$ based on compliance:

$v_{el}(P, C_{LL}) := P \cdot C_{LL}$

$$v_{pl}(P, v, C_{LL}) := \begin{vmatrix} v - v_{el}(P, C_{LL}) & \text{if } v_{el}(P, C_{LL}) \le v \\ 0 & \text{otherwise} \end{vmatrix}$$

Calculate Plastic Area under load-displacement curve

$$v_{plastic_k} := v_{pl}\left(P_k, v_k, \text{LLCompliance}\left(\frac{a_{pred_k}}{W}\right)\right)$$

$\text{AreaPl}_0 := 0$

$$\text{AreaPl}_{kk} := \text{AreaPl}_{kk-1} + \frac{P_{kk} + P_{kk-1}}{2} \cdot \left(v_{plastic_{kk}} - v_{plastic_{kk-1}}\right)$$

NOTE: For a falling Load-Disp. curve, if you don't use an incremental formula for plastic area, J will be over-estimated. Amount of over-estimation increases witl crack extension.

Calculate plastic part of J:

$$CrackGrowthCorrection_{kk} := \left(1 - \gamma\left(a_{pred_{kk-1}}\right) \cdot \frac{a_{pred_{kk}} - a_{pred_{kk-1}}}{W - a_{pred_{kk-1}}}\right)$$

$$J_{pl_0} := 0$$

$$J_{pl_{kk}} := \left(J_{pl_{kk-1}} + \frac{\eta\left(a_{pred_{kk-1}}\right)}{W - a_{pred_{kk-1}}} \cdot \frac{AreaPl_{kk} - AreaPl_{kk-1}}{B_N}\right) \cdot CrackGrowthCorrection_{kk}$$

$$J_{pred_k} := Jelastic\left(P_k, a_{pred_k}\right) + J_{pl_k}$$

Define function to find array index of points inside the exclusion lines

$$Ind(\Delta a, J, offset) := \left| \begin{array}{l} j \leftarrow 0 \\ \text{while } \left(\Delta a_j < offset_j\right) \cdot \left(J_j < J_{limit_0}\right) \cdot (j < NumPoints) \\ \quad j \leftarrow j + 1 \\ j \end{array} \right.$$

Select data bewteen exclusion lines:

$$offset_k := \frac{J_{pred_k}}{2 \cdot \sigma_Y} + 0.006 \qquad I_{p1} := Ind\left(\Delta a_{pred}, J_{pred}, offset\right) \qquad I_{p1} = 59$$

$$offset_k := \frac{J_{pred_k}}{2 \cdot \sigma_Y} + 0.060 \qquad I_{p2} := Ind\left(\Delta a_{pred}, J_{pred}, offset\right) - 1 \qquad I_{p2} = 95$$

Over-ride selection limits due to excessive scatter in data:

$$I_{p1} := 56 \qquad I_{p2} := 75$$

Perform power law fit for Normalization data to find JIc:

$$ir := 0 .. I_{p2} - I_{p1}$$

$$Xv_{ir} := \ln\left(\Delta a_{pred_{ir + I_{p1}}}\right) \qquad Yv_{ir} := \ln\left(J_{pred_{ir + I_{p1}}}\right)$$

$$C_2 := slope(Xv, Yv) \qquad C_1 := \exp(intercept(Xv, Yv)) \qquad C_2 = 0.5123$$

$$C_1 = 16751$$

$$\Delta a_{Fit_k} := k \cdot \frac{\Delta a_{pred_f}}{NumPoints} \qquad J_{Fit_k} := C_1 \cdot \left(\Delta a_{Fit_k}\right)^{C_2}$$

Find JQ:

$J_{QN} := 1000 \qquad \Delta a_{QN} := 0.015$

Given

$$J_{QN} = \left(\Delta a_{QN} - 0.008\right) \cdot 2 \cdot \sigma_Y$$

$$J_{QN} = C_1 \cdot \Delta a_{QN}^{\ C_2}$$

$$\begin{bmatrix} J_{QN} \\ \Delta a_{QN} \end{bmatrix} := \mathrm{Find}\left(J_{QN}, \Delta a_{QN}\right) \qquad \Delta a_{QN} = 0.01688 \qquad J_{QN} = 2070$$

Check valaidity for thickness and initial ligament:

$$\frac{25 \cdot J_{QN}}{\sigma_Y} = 0.444 \qquad B = 0.998 \qquad b_o = 0.722$$

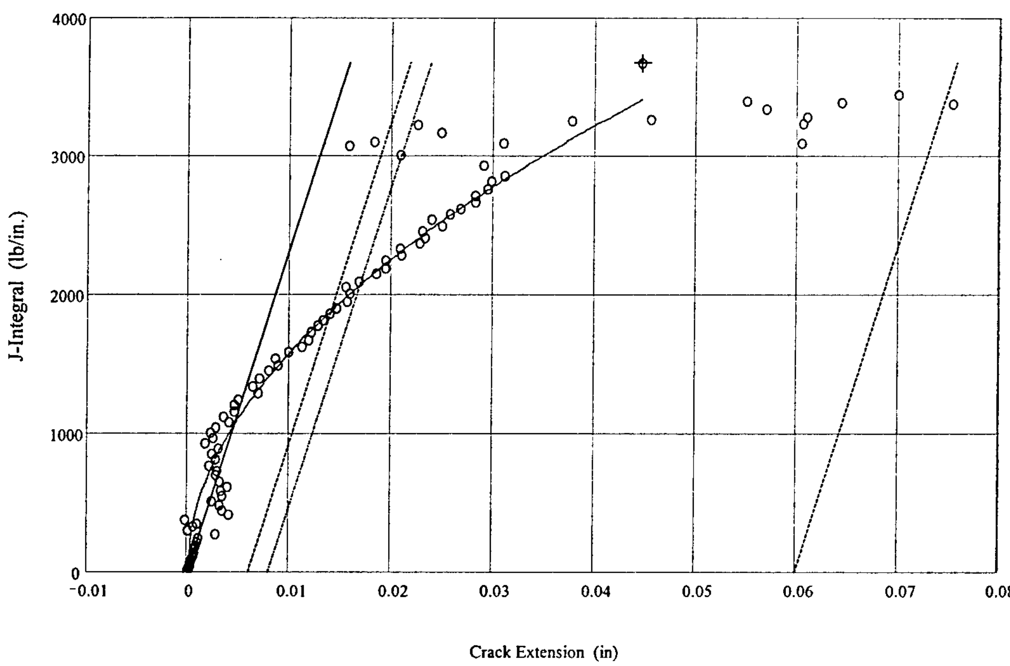

# APPENDIX B

Test Records for Quasi-Static Fracture Toughness Tests

# $J_{Ic}$ Analysis Report for ASTM E1737-96

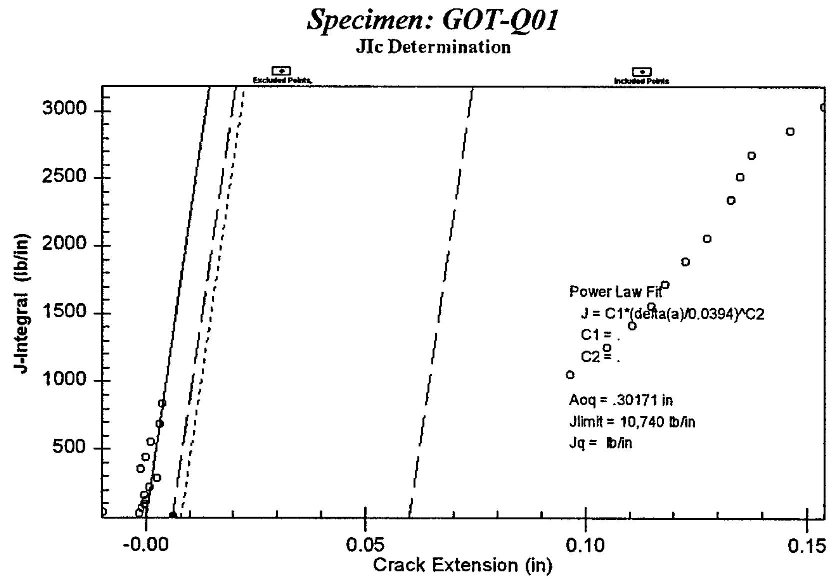


### *Test Information*

| | |
|---|---|
| Specimen Name: | GOT-Q01 |
| Specimen Type: | SE(B) |
| Test Temperature: | 28°F |
| Environment: | Air |
| Notch Orientation: | T-S |

### *Material properties*

| | |
|---|---|
| Material: | HY-100 Under-matched Weld |
| Modulus of Elasticity (Msi): | 29.00 |
| Yield Strength (ksi): | 101 |
| Tensile Strength (ksi): | 121 |
| Poisson's Ratio: | .29 |

### *Specimen Dimensions*

| | |
|---|---|
| Width, W (in.): | 1.753 |
| Thickness, B (in.): | 0.996 |
| Net Thickness, $B_n$ (in.): | 0.779 |

### *Pre-Cracking Conditions*

Max. Load at end of Pre-Cracking (lbs.): 6,059

### *Crack Growth Information*

| | | | |
|---|---|---|---|
| Initial Measured Crack Length, $a_o$ (in.): | 0.297 | Initial Predicted Crack Length, $a_{oq}$ (in.): | 0.302 |
| Final Measured Crack Length, $a_f$ (in.): | 1.500 | Final Predicted Crack Length, $a_{fq}$ (in.): | 0.456 |
| Measured Crack Extension (in.): | 1.203 | Predicted Crack Extension (in.): | 0.154 |

### *$J_{Ic}$ Qualification*

| | | | |
|---|---|---|---|
| Original Crack Size (9.7.2): | Not Checked | Max. Deviation = 0.024 | must be < 0.015 |
| Final Crack Size (9.7.3): | Not Checked | Max. Deviation = 0.024 | must be < 0.075 |
| Crack Extension (9.7.4): | Not Checked | Min. Extension = 0.000 | must be > 0.602 |
| Crack Extension Prediction (9.7.5): | Invalid | Error in $\Delta a$ = 1.049 | must be < 0.044 |
| Orig. Crack Prediction Error (9.7.6): | Valid | $\lvert a_{oq} - a_o \rvert = 0.005$ | must be < 0.018 |
| # Points for $a_{oq}$ Poly. Fit (9.7.7): | Valid | # points = 8 | must be ≥ 8 |
| Correlation for $a_{oq}$ Poly. Fit (9.7.7): | Invalid | Corr. Coeff = 0.670 | must be > 0.96 |
| # Points for Construction Line Fit (9.7.8): | | # points = N/A | must be ≥ 6 |
| Power Law Coefficient, C2 (9.7.9): | | Coeff C2 = | must be < 1.0 |
| Data Spacing for $J_{Ic}$ (9.9.1): | | # points (0.4 $J_Q$ to $J_Q$) = | must be ≥ 3 |
| # Points for Power Law Fit (9.9.3): | | # points = | must be ≥ 5 |
| Data Spacing For Power Law (9.9.3): | | # points A = # points B = | must be ≥ 1 |
| Thickness, B > 25 $J_Q / \sigma_Y$ (9.9.4.1): | | B = | must be > |
| Initial Lig., bo > 25 $J_Q / \sigma_Y$ (9.9.4.2): | | bo = | must be > |
| Power Law Fit Slope @ $\Delta a_Q$ (9.9.4.3): | | Slope = | must be < |

### *Test Results*

Construction Line Slope =

JQc NOT a Valid Jc; JQc = 888.99 (lb/in)

$\Delta a = 0.004$: < : $0.008 + J_{Qc}/(2\ \sigma_Y) = 0.012$

B, bo < $200\ J_{Qc}/\sigma_Y = 1.602$

Naval Surface Warfare Center
Carderock Division

Engineer/Technician: SMG/TS
Date: 28 April, 1999

# $J_{Ic}$ Analysis Report for ASTM E1737-96

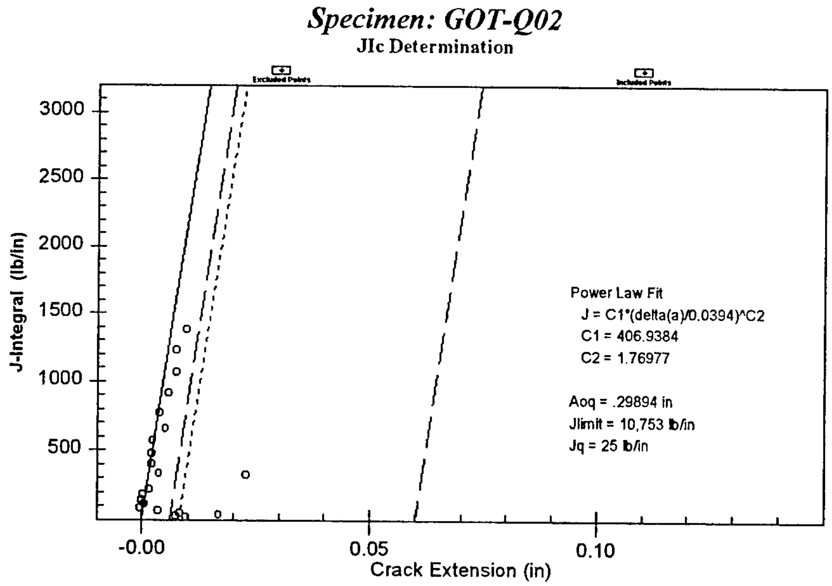


### *Test Information*

| | |
|---|---|
| Specimen Name: | GOT-Q02 |
| Specimen Type: | SE(B) |
| Test Temperature: | 28°F |
| Environment: | Air |
| Notch Orientation: | T-S |

### *Specimen Dimensions*

| | |
|---|---|
| Width, W (in.): | 1.752 |
| Thickness, B (in.): | 0.998 |
| Net Thickness, $B_n$ (in.): | 0.775 |

### *Material properties*

Material: HY-100 Under-matched Weld

| | |
|---|---|
| Modulus of Elasticity (Msi): | 29.00 |
| Yield Strength (ksi): | 101 |
| Tensile Strength (ksi): | 121 |
| Poisson's Ratio: | .29 |

### *Pre-Cracking Conditions*

Max. Load at end of Pre-Cracking (lbs.): 6,061

### *Crack Growth Information*

| | | | |
|---|---|---|---|
| Initial Measured Crack Length, $a_o$ (in.): | 0.306 | Initial Predicted Crack Length, $a_{oq}$ (in.): | 0.299 |
| Final Measured Crack Length, $a_f$ (in.): | 0.769 | Final Predicted Crack Length, $a_{fq}$ (in.): | 0.309 |
| Measured Crack Extension (in.): | 0.463 | Predicted Crack Extension (in.): | 0.010 |

### *$J_{Ic}$ Qualification*

| | | | |
|---|---|---|---|
| Original Crack Size (9.7.2): | Invalid | Max. Deviation = 0.029 | must be < 0.015 |
| Final Crack Size (9.7.3): | Valid | Max. Deviation = 0.038 | must be < 0.038 |
| Crack Extension (9.7.4): | Valid | Min. Extension = 0.450 | must be > 0.232 |
| Crack Extension Prediction (9.7.5): | Invalid | Error in $\Delta a$ = 0.453 | must be < 0.043 |
| Orig. Crack Prediction Error (9.7.6): | Valid | $\lvert a_{oq} - a_o \rvert$ = 0.007 | must be < 0.018 |
| # Points for $a_{oq}$ Poly. Fit (9.7.7): | Valid | # points = 13 | must be ≥ 8 |
| Correlation for $a_{oq}$ Poly. Fit (9.7.7): | Invalid | Corr. Coeff = 0.953 | must be > 0.96 |
| # Points for Construction Line Fit (9.7.8): | | # points = N/A | must be ≥ 6 |
| Power Law Coefficient, C2 (9.7.9): | | Coeff C2 = | must be < 1.0 |
| Data Spacing for $J_{Ic}$ (9.9.1): | | # points (0.4 $J_Q$ to $J_Q$) = | must be ≥ 3 |
| # Points for Power Law Fit (9.9.3): | | # points = | must be ≥ 5 |
| Data Spacing For Power Law (9.9.3): | | # points A = # points B = | must be ≥ 1 |
| Thickness, B > 25 $J_Q / \sigma_Y$ (9.9.4.1): | | B = | must be > |
| Initial Lig., bo > 25 $J_Q / \sigma_Y$ (9.9.4.2): | | bo = | must be > |
| Power Law Fit Slope @ $\Delta a_Q$ (9.9.4.3): | | Slope = | must be < |

### *Test Results*

Construction Line Slope =

JQc NOT a Valid Jc; JQc = 1,426.59 (lb/in)
$\Delta a$ = 0.007: < : 0.008 + $J_{Qc}/(2\ \sigma_Y)$ = 0.014
B, bo < 200 $J_{Qc}/\sigma_Y$ = 2.570

Naval Surface Warfare Center
Carderock Division

Engineer/Technician: SMG/TS
Date: 28 April, 1999

# $J_{Ic}$ Analysis Report for ASTM E1737-96

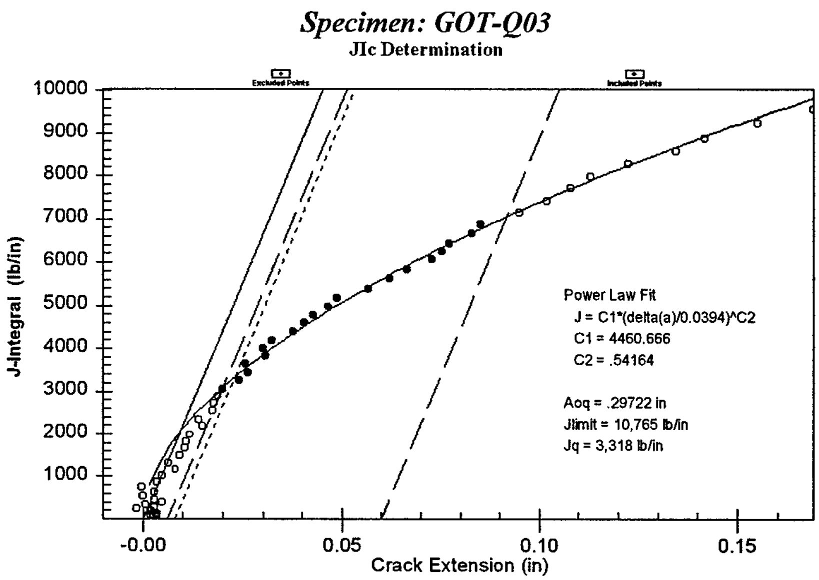


### *Test Information*

Specimen Name: GOT-Q03
Specimen Type: SE(B)
Test Temperature: 28°F
Environment: Air
Notch Orientation: T-S

### *Specimen Dimensions*

Width, W (in.): 1.752
Thickness, B (in.): 0.986
Net Thickness, $B_n$ (in.): 0.798

### *Material properties*

Material: HY-100 Under-matched Weld
Modulus of Elasticity (Msi): 29.00
Yield Strength (ksi): 101
Tensile Strength (ksi): 121
Poisson's Ratio: .29

### *Pre-Cracking Conditions*

Max. Load at end of Pre-Cracking (lbs.): 6,041

### *Crack Growth Information*

Initial Measured Crack Length, $a_o$ (in.): 0.300
Final Measured Crack Length, $a_f$ (in.): 1.040
Measured Crack Extension (in.): 0.740

Initial Predicted Crack Length, $a_{oq}$ (in.): 0.297
Final Predicted Crack Length, $a_{fq}$ (in.): 0.466
Predicted Crack Extension (in.): 0.169

### *$J_{Ic}$ Qualification*

| | | | |
|---|---|---|---|
| Original Crack Size (9.7.2): | Invalid | Max. Deviation = 0.017 | must be < 0.015 |
| Final Crack Size (9.7.3): | Invalid | Max. Deviation = 0.385 | must be < 0.052 |
| Crack Extension (9.7.4): | Invalid | Min. Extension = 0.368 | must be > 0.370 |
| Crack Extension Prediction (9.7.5): | Invalid | Error in $\Delta a$ = 0.571 | must be < 0.044 |
| Orig. Crack Prediction Error (9.7.6): | Valid | $\lvert a_{oq} - a_o \rvert = 0.003$ | must be < 0.018 |
| # Points for $a_{oq}$ Poly. Fit (9.7.7): | Valid | # points = 44 | must be ≥ 8 |
| Correlation for $a_{oq}$ Poly. Fit (9.7.7): | Valid | Corr. Coeff = 0.998 | must be > 0.96 |
| # Points for Construction Line Fit (9.7.8): | | # points = N/A | must be ≥ 6 |
| Power Law Coefficient, C2 (9.7.9): | Valid | Coeff C2 = 0.542 | must be < 1.0 |
| Data Spacing for $J_{Ic}$ (9.9.1): | Valid | # points (0.4 $J_Q$ to $J_Q$) = 11 | must be ≥ 3 |
| # Points for Power Law Fit (9.9.3): | Valid | # points = 20 | must be ≥ 5 |
| Data Spacing For Power Law (9.9.3): | Valid | # points A = 9 # points B = 11 | must be ≥ 1 |
| Thickness, B > 25 $J_Q / \sigma_Y$ (9.9.4.1): | Valid | B = 0.986 | must be > 0.747 |
| Initial Lig., bo > 25 $J_Q / \sigma_Y$ (9.9.4.2): | Valid | bo = 1.452 | must be > 0.747 |
| Power Law Fit Slope @ $\Delta a_Q$ (9.9.4.3): | Valid | Slope = 3,103.40 | must be < 111,000 |

### *Test Results*

JQ NOT a Valid JIc; JQ = 3,318.32 (lb/in)
Construction Line Slope = 2.00

Ju = 7,490.61 (lb/in)
$\Delta a$ = 0.155: > : 0.008 + $J_Q/(2\ \sigma_Y)$ = 0.042
B, bo 200 $J_Q/\sigma_Y$ = N/A

Naval Surface Warfare Center
Carderock Division

Engineer/Technician: SMG/TS
Date: 28 April, 1999

# $J_{Ic}$ Analysis Report for ASTM E1737-96

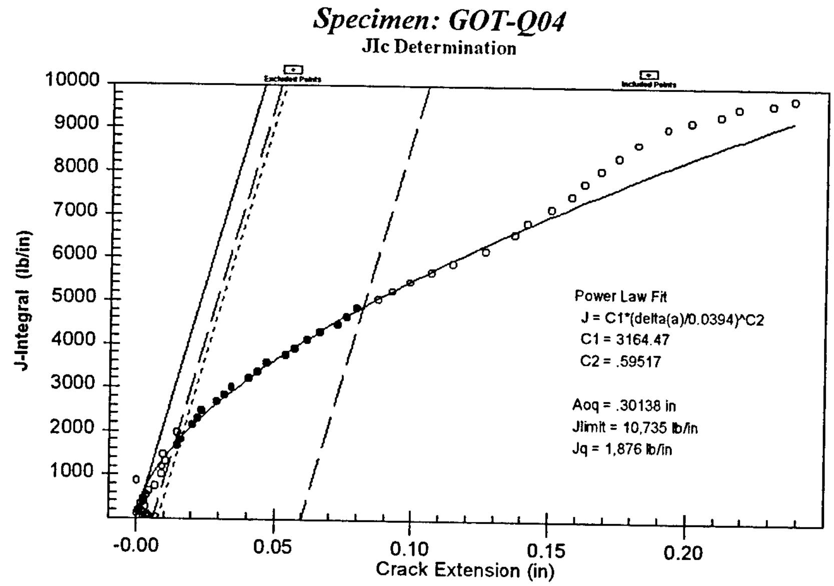


### *Test Information*

| | |
|---|---|
| Specimen Name: | GOT-Q04 |
| Specimen Type: | SE(B) |
| Test Temperature: | 28°F |
| Environment: | Air |
| Notch Orientation: | T-S |

### *Specimen Dimensions*

| | |
|---|---|
| Width, W (in.): | 1.752 |
| Thickness, B (in.): | 0.998 |
| Net Thickness, $B_n$ (in.): | 0.791 |

### *Material properties*

| | |
|---|---|
| Material: | HY-100 Under-matched Weld |
| Modulus of Elasticity (Msi): | 29.00 |
| Yield Strength (ksi): | 101 |
| Tensile Strength (ksi): | 121 |
| Poisson's Ratio: | .29 |

### *Pre-Cracking Conditions*

Max. Load at end of Pre-Cracking (lbs.): 6,035

### *Crack Growth Information*

| | |
|---|---|
| Initial Measured Crack Length, $a_o$ (in.): | 0.292 |
| Final Measured Crack Length, $a_f$ (in.): | 1.057 |
| Measured Crack Extension (in.): | 0.766 |
| Initial Predicted Crack Length, $a_{oq}$ (in.): | 0.301 |
| Final Predicted Crack Length, $a_{fq}$ (in.): | 0.540 |
| Predicted Crack Extension (in.): | 0.238 |

### *$J_{Ic}$ Qualification*

| | | | |
|---|---|---|---|
| Original Crack Size (9.7.2): | Valid | Max. Deviation = 0.008 | must be < 0.015 |
| Final Crack Size (9.7.3): | Valid | Max. Deviation = 0.028 | must be < 0.053 |
| Crack Extension (9.7.4): | Valid | Min. Extension = 0.742 | must be > 0.383 |
| Crack Extension Prediction (9.7.5): | Invalid | Error in $\Delta a$ = 0.528 | must be < 0.044 |
| Orig. Crack Prediction Error (9.7.6): | Valid | $\lvert a_{oq} - a_o \rvert = 0.010$ | must be < 0.018 |
| # Points for $a_{oq}$ Poly. Fit (9.7.7): | Valid | # points = 35 | must be ≥ 8 |
| Correlation for $a_{oq}$ Poly. Fit (9.7.7): | Valid | Corr. Coeff = 0.998 | must be > 0.96 |
| # Points for Construction Line Fit (9.7.8): | | # points = N/A | must be ≥ 6 |
| Power Law Coefficient, C2 (9.7.9): | Valid | Coeff C2 = 0.595 | must be < 1.0 |
| Data Spacing for $J_{Ic}$ (9.9.1): | Valid | # points (0.4 $J_Q$ to $J_Q$) = 7 | must be ≥ 3 |
| # Points for Power Law Fit (9.9.3): | Valid | # points = 18 | must be ≥ 5 |
| Data Spacing For Power Law (9.9.3): | Valid | # points A = 7 # points B = 11 | must be ≥ 1 |
| Thickness, B > 25 $J_Q / \sigma_Y$ (9.9.4.1): | Valid | B = 0.998 | must be > 0.422 |
| Initial Lig., bo > 25 $J_Q / \sigma_Y$ (9.9.4.2): | Valid | bo = 1.460 | must be > 0.422 |
| Power Law Fit Slope @ $\Delta a_Q$ (9.9.4.3): | Valid | Slope = 2,688.00 | must be < 111,000 |

### *Test Results*

JQ NOT a Valid JIc; JQ = 1,875.77 (lb/in)
Construction Line Slope = 2.00

Ju = 7,118.71 (lb/in)
$\Delta a = 0.230$: > : $0.008 + J_{Qc}/(2\ \sigma_Y) = 0.040$
B, bo 200 $J_{Qc}/\sigma_Y$ = N/A

# $J_{Ic}$ Analysis Report for ASTM E1737-96

*Specimen: GOT-Q05*
JIc Determination

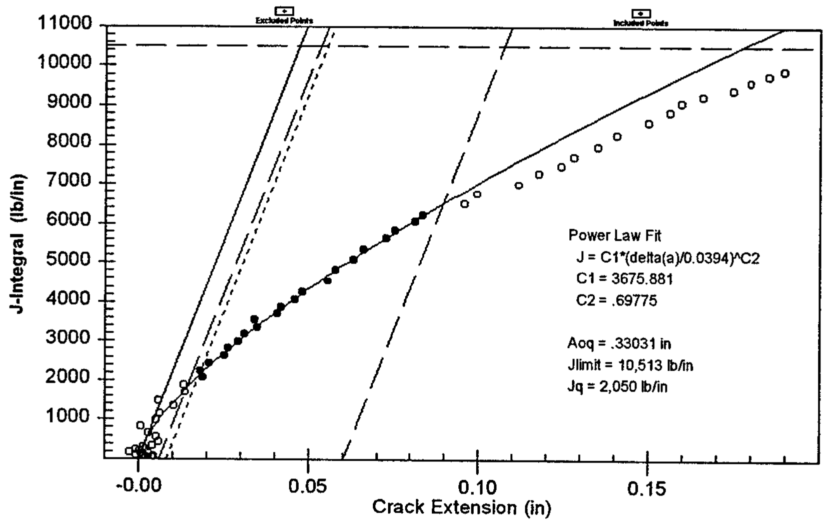


### *Test Information*
Specimen Name: GOT-Q05
Specimen Type: SE(B)
Test Temperature: 28°F
Environment: Air
Notch Orientation: T-S

### *Specimen Dimensions*
Width, W (in.): 1.751
Thickness, B (in.): 1.001
Net Thickness, $B_n$ (in.): 0.776

### *Material properties*
Material: HY-100 Under-matched Weld
Modulus of Elasticity (Msi): 29.00
Yield Strength (ksi): 101
Tensile Strength (ksi): 121
Poisson's Ratio: .29

### *Pre-Cracking Conditions*
Max. Load at end of Pre-Cracking (lbs.): 3,000

### *Crack Growth Information*

| | | | |
|---|---|---|---|
| Initial Measured Crack Length, $a_o$ (in.): | 0.329 | Initial Predicted Crack Length, $a_{oq}$ (in.): | 0.330 |
| Final Measured Crack Length, $a_f$ (in.): | 0.522 | Final Predicted Crack Length, $a_{fq}$ (in.): | 0.520 |
| Measured Crack Extension (in.): | 0.193 | Predicted Crack Extension (in.): | 0.190 |

### *$J_{Ic}$ Qualification*

| | | | |
|---|---|---|---|
| Original Crack Size (9.7.2): | Invalid | Max. Deviation = 0.023 | must be < 0.016 |
| Final Crack Size (9.7.3): | Invalid | Max. Deviation = 0.148 | must be < 0.026 |
| Crack Extension (9.7.4): | Invalid | Min. Extension = 0.053 | must be > 0.097 |
| Crack Extension Prediction (9.7.5): | Valid | Error in Δa = 0.003 | must be < 0.029 |
| Orig. Crack Prediction Error (9.7.6): | Valid | $\lvert a_{oq} - a_o \rvert = 0.002$ | must be < 0.018 |
| # Points for $a_{oq}$ Poly. Fit (9.7.7): | Valid | # points = 40 | must be ≥ 8 |
| Correlation for $a_{oq}$ Poly. Fit (9.7.7): | Valid | Corr. Coeff = 0.998 | must be > 0.96 |
| # Points for Construction Line Fit (9.7.8): | | # points = N/A | must be ≥ 6 |
| Power Law Coefficient, C2 (9.7.9): | Valid | Coeff C2 = 0.698 | must be < 1.0 |
| Data Spacing for $J_{Ic}$ (9.9.1): | Valid | # points (0.4 $J_Q$ to $J_Q$) = 7 | must be ≥ 3 |
| # Points for Power Law Fit (9.9.3): | Valid | # points = 21 | must be ≥ 5 |
| Data Spacing For Power Law (9.9.3): | Valid | # points A = 9 # points B = 12 | must be ≥ 1 |
| Thickness, B > 25 $J_Q / \sigma_Y$ (9.9.4.1): | Valid | B = 1.001 | must be > 0.462 |
| Initial Lig., bo > 25 $J_Q / \sigma_Y$ (9.9.4.2): | Valid | bo = 1.422 | must be > 0.462 |
| Power Law Fit Slope @ $\Delta a_Q$ (9.9.4.3): | Valid | Slope = 3,303.02 | must be < 111,000 |

### *Test Results*
JQ NOT a Valid JIc; JQ = 2,050.07 (lb/in)
Construction Line Slope = 2.00

Ju = 7,896.86 (lb/in)
Δa = 0.185: > : $0.008 + J_{Qc}/(2\,\sigma_Y) = 0.044$
B, bo 200 $J_{Qc}/\sigma_Y$ = N/A

# $J_{Ic}$ Analysis Report for ASTM E1737-96

*Specimen: GOT-D01*

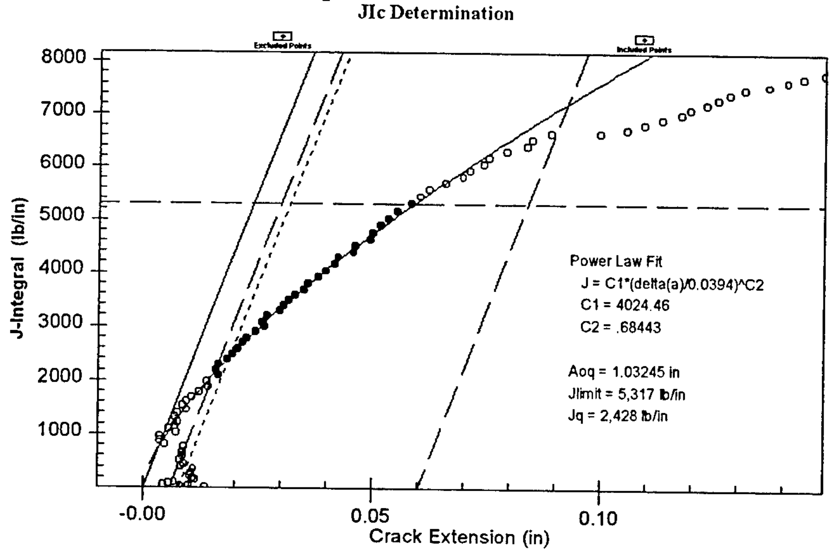


### Test Information

| | |
|---|---|
| Specimen Name: | GOT-D01 |
| Specimen Type: | SE(B) |
| Test Temperature: | 28°F |
| Environment: | Air |
| Notch Orientation: | T-S |

### Specimen Dimensions

| | |
|---|---|
| Width, W (in.): | 1.751 |
| Thickness, B (in.): | 0.998 |
| Net Thickness, $B_n$ (in.): | 0.800 |

### Material properties

| | |
|---|---|
| Material: | HY-100 Matched Weld |
| Modulus of Elasticity (Msi): | 29.00 |
| Yield Strength (ksi): | 101 |
| Tensile Strength (ksi): | 121 |
| Poisson's Ratio: | .29 |

### Pre-Cracking Conditions

Max. Load at end of Pre-Cracking (lbs.): 2,463

### Crack Growth Information

| | | | |
|---|---|---|---|
| Initial Measured Crack Length, $a_o$ (in.): | 1.028 | Initial Predicted Crack Length, $a_{oq}$ (in.): | 1.032 |
| Final Measured Crack Length, $a_f$ (in.): | 1.208 | Final Predicted Crack Length, $a_{fq}$ (in.): | 1.181 |
| Measured Crack Extension (in.): | 0.179 | Predicted Crack Extension (in.): | 0.149 |

### $J_{Ic}$ Qualification

| | | | |
|---|---|---|---|
| Original Crack Size (9.7.2): | Invalid | Max. Deviation = 0.058 | must be < 0.051 |
| Final Crack Size (9.7.3): | Valid | Max. Deviation = 0.055 | must be < 0.060 |
| Crack Extension (9.7.4): | Valid | Min. Extension = 0.140 | must be > 0.090 |
| Crack Extension Prediction (9.7.5): | Invalid | Error in $\Delta a$ = 0.030 | must be < 0.022 |
| Orig. Crack Prediction Error (9.7.6): | Valid | $\lvert a_{oq} - a_o \rvert = 0.004$ | must be < 0.018 |
| # Points for $a_{oq}$ Poly. Fit (9.7.7): | Valid | # points = 57 | must be ≥ 8 |
| Correlation for $a_{oq}$ Poly. Fit (9.7.7): | Valid | Corr. Coeff = 0.999 | must be > 0.96 |
| # Points for Construction Line Fit (9.7.8): | | # points = N/A | must be ≥ 6 |
| Power Law Coefficient, C2 (9.7.9): | Valid | Coeff C2 = 0.684 | must be < 1.0 |
| Data Spacing for $J_{Ic}$ (9.9.1): | Valid | # points (0.4 $J_Q$ to $J_Q$) = 17 | must be ≥ 3 |
| # Points for Power Law Fit (9.9.3): | Valid | # points = 30 | must be ≥ 5 |
| Data Spacing For Power Law (9.9.3): | Valid | # points A = 18 # points B = 12 | must be ≥ 1 |
| Thickness, B > 25 $J_Q / \sigma_Y$ (9.9.4.1): | Valid | B = 0.998 | must be > 0.547 |
| Initial Lig., bo > 25 $J_Q / \sigma_Y$ (9.9.4.2): | Valid | bo = 0.723 | must be > 0.547 |
| Power Law Fit Slope @ $\Delta a_Q$ (9.9.4.3): | Valid | Slope = 3,477.16 | must be < 111,000 |

### Test Results

JQ NOT a Valid JIc; JQ = 2,427.99 (lb/in)
Construction Line Slope = 2.00

No Instability or Jc not Calculated
$\Delta a$ = : : 0.008 + $J_{Qc}/(2\ \sigma_Y)$ =
B, bo 200 $J_{Qc}/\sigma_Y$ =

**Naval Surface Warfare Center**
**Carderock Division**

**Engineer/Technician: SMG/TS**
**Date: 27 April, 1999**

# $J_{Ic}$ Analysis Report for ASTM E1737-96

*Specimen: GOS-Q01B*
JIc Determination

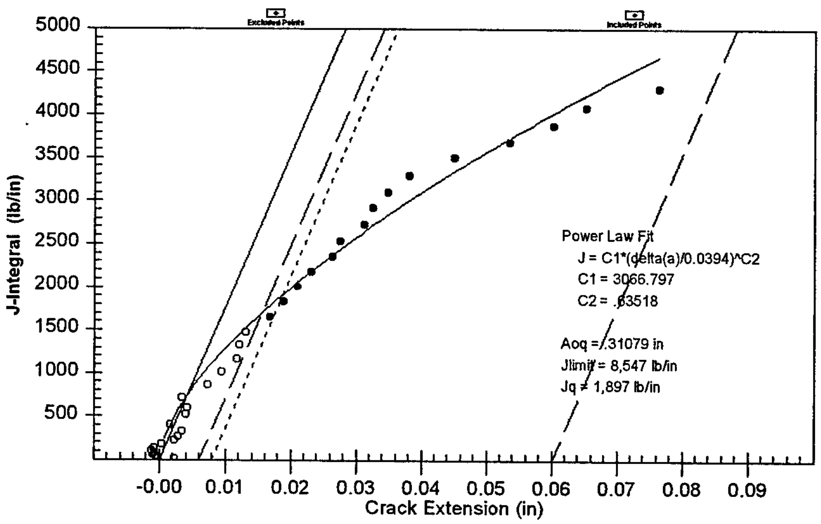


### *Test Information*

Specimen Name: GOS-Q01B
Specimen Type: SE(B)
Test Temperature: 28°F
Environment: Air
Notch Orientation: T-S

### *Specimen Dimensions*

Width, W (in.): 1.753
Thickness, B (in.): 1.003
Net Thickness, $B_n$ (in.): 0.776

### *Material properties*

Material: HY-80 Under-matched Weld
Modulus of Elasticity (Msi): 29.00
Yield Strength (ksi): 81
Tensile Strength (ksi): 97
Poisson's Ratio: .29

### *Pre-Cracking Conditions*

Max. Load at end of Pre-Cracking (lbs.): 6,049

### *Crack Growth Information*

Initial Measured Crack Length, $a_o$ (in.): 0.306
Final Measured Crack Length, $a_f$ (in.): 0.893
Measured Crack Extension (in.): 0.587

Initial Predicted Crack Length, $a_{oq}$ (in.): 0.311
Final Predicted Crack Length, $a_{fq}$ (in.): 0.387
Predicted Crack Extension (in.): 0.076

### *$J_{Ic}$ Qualification*

| | | | |
|---|---|---|---|
| Original Crack Size (9.7.2): | Valid | Max. Deviation = 0.014 | must be < 0.015 |
| Final Crack Size (9.7.3): | Valid | Max. Deviation = 0.026 | must be < 0.045 |
| Crack Extension (9.7.4): | Valid | Min. Extension = 0.569 | must be > 0.294 |
| Crack Extension Prediction (9.7.5): | Invalid | Error in $\Delta a$ = 0.511 | must be < 0.043 |
| Orig. Crack Prediction Error (9.7.6): | Valid | $\lvert a_{oq} - a_o \rvert = 0.005$ | must be < 0.018 |
| # Points for $a_{oq}$ Poly. Fit (9.7.7): | Valid | # points = 26 | must be ≥ 8 |
| Correlation for $a_{oq}$ Poly. Fit (9.7.7): | Valid | Corr. Coeff = 0.997 | must be > 0.96 |
| # Points for Construction Line Fit (9.7.8): | | # points = N/A | must be ≥ 6 |
| Power Law Coefficient, C2 (9.7.9): | Valid | Coeff C2 = 0.635 | must be < 1.0 |
| Data Spacing for $J_{Ic}$ (9.9.1): | Valid | # points (0.4 $J_Q$ to $J_Q$) = 7 | must be ≥ 3 |
| # Points for Power Law Fit (9.9.3): | Valid | # points = 15 | must be ≥ 5 |
| Data Spacing For Power Law (9.9.3): | Valid | # points A = 10 # points B = 5 | must be ≥ 1 |
| Thickness, B > 25 $J_Q / \sigma_Y$ (9.9.4.1): | Valid | B = 1.003 | must be > 0.534 |
| Initial Lig., bo > 25 $J_Q / \sigma_Y$ (9.9.4.2): | Valid | bo = 1.447 | must be > 0.534 |
| Power Law Fit Slope @ $\Delta a_Q$ (9.9.4.3): | Valid | Slope = 2,566.63 | must be < 88,895 |

### *Test Results*

JQ NOT a Valid JIc; JQ = 1,897.30 (lb/in)
Construction Line Slope = 2.00

Ju = 3,885.46 (lb/in)
$\Delta a$ = 0.065: > : 0.008 + $J_Q/(2\,\sigma_Y)$ = 0.030
B, bo 200 $J_Q/\sigma_Y$ = N/A

Naval Surface Warfare Center
Carderock Division

Engineer/Technician: SMG/TS
Date: 28 April, 1999

# $J_{Ic}$ Analysis Report for ASTM E1737-96

***Specimen: GOS-Q02***

JIc Determination

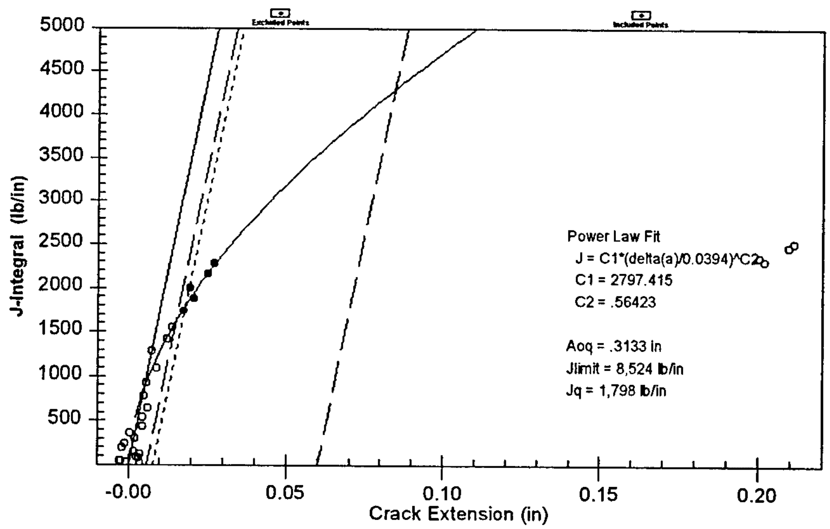


### *Test Information*

| | |
|---|---|
| Specimen Name: | GOS-Q02 |
| Specimen Type: | SE(B) |
| Test Temperature: | 28°F |
| Environment: | Air |
| Notch Orientation: | T-S |

### *Specimen Dimensions*

| | |
|---|---|
| Width, W (in.): | 1.750 |
| Thickness, B (in.): | 0.994 |
| Net Thickness, $B_n$ (in.): | 0.790 |

### *Material properties*

| | |
|---|---|
| Material: | HY-80 Under-matched Weld |
| Modulus of Elasticity (Msi): | 29.00 |
| Yield Strength (ksi): | 81 |
| Tensile Strength (ksi): | 97 |
| Poisson's Ratio: | .29 |

### *Pre-Cracking Conditions*

Max. Load at end of Pre-Cracking (lbs.): 6,256

### *Crack Growth Information*

| | | | |
|---|---|---|---|
| Initial Measured Crack Length, $a_o$ (in.): | 0.309 | Initial Predicted Crack Length, $a_{oq}$ (in.): | 0.313 |
| Final Measured Crack Length, $a_f$ (in.): | 0.510 | Final Predicted Crack Length, $a_{fq}$ (in.): | 0.525 |
| Measured Crack Extension (in.): | 0.201 | Predicted Crack Extension (in.): | 0.211 |

### *$J_{Ic}$ Qualification*

| | | | |
|---|---|---|---|
| Original Crack Size (9.7.2): | Valid | Max. Deviation = 0.014 | must be < 0.015 |
| Final Crack Size (9.7.3): | Invalid | Max. Deviation = 0.094 | must be < 0.025 |
| Crack Extension (9.7.4): | Valid | Min. Extension = 0.121 | must be > 0.100 |
| Crack Extension Prediction (9.7.5): | Valid | Error in $\Delta a$ = 0.011 | must be < 0.030 |
| Orig. Crack Prediction Error (9.7.6): | Valid | $\lvert a_{oq} - a_o \rvert = 0.004$ | must be < 0.018 |
| # Points for $a_{oq}$ Poly. Fit (9.7.7): | Valid | # points = 25 | must be ≥ 8 |
| Correlation for $a_{oq}$ Poly. Fit (9.7.7): | Valid | Corr. Coeff = 0.976 | must be > 0.96 |
| # Points for Construction Line Fit (9.7.8): | | # points = N/A | must be ≥ 6 |
| Power Law Coefficient, C2 (9.7.9): | Valid | Coeff C2 = 0.564 | must be < 1.0 |
| Data Spacing for $J_{Ic}$ (9.9.1): | Valid | # points (0.4 $J_Q$ to $J_Q$) = 7 | must be ≥ 3 |
| # Points for Power Law Fit (9.9.3): | Valid | # points = 5 | must be ≥ 5 |
| Data Spacing For Power Law (9.9.3): | Invalid | # points A = 5   # points B = 0 | must be ≥ 1 |
| Thickness, B > 25 $J_Q / \sigma_Y$ (9.9.4.1): | Valid | B = 0.994 | must be > 0.505 |
| Initial Lig., bo > 25 $J_Q / \sigma_Y$ (9.9.4.2): | Valid | bo = 1.441 | must be > 0.505 |
| Power Law Fit Slope @ $\Delta a_Q$ (9.9.4.3): | Valid | Slope = 2,220.97 | must be < 89,000 |

### *Test Results*

JQ NOT a Valid JIc; JQ = 1,797.63 (lb/in)

Construction Line Slope = 2.00

Ju = 2,231.57 (lb/in)

$\Delta a$ = 0.027: > : 0.008 + $J_{Qc}/(2\ \sigma_Y)$ = 0.021

B, bo   200 $J_{Qc}/\sigma_Y$ = N/A

**Naval Surface Warfare Center**
**Carderock Division**

**Engineer/Technician: SMG/TS**
**Date: 28 April, 1999**

# $J_{Ic}$ Analysis Report for ASTM E1737-96

*Specimen: GOS-Q03*
**JIc Determination**

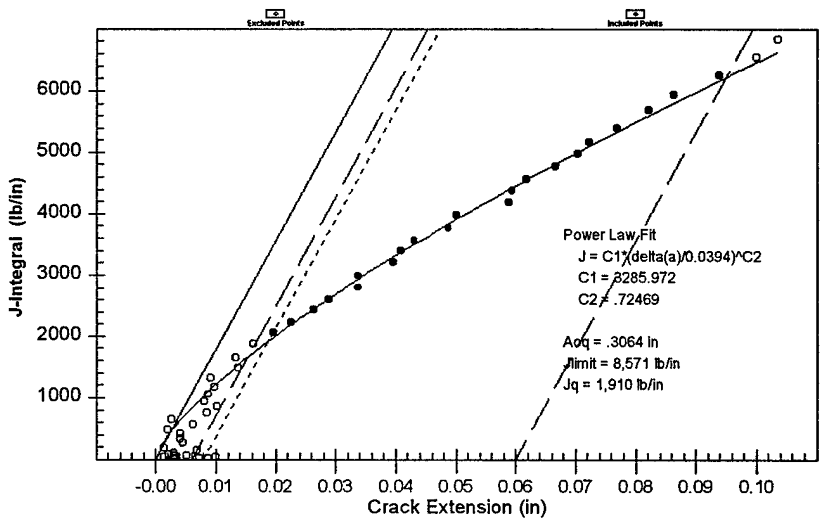


### *Test Information*

| | |
|---|---|
| Specimen Name: | GOS-Q03 |
| Specimen Type: | SE(B) |
| Test Temperature: | 28°F |
| Environment: | Air |
| Notch Orientation: | T-S |

### *Specimen Dimensions*

| | |
|---|---|
| Width, W (in.): | 1.751 |
| Thickness, B (in.): | 1.001 |
| Net Thickness, $B_n$ (in.): | 0.775 |

### *Material properties*

| | |
|---|---|
| Material: | HY-80 Under-matched Weld |
| Modulus of Elasticity (Msi): | 29.00 |
| Yield Strength (ksi): | 81 |
| Tensile Strength (ksi): | 97 |
| Poisson's Ratio: | .29 |

### *Pre-Cracking Conditions*

Max. Load at end of Pre-Cracking (lbs.): 6,048

### *Crack Growth Information*

| | | | |
|---|---|---|---|
| Initial Measured Crack Length, $a_o$ (in.): | 0.292 | Initial Predicted Crack Length, $a_{oq}$ (in.): | 0.306 |
| Final Measured Crack Length, $a_f$ (in.): | 0.919 | Final Predicted Crack Length, $a_{fq}$ (in.): | 0.410 |
| Measured Crack Extension (in.): | 0.627 | Predicted Crack Extension (in.): | 0.104 |

### *$J_{Ic}$ Qualification*

| | | | |
|---|---|---|---|
| Original Crack Size (9.7.2): | Invalid | Max. Deviation = 0.022 | must be < 0.015 |
| Final Crack Size (9.7.3): | Valid | Max. Deviation = 0.034 | must be < 0.046 |
| Crack Extension (9.7.4): | Valid | Min. Extension = 0.609 | must be > 0.314 |
| Crack Extension Prediction (9.7.5): | Invalid | Error in $\Delta a$ = 0.524 | must be < 0.044 |
| Orig. Crack Prediction Error (9.7.6): | Valid | $\lvert a_{oq} - a_o \rvert = 0.014$ | must be < 0.018 |
| # Points for $a_{oq}$ Poly. Fit (9.7.7): | Valid | # points = 35 | must be ≥ 8 |
| Correlation for $a_{oq}$ Poly. Fit (9.7.7): | Valid | Corr. Coeff = 0.999 | must be > 0.96 |
| # Points for Construction Line Fit (9.7.8): | | # points = N/A | must be ≥ 6 |
| Power Law Coefficient, C2 (9.7.9): | Valid | Coeff C2 = 0.725 | must be < 1.0 |
| Data Spacing for $J_{Ic}$ (9.9.1): | Valid | # points (0.4 $J_Q$ to $J_Q$) = 8 | must be ≥ 3 |
| # Points for Power Law Fit (9.9.3): | Valid | # points = 21 | must be ≥ 5 |
| Data Spacing For Power Law (9.9.3): | Valid | # points A = 6 # points B = 15 | must be ≥ 1 |
| Thickness, B > 25 $J_Q / \sigma_Y$ (9.9.4.1): | Valid | B = 1.001 | must be > 0.536 |
| Initial Lig., bo > 25 $J_Q / \sigma_Y$ (9.9.4.2): | Valid | bo = 1.459 | must be > 0.536 |
| Power Law Fit Slope @ $\Delta a_Q$ (9.9.4.3): | Valid | Slope = 2,926.60 | must be < 89,000 |

### *Test Results*

JQ NOT a Valid JIc; JQ = 1,909.64 (lb/in)

Construction Line Slope = 2.00

Ju = 5,747.19 (lb/in)

$\Delta a = 0.100$: > : $0.008 + J_{Qc}/(2\ \sigma_Y) = 0.040$

B, bo 200 $J_{Qc}/\sigma_Y$ = N/A

# $J_{Ic}$ Analysis Report for ASTM E1737-96

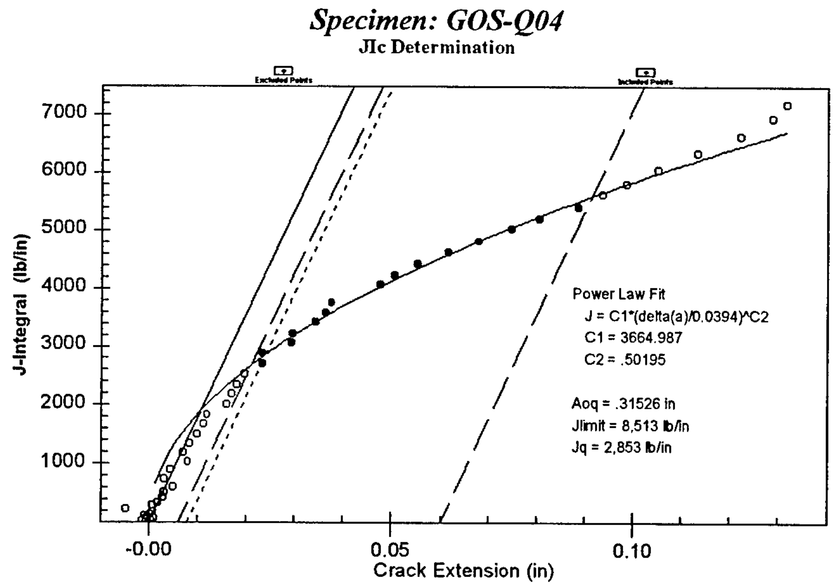


### Test Information

| | |
|---|---|
| Specimen Name: | GOS-Q04 |
| Specimen Type: | SE(B) |
| Test Temperature: | 28°F |
| Environment: | Air |
| Notch Orientation: | T-S |

### Material properties

| | |
|---|---|
| Material: | HY-80 Under-matched Weld |
| Modulus of Elasticity (Msi): | 29.00 |
| Yield Strength (ksi): | 81 |
| Tensile Strength (ksi): | 97 |
| Poisson's Ratio: | .29 |

### Specimen Dimensions

| | |
|---|---|
| Width, W (in.): | 1.750 |
| Thickness, B (in.): | 1.001 |
| Net Thickness, $B_n$ (in.): | 0.790 |

### Pre-Cracking Conditions

Max. Load at end of Pre-Cracking (lbs.): 6,042

### Crack Growth Information

| | | | |
|---|---|---|---|
| Initial Measured Crack Length, $a_o$ (in.): | 0.308 | Initial Predicted Crack Length, $a_{oq}$ (in.): | 0.315 |
| Final Measured Crack Length, $a_f$ (in.): | 1.502 | Final Predicted Crack Length, $a_{fq}$ (in.): | 0.447 |
| Measured Crack Extension (in.): | 1.194 | Predicted Crack Extension (in.): | 0.132 |

### $J_{Ic}$ Qualification

| | | | |
|---|---|---|---|
| Original Crack Size (9.7.2): | Invalid | Max. Deviation = 0.025 | must be < 0.015 |
| Final Crack Size (9.7.3): | Valid | Max. Deviation = 0.042 | must be < 0.075 |
| Crack Extension (9.7.4): | Valid | Min. Extension = 1.159 | must be > 0.597 |
| Crack Extension Prediction (9.7.5): | Invalid | Error in $\Delta a$ = 1.063 | must be < 0.043 |
| Orig. Crack Prediction Error (9.7.6): | Valid | $\lvert a_{oq} - a_o \rvert = 0.007$ | must be < 0.018 |
| # Points for $a_{oq}$ Poly. Fit (9.7.7): | Valid | # points = 36 | must be ≥ 8 |
| Correlation for $a_{oq}$ Poly. Fit (9.7.7): | Valid | Corr. Coeff = 0.999 | must be > 0.96 |
| # Points for Construction Line Fit (9.7.8): | | # points = N/A | must be ≥ 6 |
| Power Law Coefficient, C2 (9.7.9): | Valid | Coeff C2 = 0.502 | must be < 1.0 |
| Data Spacing for $J_{Ic}$ (9.9.1): | Valid | # points (0.4 $J_Q$ to $J_Q$) = 10 | must be ≥ 3 |
| # Points for Power Law Fit (9.9.3): | Valid | # points = 15 | must be ≥ 5 |
| Data Spacing For Power Law (9.9.3): | Valid | # points A = 7 # points B = 8 | must be ≥ 1 |
| Thickness, B > 25 $J_Q / \sigma_Y$ (9.9.4.1): | Valid | B = 1.001 | must be > 0.801 |
| Initial Lig., bo > 25 $J_Q / \sigma_Y$ (9.9.4.2): | Valid | bo = 1.442 | must be > 0.801 |
| Power Law Fit Slope @ $\Delta a_Q$ (9.9.4.3): | Valid | Slope = 2,358.69 | must be < 89,000 |

### Test Results

JQ NOT a Valid JIc; JQ = 2,852.92 (lb/in)

Construction Line Slope = 2.00

Ju = 5,825.63 (lb/in)

$\Delta a = 0.129$: > : $0.008 + J_{Qc}/(2\ \sigma_Y) = 0.041$

B, bo 200 $J_{Qc}/\sigma_Y$ = N/A

Naval Surface Warfare Center
Carderock Division

Engineer/Technician: SMG/TS
Date: 28 April, 1999

# $J_{Ic}$ Analysis Report for ASTM E1737-96

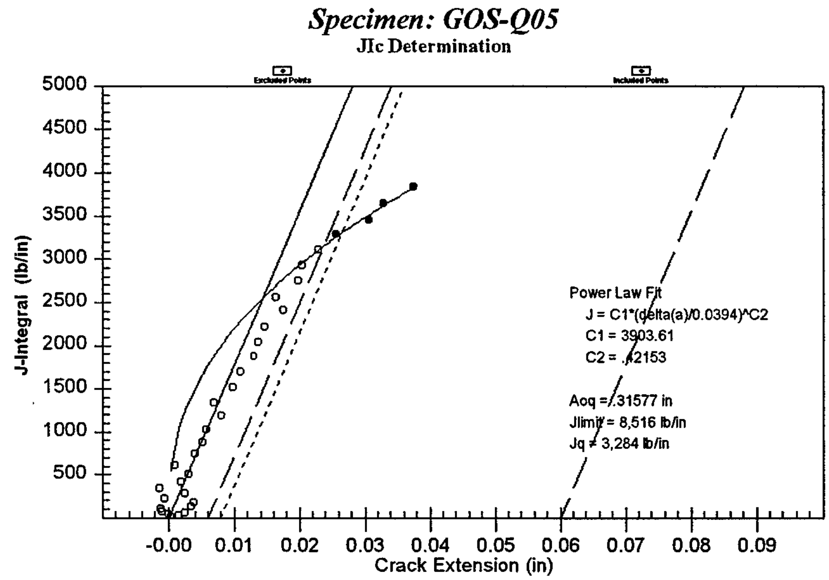


### Test Information

| | |
|---|---|
| Specimen Name: | GOS-Q05 |
| Specimen Type: | SE(B) |
| Test Temperature: | 28°F |
| Environment: | Air |
| Notch Orientation: | T-S |

### Material properties

| | |
|---|---|
| Material: | HY-80 Under-matched Weld |
| Modulus of Elasticity (Msi): | 29.00 |
| Yield Strength (ksi): | 81 |
| Tensile Strength (ksi): | 97 |
| Poisson's Ratio: | .29 |

### Specimen Dimensions

| | |
|---|---|
| Width, W (in.): | 1.751 |
| Thickness, B (in.): | 0.998 |
| Net Thickness, $B_n$ (in.): | 0.797 |

### Pre-Cracking Conditions

Max. Load at end of Pre-Cracking (lbs.): 5,940

### Crack Growth Information

| | | | |
|---|---|---|---|
| Initial Measured Crack Length, $a_o$ (in.): | 0.303 | Initial Predicted Crack Length, $a_{oq}$ (in.): | 0.316 |
| Final Measured Crack Length, $a_f$ (in.): | 1.356 | Final Predicted Crack Length, $a_{fq}$ (in.): | 0.353 |
| Measured Crack Extension (in.): | 1.053 | Predicted Crack Extension (in.): | 0.038 |

### $J_{Ic}$ Qualification

| | | | | |
|---|---|---|---|---|
| Original Crack Size (9.7.2): | Valid | Max. Deviation = 0.015 | must be < 0.015 | |
| Final Crack Size (9.7.3): | Valid | Max. Deviation = 0.040 | must be < 0.068 | |
| Crack Extension (9.7.4): | Valid | Min. Extension = 1.028 | must be > 0.526 | |
| Crack Extension Prediction (9.7.5): | Invalid | Error in $\Delta a$ = 1.015 | must be < 0.043 | |
| Orig. Crack Prediction Error (9.7.6): | Valid | $\lvert a_{oq} - a_o \rvert$ = 0.013 | must be < 0.018 | |
| # Points for $a_{oq}$ Poly. Fit (9.7.7): | Valid | # points = 19 | must be ≥ 8 | |
| Correlation for $a_{oq}$ Poly. Fit (9.7.7): | Valid | Corr. Coeff = 0.994 | must be > 0.96 | |
| # Points for Construction Line Fit (9.7.8): | | # points = N/A | must be ≥ 6 | |
| Power Law Coefficient, C2 (9.7.9): | Valid | Coeff C2 = 0.422 | must be < 1.0 | |
| Data Spacing for $J_{Ic}$ (9.9.1): | Valid | # points (0.4 $J_Q$ to $J_Q$) = 11 | | must be ≥ 3 |
| # Points for Power Law Fit (9.9.3): | Invalid | # points = 4 | must be ≥ 5 | |
| Data Spacing For Power Law (9.9.3): | Invalid | # points A = 4 | # points B = 0 | must be ≥ 1 |
| Thickness, B > 25 $J_Q / \sigma_Y$ (9.9.4.1): | Valid | B = 0.998 | must be > 0.923 | |
| Initial Lig., bo > 25 $J_Q / \sigma_Y$ (9.9.4.2): | Valid | bo = 1.448 | must be > 0.923 | |
| Power Law Fit Slope @ $\Delta a_Q$ (9.9.4.3): | Valid | Slope = 2,085.73 | must be < 89,000 | |

### Test Results

JQ NOT a Valid JIc; JQ = 3,284.27 (lb/in)
Construction Line Slope = 2.00

Ju = 3,621.17 (lb/in)
$\Delta a$ = 0.033: > : 0.008 + $J_{Qc}/(2\ \sigma_Y)$ = 0.028
B, bo 200 $J_{Qc}/\sigma_Y$ = N/A

Naval Surface Warfare Center
Carderock Division

Engineer/Technician: SMG/TS
Date: 14 April, 1999

# $J_{Ic}$ Analysis Report for ASTM E1737-96

*Specimen: GOS-D03*
JIc Determination

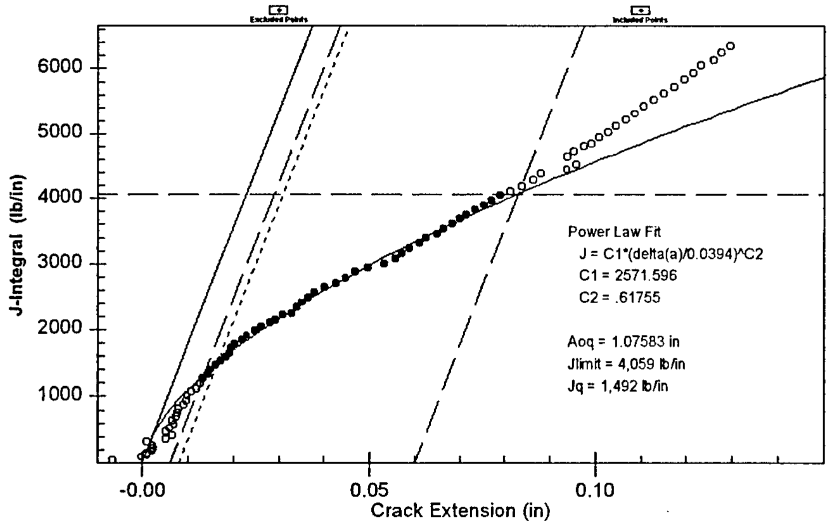


### *Test Information*

| | |
|---|---|
| Specimen Name: | GOS-D03 |
| Specimen Type: | SE(B) |
| Test Temperature: | 28°F |
| Environment: | Air |
| Notch Orientation: | T-S |

### *Material properties*

| | |
|---|---|
| Material: | HY-80 Under-matched Weld |
| Modulus of Elasticity (Msi): | 30.00 |
| Yield Strength (ksi): | 81 |
| Tensile Strength (ksi): | 97 |
| Poisson's Ratio: | .29 |

### *Specimen Dimensions*

| | |
|---|---|
| Width, W (in.): | 1.760 |
| Thickness, B (in.): | 0.998 |
| Net Thickness, $B_n$ (in.): | 0.801 |

### *Pre-Cracking Conditions*

Max. Load at end of Pre-Cracking (lbs.): 2,492

### *Crack Growth Information*

| | | | |
|---|---|---|---|
| Initial Measured Crack Length, $a_o$ (in.): | 1.079 | Initial Predicted Crack Length, $a_{oq}$ (in.): | 1.076 |
| Final Measured Crack Length, $a_f$ (in.): | 1.352 | Final Predicted Crack Length, $a_{fq}$ (in.): | 1.336 |
| Measured Crack Extension (in.): | 0.274 | Predicted Crack Extension (in.): | 0.260 |

### *$J_{Ic}$ Qualification*

| | | | |
|---|---|---|---|
| Original Crack Size (9.7.2): | Invalid | Max. Deviation = 0.124 | must be < 0.054 |
| Final Crack Size (9.7.3): | Invalid | Max. Deviation = 0.112 | must be < 0.068 |
| Crack Extension (9.7.4): | Valid | Min. Extension = 0.191 | must be > 0.137 |
| Crack Extension Prediction (9.7.5): | Valid | Error in $\Delta a$ = 0.014 | must be < 0.020 |
| Orig. Crack Prediction Error (9.7.6): | Valid | $\lvert a_{oq} - a_o \rvert = 0.003$ | must be < 0.018 |
| # Points for $a_{oq}$ Poly. Fit (9.7.7): | Valid | # points = 72 | must be ≥ 8 |
| Correlation for $a_{oq}$ Poly. Fit (9.7.7): | Valid | Corr. Coeff = 0.998 | must be > 0.96 |
| # Points for Construction Line Fit (9.7.8): | | # points = N/A | must be ≥ 6 |
| Power Law Coefficient, C2 (9.7.9): | Valid | Coeff C2 = 0.618 | must be < 1.0 |
| Data Spacing for $J_{Ic}$ (9.9.1): | Valid | # points (0.4 $J_Q$ to $J_Q$) = 14 | must be ≥ 3 |
| # Points for Power Law Fit (9.9.3): | Valid | # points = 41 | must be ≥ 5 |
| Data Spacing For Power Law (9.9.3): | Valid | # points A = 16 # points B = 25 | must be ≥ 1 |
| Thickness, B > 25 $J_Q / \sigma_Y$ (9.9.4.1): | Valid | B = 0.998 | must be > 0.419 |
| Initial Lig., bo > 25 $J_Q / \sigma_Y$ (9.9.4.2): | Valid | bo = 0.681 | must be > 0.419 |
| Power Law Fit Slope @ $\Delta a_Q$ (9.9.4.3): | Valid | Slope = 2,224.74 | must be < 89,000 |

### *Test Results*

JQ NOT a Valid JIc; JQ = 1,492.12 (lb/in)
Construction Line Slope = 2.00

No Instability or Jc not Calculated
$\Delta a$ = : : 0.008 + $J_{Qc}/(2\,\sigma_Y)$ =
B, bo 200 $J_{Qc}/\sigma_Y$ =

# INITIAL DISTRIBUTION

| Copies | | | |
|---|---|---|---|
| 9 | **NAVSEA** | | |
| | 1 SEA 05M2 (Null) | | |
| | 1 SEA 05M2 (Mitchell) | | |
| | 1 SEA 05P (McCarthy) | | |
| | 1 SEA 05P1(Packard) | | |
| | 1 SEA 05P1(Sieve) | | |
| | 1 SEA 05P2(Nichols) | | |
| | 1 SEA 05P3 (Miles) | | |
| | 1 SEA 05P4 (Manuel) | | |
| | 1 SEA 05P4 (Moussouros) | | |
| 3 | **US Naval Academy** | | |
| | 1 (Link) | | |
| | 1 (Joyce) | | |
| | 1 (Gaudett) | | |
| 2 | **Office of Naval Research** | | |
| | 1 332 (Yoder) | | |
| | 1 334 (Barsoum) | | |
| 2 | **DTIC** | | |

**DIVISION DISTRIBUTION**

| Copies | |
|---|---|
| 1 | 61 (DeNale) |
| 1 | 614 (Montemarano) |
| 1 | 614 (Czyryca) |
| 1 | 614 (Roe) |
| 1 | 614 (Tregoning) |
| 1 | 614 (L'Heureux) |
| 1 | 614 (Focht) |
| 1 | 614 (Zhang) |
| 1 | 614 (McKirgan) |
| 5 | 614 (Graham) |
| 1 | 615 (DeLoach) |
| 1 | 65 (Beach) |
| 1 | 653 (Hay) |
| 1 | 653 (Gifford) |
| 1 | 654 (Lerner) |
| 1 | 60 |
| 1 | 602 |
| 1 | 604 |
| 1 | 62 |
| 1 | 63 |
| 1 | 64 |
| 1 | 66 (SF 298 only) |